

**ISSUE RESOLUTION STATUS REPORT
KEY TECHNICAL ISSUE:
IGNEOUS ACTIVITY**

**Division of Waste Management
Office of Nuclear Material Safety and Safeguards
U.S. Nuclear Regulatory Commission**

Revision 0

March 1998

9804160162 980327
PDR WASTE PDR
WM-11

102.8

CONTENTS

Section	Page
FIGURES	iv
ACKNOWLEDGMENTS	vi
QUALITY OF DATA, ANALYSES, AND CODE DEVELOPMENT	vi
1.0 INTRODUCTION	1
2.0 KEY TECHNICAL ISSUE AND SUBISSUES	3
3.0 IMPORTANCE OF ISSUE TO REPOSITORY PERFORMANCE	5
3.1 RELATIONSHIP AND IMPORTANCE OF SUBISSUE TO TOTAL SYSTEM PERFORMANCE	5
3.2 RELATIONSHIP OF SUBISSUES TO DOE'S REPOSITORY SAFETY STRATEGY	8
3.3 CONSIDERATION OF IGNEOUS ACTIVITY IN PREVIOUS PERFORMANCE ASSESSMENTS	8
3.3.1 Link, et al., 1982	8
3.3.2 TSPA 91	8
3.3.3 TSPA 93	9
3.3.4 NRC Iterative Performance Assessment Phase 2 - 1995	9
3.4 NRC/CNWRA SENSITIVITY STUDIES	10
4.0 REVIEW METHODS AND ACCEPTANCE CRITERIA	13
4.1 PROBABILITY	13
4.1.1 Probability Criterion 1	14
4.1.1.1 Acceptance Criterion	14
4.1.1.2 Review Method	14
4.1.1.3 Technical Basis	14
4.1.1.4 Summary	18
4.1.2 Probability Criterion 2	19
4.1.2.1 Acceptance Criterion	19
4.1.2.2 Review Method	19
4.1.2.3 Technical Basis	19
4.1.2.3.1 Individual Eruptive Units	20
4.1.2.3.2 Episodes of Vent or Vent-Alignment Formation	21
4.1.2.3.3 Emplacement of an Igneous Intrusion	25
4.1.2.3.4 Volcanic Eruptions with Accompanying Dike Injection	25
4.1.2.4 Summary	27
4.1.3 Probability Criterion 3	27
4.1.3.1 Acceptance Criterion	27

4.1.3.2	Review Method	27
4.1.3.3	Technical Basis	28
4.1.3.3.1	Shifts in the Location of Basaltic Volcanism	28
4.1.3.3.2	Vent Clustering	29
4.1.3.3.3	Vent Alignments and Correlation of Vent Alignments and Faults	31
4.1.3.4	Summary	34
4.1.4	Probability Criterion 4	34
4.1.4.1	Acceptance Criterion	34
4.1.4.2	Review Method	34
4.1.4.3	Technical Basis	34
4.1.4.3.1	Temporal Recurrence Rate	35
4.1.4.3.2	Spatial Recurrence Rate	37
4.1.4.3.3	Area Affected by Igneous Events	44
4.1.4.4	Summary	48
4.1.5	Probability Criterion 5	50
4.1.5.1	Acceptance Criterion	50
4.1.5.2	Review Method	50
4.1.5.3	Technical Basis	50
4.1.5.3.1	Regional Tectonic Models	51
4.1.5.3.2	Mechanistic Relationship Between Crustal Extension and Magma Generation	55
4.1.5.3.3	Local Structural Controls on Magma Ascent	64
4.1.5.4	Summary	66
4.1.6	Probability Criterion 6	67
4.1.6.1	Acceptance Criterion	67
4.1.6.2	Review Method	67
4.1.6.3	Technical Basis	67
4.1.6.3.1	Individual Mappable Eruptive Units and Vents	68
4.1.6.3.2	Vent Alignments	70
4.1.6.3.3	Vent Alignments with Tectonic Control	72
4.1.6.3.4	Igneous Intrusions	77
4.1.6.4	Summary	78
4.1.7	Probability Criterion 7	79
4.1.7.1	Acceptance Criterion	79
4.1.7.2	Review Method	79
4.1.7.3	Technical Basis	80
4.1.7.4	Summary	80
4.1.8	Probability Criterion 8	80
4.1.8.1	Acceptance Criterion	80
4.1.8.2	Review Method	81
4.1.8.3	Technical Basis	81

	4.1.8.4	Summary	82
4.1.9	Probability Criterion 9		83
	4.1.9.1	Acceptance Criterion	83
	4.1.9.2	Review Method	83
	4.1.9.3	Technical Basis	83
	4.1.9.4	Summary	84
4.2	CONSEQUENCES		84
	4.2.1	Acceptance Criteria - Consequences	84
	4.2.2	Review Method - Consequences	84
	4.2.3	Technical Basis - Consequences	85
	4.2.4	Summary - Consequences	85
5.0	STATUS OF ISSUE RESOLUTION AT STAFF LEVEL		87
5.1	STATUS OF RESOLUTION OF PROBABILITY ISSUES		87
	5.1.1	Probability Criterion 1	87
	5.1.2	Probability Criterion 2	88
	5.1.3	Probability Criterion 3	88
	5.1.4	Probability Criterion 4	88
	5.1.5	Probability Criterion 5	89
	5.1.6	Probability Criterion 6	89
	5.1.7	Probability Criterion 7	90
	5.1.8	Probability Criterion 8	90
	5.1.9	Probability Criterion 9	90
5.2	STATUS OF CONSEQUENCE ANALYSIS		91
5.3	NRC DISPOSITION OF COMMENTS RELATED TO IGNEOUS ACTIVITY		91
6.0	REFERENCES		99

**APPENDIX A: COMPILATION OF DATES FOR BASALTIC ROCKS OF THE YUCCA
MOUNTAIN REGION**

FIGURES

Figure		Page
1	Flowdown diagram for total system performance assessment.	6
2	CCDF for volcanism disruptive scenario, all parameters sampled from ranges, receptor location 20 km south of repository, 10,000 yr performance period..	11
3	Basaltic volcanic rocks of the Western Great Basin since about 12 Ma, from Luedke and Smith (1981) and references in Connor and Hill (1994) and Appendix A.	16
4	Basaltic volcanic rocks of the Yucca Mountain region since about 11 Ma.	17
5	Development of multiple vent alignments along a fault is illustrated by the Mesa Butte alignment in the San Francisco volcanic field, Arizona.	22
6	Detailed geochronology shows that the Mesa Butte alignment formed over a period of more than 1 m.y. through several distinct episodes of volcanism.	23
7	Basaltic volcanic rocks of the Crater Flat area, Nevada.	24
8	Distribution of dikes, breccia zones, sills, and vents in the San Rafael volcanic field, Utah.	26
9	Ground magnetic map of Amargosa Aeromagnetic Anomaly A showing three aligned anomalies	30
10	Ground magnetic map of the Northern Cone area, Crater Flat, Nevada	33
11	Comparison of observed fraction of volcanoes within a given distance of their nearest-neighbor volcano with Gaussian kernel models calculated using $h = 3$ km, 5 km, and 7 km.	41
12	Comparison of observed fraction of volcanic events within a given distance of their nearest-neighbor volcanic event with Gaussian kernel models calculated using $h = 5$ km and $h = 7$ km.	42
13	Comparison of observed fraction of volcanoes within a given distance of their nearest-neighbor volcano with Epanechnikov kernel models calculated using $h = 5$ km, 10 km, and 18 km.	43
14	Distribution of Plio-Quaternary vents by vent alignment half-length.	46
15	Distribution of the orientation of fault segments with respect to north	48

16	Simplified geologic map of the area around Yucca Mountain showing major geologic units, including Plio-Quaternary volcanoes and faults.	52
17	Two balanced cross sections across Bare Mountain, Crater Flat, and Yucca Mountain (from Ferrill, et al., 1996b).	53
18	Comparison of density profiles beneath Bare Mountain (BM) and Crater Flat (CF) . . .	56
19	Conceptual model of melt generation in response to crustal extension	58
20	Bouguer gravity anomaly map of the Yucca Mountain region	59
21	Apparent density variation across the Yucca Mountain region, derived from gravity data	62
22	Schmidt plot of fault dilation tendency for Yucca Mountain region stresses	65
23	Annual probability of volcanic eruptions within the repository boundary. Igneous events are defined as individual mappable eruptive units and vents.	69
24	Annual probability of volcanic eruptions within the repository boundary. Igneous events are defined as vents and vent alignments.	71
25	The weighting function, $f_r(x,y)$, is derived from changes in average crustal densities under the locations of Plio-Quaternary YMR volcanoes.	73
26	The spatial recurrence rate (v/km^2) is contoured in the area of Yucca Mountain, using the Gaussian kernel function (Eq. 35).	74
27	The spatial recurrence rate (v/km^2) is contoured in the area of Yucca Mountain, using the modified Gaussian kernel function (Eqs. 37 to 39) to incorporate tectonic control on the probability estimate.	75
28	Annual probability of volcanic eruptions within the repository boundary using a modified Gaussian kernel. Igneous events are defined as vents and vent alignments	76
29	Annual probability of volcanic eruptions within the repository boundary using regional recurrence rates of $\lambda_r = 1 \times 10^{-6}$, 2×10^{-6} , 3×10^{-6} , 4×10^{-6} , and $5 \times 10^{-6}/\text{yr}$	77

ACKNOWLEDGMENTS

This report was prepared jointly by the U.S. Nuclear Regulatory Commission and the Center for Nuclear Waste Regulatory Analyses (CNWRA) staffs. Primary authors of the report are Charles B. Connor (CNWRA), Brittain E. Hill (CNWRA), and John S. Trapp (NRC). The authors thank David Ferrill (CNWRA), F. Michael Conway (CNWRA), Goodluck Ofoegbu (CNWRA), Philip Justus (NRC), and Mark Jarzempa (CNWRA) for their assistance on the discussions and interpretations of the models presented herein; John Stamatakos (CNWRA), H. Lawrence McKague (CNWRA), Budhi Sagar (CNWRA), N. King Stablein (NRC) and David J. Brooks (NRC) for their review of this report; Ron Martin (CNWRA), Peter La Femina (CNWRA), and Samantha Magsino (CNWRA) for their expert technical assistance; and Annette Mandujano (CNWRA) and Carrie Crawford (NRC) for their assistance in preparing this report.

QUALITY OF DATA, ANALYSIS, AND CODE DEVELOPMENT

DATA: CNWRA-generated data contained within this report meet quality assurance requirements described in the CNWRA Quality Assurance Manual. Sources for other data should be consulted for determining the level of quality for those data.

ANALYSIS AND CODES: Probability models that form the basis of this report have been tested for accuracy. The calculations were checked as required by QAP-014, Documentation and Verification of Scientific and Engineering Calculations, and recorded in a scientific notebook.

1.0 INTRODUCTION

One of the primary objectives of the U.S. Nuclear Regulatory Commission's refocused precicensing program is to direct all activities towards resolving 10 key technical issues (KTIs) considered most important to repository performance. This approach is summarized in Chapter 1 of the staff's fiscal year (FY) 1996 Annual Progress Report (Sagar, 1997). Other chapters address each of the 10 KTIs by describing the scope of the issue and subissues, path to resolution, and progress achieved during FY96. For the purposes of this report, "staff" shall refer to NRC and Center for Nuclear Waste Regulatory Analyses (CNWRA) staff.

Consistent with NRC regulations on precicensing consultations and a 1992 agreement with the U.S. Department of Energy (DOE), staff-level issue resolution can be achieved during the precicensing consultation period; however, such resolution at the staff level would not preclude the issue being raised and considered during licensing proceedings. Issue resolution at the staff level during precicensing is achieved when the staff has no further questions or comments (i.e., open items), at a point in time, regarding how the DOE program is addressing an issue. There may be some cases where resolution at the staff level may be limited to documenting a common understanding regarding differences in the NRC and the DOE technical positions. Pertinent, additional information could raise new questions or comments regarding a previously-resolved issue.

An important step in the staff's approach to issue resolution is to provide DOE with feedback regarding issue resolution before viability assessment. Issue Resolution Status Reports (IRSRs) are the primary mechanism that NRC and CNWRA staff will use to provide DOE with feedback on KTI subissues. IRSRs focus on: (i) acceptance criteria for issue resolution; and (ii) the status of resolution, including areas of agreement or when the staff currently has comments or questions. Feedback is also contained in the staff's Annual Progress Report, which summarizes the significant technical work toward resolution of all KTIs during the preceding fiscal year. Finally, open meetings and technical exchanges with DOE provide opportunities to discuss issue resolution, identify areas of agreement and disagreement, and develop plans to resolve such disagreements.

In addition to providing feedback, the IRSRs will guide the staff's review of information in the DOE viability assessment. The staff also plans to use the IRSRs in the future to develop the Standard Review Plan for the repository license application.

Each IRSR contains five sections. This Introduction is Section 1.0. Section 2.0 defines the KTI, all the related subissues, and the scope of the particular subissue that is the subject of the IRSR. Section 3.0 discusses the importance of the subissue to repository performance including: (i) qualitative descriptions; (ii) reference to total system performance (TSP); (iii) results of available sensitivity analyses; and (iv) relationship to the DOE Repository Safety Strategy (RSS), that is, their approach to the viability assessment. Section 4.0 provides the staff's review methods and acceptance criteria, which indicate the technical basis for resolution of the subissue and that will be used by the staff in subsequent reviews of DOE submittals. These acceptance criteria are guidance for the staff and, indirectly, for DOE as well. The staff's technical basis for the acceptance criteria is also explained in detail to further document the rationale for staff decisions. Section 5.0 concludes the IRSR with the status of resolution, indicating those items resolved at the staff level or those items remaining open. These open items will be tracked by the staff, and resolution will be documented in future IRSRs.

THIS PAGE INTENTIONALLY BLANK

2.0 KEY TECHNICAL ISSUE AND SUBISSUES

The Igneous Activity KTI (IA KTI) has been defined by the NRC as "predicting the consequence and probability of igneous activity affecting the repository in relationship to the overall system performance objective." Igneous activity is the process of the formation of igneous rocks from molten or partially-molten material (magma). Igneous processes are normally divided into two classes; intrusive activity, whereby magma is emplaced into preexisting rocks, and extrusive or volcanic activity, whereby magma and its associated materials rise into the crust and are deposited on the earth's surface. The dividing line between intrusive and extrusive processes and events can be very blurred. Dikes, which are by definition intrusive features, can break through to the earth's surface and are responsible for many lava flows. In addition, many volcanoes first start as a dike in which flow becomes constricted to a certain location, the volcanic vent. For purposes of this IRSR, volcanic activity is restricted to mean only those features and processes associated with the volcano and volcanic vent itself.

The main objective of work within the IA KTI is to evaluate the significance of igneous activity to repository performance by reviewing and independently confirming critical data, and evaluating and developing alternative conceptual models for estimating the probability and consequence of igneous activity at the proposed repository site. The scope of work includes review of various DOE documents as well as applicable documents in the open literature, participation in meetings with DOE to discuss issues related to the KTI, observation of Quality Assurance (QA) audits of DOE, independent technical investigations, and performing sensitivity studies related to igneous activity and TSP.

The IA KTI has been factored by NRC into two subissues, which contain specific technical components. The first subissue, probability, focuses on: (i) definition of igneous events, (ii) determination of recurrence rates, and (iii) examination of geologic factors that control the timing and location of igneous activity. Under this subissue, nine acceptance criteria have been developed that relate to these areas of focus and use this information to develop probability values. The second subissue considers the consequences of igneous activity within the repository setting. Primary focus areas for the second subissue are: (i) definition of the physical characteristics of igneous events, (ii) determination of the eruption characteristics for modern and ancient basaltic igneous features in the Yucca Mountain Region (YMR) and analogous geologic settings, (iii) models of the effect of the geologic repository setting on igneous processes, (iv) evaluation of waste and repository characteristics with regard to behavior during igneous events, and (v) determination of geologic system characteristics relevant to the probability and consequences of igneous activity. This IRSR addresses Subissue 1 (probability) with specific emphasis on the probability of volcanic activity disrupting the repository. Subissue 2 will be addressed in Revision 1 of this IRSR.

Issue resolution regarding probability has been achieved by gaining agreement on reasonable mechanisms and realistic ranges of the critical parameters necessary to evaluate the likelihood and character of future igneous activity at or near the proposed repository site. This required an evaluation of existing data and models from DOE, the CNWRA, and others to arrive at a reasonably conservative value for the probability of future igneous activity at the proposed repository site. Probability models will need to reflect the limitations of YMR characterization activities along with the uncertainties associated with understanding igneous processes.

Reasonably conservative values are needed due to the limitations and uncertainty in our understanding of igneous processes in general, and within the YMR in particular. Further, there must be reasonable assurance that the values used do not underestimate possible effects of igneous activity on the proposed repository site.

Issue resolution for the consequences of igneous activity will be achieved through comparison of results from independent estimates of the staff with those from the DOE program and through agreement on reasonable or bounding mechanisms and realistic or bounding ranges of parameters necessary to evaluate igneous activity on repository TSP. This will require an evaluation of direct and indirect effects of both the intrusive and extrusive aspects of igneous disruption of a waste repository, to include the physical, chemical, and thermal effects of magma on engineered systems. Critical to this resolution is the building of confidence in the consequence models by testing some of their components (e.g., ash dispersal) against known data from analogous basaltic volcanoes.

3.0 IMPORTANCE OF ISSUE TO REPOSITORY PERFORMANCE

Basaltic igneous activity has been characteristic of the region around the proposed repository site since cessation of caldera magmatism at about 11 Ma. Prior to this time, silicic volcanic activity had been characteristic of the YMR, however, since about 10 Ma, such activity has been absent from the YMR. As a result, during the Technical Exchange between NRC and DOE on February 25-26, 1997, NRC and DOE agreed that silicic activity need not be considered in performance assessment of the Yucca Mountain site. Since about 1 Ma, five basaltic volcanoes have erupted within 20 km of the proposed repository site. Based on the long record of scattered, small-volume basaltic volcanism in the region and large time-scales of geological processes that likely control the production and distribution of basaltic volcanism, the YMR has the potential for a basaltic volcano to erupt during the next 10,000 to 1,000,000 years. Staff from NRC, CNWRA, DOE, and the State of Nevada have conducted numerous investigations regarding the probability and likely consequences of repository disruption by basaltic igneous activity. Results of these investigations demonstrate that the probability and likely consequences of future igneous activity are sufficiently large, such that basaltic igneous activity needs to be considered in repository performance assessments.

3.1 RELATIONSHIP AND IMPORTANCE OF SUBISSUES TO TOTAL SYSTEM PERFORMANCE

The staff is developing a strategy for evaluating the performance of a proposed repository at Yucca Mountain. As is currently visualized by the staff, key elements of this strategy are defined by those elements necessary for DOE to demonstrate repository performance. These elements are illustrated in Figure 1. Figure 1 is a simplified illustration of the key elements of system and subsystem abstraction that are needed for input into the performance assessment models. The probability of volcanism, the focus of this IRSR, is a key element for evaluating the significance of direct release on repository performance.

If igneous activity were to resume in the YMR, there are four possible outcomes: (i) the activity would not intersect the repository and would have no effect on repository performance; (ii) such activity would result in features and processes that would not directly intersect the repository, but would have indirect effects on the repository; (iii) the igneous features would directly intersect the repository, have direct and indirect effects on the repository, but a volcano would not form within the repository boundary, and (iv) basaltic volcanic activity would directly intersect the repository, and both directly and indirectly affect repository performance.

The most probable outcome of basaltic igneous activity in the YMR would be outcome (i); there would be no effect on repository performance. It is believed that as a result of outcome (ii), the results of such features as dikes modifying the groundwater flow system (modification of both unsaturated (UZ) and saturated (SZ) flow, Figure 1), or dikes and/or sills changing the thermal regime and possibly resulting in release of volcanic gases that could result in degradation of the waste package/waste form and modification of the geochemistry of the system (effects on waste package corrosion, Figure 1) would have relatively minor consequences. Outcome (iii) could occur either solely through intrusive activity developing features that directly intersect

TOTAL SYSTEM

REPOSITORY PERFORMANCE
(Individual Dose or Risk)

SUBSYSTEMS

ENGINEERED SYSTEM

GEOSPHERE

BIOSPHERE

(Intermediate calculations of key contributors to system-level performance)

COMPONENTS OF SUBSYSTEM

Engineered Barriers

UZ Flow and Transport

SZ Flow and Transport

Direct Release and Transport

Dose Calculation

KEY ELEMENTS OF SUBSYSTEM ABSTRACTIONS

- WP corrosion (temperature, humidity and chemistry)
- mechanical disruption of WPs (seismicity, faulting, rockfall and dike intrusion)
- quantity and chemistry of water contacting WPs and waste forms
- radionuclide release rates and solubility limits

- spatial and temporal distribution of flow
- distribution of mass flux between fracture and matrix
- retardation in fractures in the unsaturated zone

- flow rates in water-production zones
- retardation in water-production zones and alluvium

- volcanic disruption of waste packages
- airborne transport of radionuclides

- dilution of radionuclides in ground water (well pumping)
- dilution of radionuclides in soil (surface processes)
- location and lifestyle of critical group

Figure 1. Flowdown diagram for total system performance assessment.

the repository causing thermal, mechanical, and chemical changes to the repository, waste package, and waste form or by development of a volcano outside the repository boundary with the associated dikes intersecting the repository causing the same effects. Such an outcome could increase waste package/waste form degradation by corrosion, mechanical disruption or changing the quantity and chemistry of water contacting the waste packages and waste form allowing more rapid release of radionuclides, and could locally modify the UZ and SZ flow systems (Figure 1). Waste material could be brought to the surface by a dike, but in this case the material would be incorporated into the lava, and although it would be available for leaching and erosion, for all practical purposes, the waste material would be immobilized, and the only potentially significant health effect would be through direct exposure to an individual in the vicinity of the dike or associated flows. Scoping calculations are planned to evaluate outcomes (ii) and (iii).

The fourth outcome, intersection of the repository by a volcano with resulting direct release of the material to the accessible environment, is the scenario that the NRC has spent the most time analyzing, as it appears to be the most significant from a dose- or risk-based perspective. This is illustrated by the Direct Release path on Figure 1. The emplacement of basaltic magma (i.e., molten rock) in or through a high-level radioactive waste repository introduces thermal, mechanical, and chemical loads on engineered and surrounding geologic systems that are difficult to evaluate. Basaltic magma can be generally described as a material with a temperature of about 1,100 °C, density around 2,600 kg m⁻³, viscosities between about 10–100 Pa s, and a chemical composition that produces acidic gases in addition to very low oxygen fugacities (roughly 10 log units below atmospheric conditions). During initial dike ascent or lava flow through open drifts, magma velocities will be on the order of 1 m s⁻¹. Flow velocities in the magma conduit, however, can reach 100 m s⁻¹ once a volcano is established at the surface. There has been little quantitative evaluation of the effect of these thermal, mechanical, and chemical loads on the engineered repository systems. All previous total system performance assessments (TSPA) sponsored by DOE (Link, et al., 1982; Barnard, et al., 1992; Barr, et al., 1993; Wilson, et al., 1994) have assumed that a waste package fails upon contact with basaltic magma. This assumption appears reasonable, based on current information, but will be re-evaluated as new data or models become available.

The consequences of the extrusive component of basaltic volcanic activity are governed by two primary processes and associated assumptions. First, radioactive waste is incorporated into the ascending magma under the physical conditions outlined in the preceding paragraph. Particle diameter is a critical parameter because of the difficulty in transporting dense spent-fuel (about 10,000 kg m⁻³) in viscous, ascending 2,600-kg m⁻³ basaltic magma. Although spent-fuel pellets are originally 1 cm diameter, they are highly fractured and have average particle diameters on the order of 1 mm (Jarzempa and LaPlante, 1996). These spent-fuel grains are relatively friable and under tests in which spent fuel is subject to simple physical disruption (impact from a steel plate) degrade to an average particle diameter of 0.001–0.01 mm. during disruptive events (Ayer, et al., 1988). In addition, during heating, oxidation of the fuel proceeds rapidly to U₃O₈, producing micron size particles (Einzigler, et al., 1992). Under the thermal and physical conditions of a volcanic event, it appears reasonable to assume that the spent fuel can degrade to the millimeter to micron size. The NRC model, discussed in Section 3.4, assumes that small waste particles will be incorporated into larger ash particles (Jarzempa, et al., 1997). The second primary process concerns transport and dispersal of contaminated tephra to

subaerial locations. Only traces remain of the distributed tephra erupted from YMR volcanoes, requiring comparison with analog volcanoes to determine suitable dispersal characteristics (e.g., Connor, 1993). Historically active basaltic volcanoes are capable of dispersing tephra particles >0.1-mm diameter at least 30 km from the vent, resulting in 1- to 100-mm thick deposits (Hill, et al., 1996). Based on the highly-fragmented character of some Quaternary YMR volcanoes (Crowe and Perry, 1991; Crowe, et al., 1995; Hill, 1996), YMR volcanoes were potentially capable of transporting material these distances. A repository-disrupting volcano would likely be capable of directly transporting some amount of high-level waste at least 30-km downwind. Basaltic volcanism, thus, appears capable of breaching waste canisters, incorporating some finite amount of spent fuel, and potentially transporting some portion of the incorporated spent-fuel to likely inhabited regions (e.g., Link, et al., 1982).

3.2 Relationship of Subissues to DOE'S Repository Safety Strategy

The IA KTI has been defined by NRC as "predicting the consequence and probability of igneous activity affecting the repository in relationship to the overall system performance objective." This definition is a comparable but broader definition than the hypothesis evaluated in the DOE RSS that "volcanic events within the controlled area will be rare and the dose consequences of volcanism will be too small to significantly affect waste isolation." As the majority of the NRC effort has been directed toward understanding the effects of volcanic activity, the differences in the focus of the two programs has been minor. The probability and consequence subissues of the overall issue are directly incorporated in both the NRC issue and the DOE RSS.

3.3 Consideration of Igneous Activity in Previous Performance Assessments

3.3.1 Link, et al., 1982

Link, et al., 1982, provides the most detailed analysis of the effects of igneous activity on a site in the YMR. This report considered thermal effects from a dike, the effects of dispersion of radioactive waste particles, and carried the analysis through ingestion, exposure and dose. While the input values, assumptions, and methodology are outdated, the report does provide a good first approximation of the relative contributions of the various possible exposure scenarios on overall dose. Volcanism was assumed to occur through development of a dike that localized into a volcanic vent within the repository. The probability assumed in the report for disruption of the repository by the dike was 2.9×10^{-6} /year.

3.3.2 TSPA 91

In TSPA 91 (Barnard, et al., 1992), the effects of igneous activity were modeled as a dike, which localized into a volcano, intersecting the repository. The probability of the dike intersection was 2.4×10^{-4} in 10,000 years. This probability is within the low end of the general range that NRC considers representative for a volcano erupting through a repository. However, this analysis was based on the remanded EPA standard. Therefore, the consequence analysis was only concerned with transporting waste to the "accessible environment" (the ground surface), rather than to a "critical group." Nevertheless, the values used to represent the incorporation or the entrainment of waste moved to the surface (i.e. the relative relationship of waste volume to magma volume) did not reflect values that are representative of the expected conditions in the YMR.

For example, the TSPA analysis assumed a mean entrainment factor of 0.03%. Since there is no actual data on "waste" entrainment in magma, a practical approach is to assume that the entrainment of lithic fragments in magma in the YMR provides a reasonable approximation. Crowe, et al., 1986, performed such an analysis with respect to materials from Lathrop Wells. That study found that for "normal" eruptive sequences, an average value for the entrainment of lithic fragments was approximately 1%, and that values for "hydrovolcanic" sequences reached 17%. While other values for other regions can be found in the literature, the work by Crowe, et al., 1986, is the only published report with data for volcanoes in the YMR. Consequently, the use of .03% in TSPA 91 instead of the values reported by Crowe, et al., 1986, appears to substantially underestimate entrainment, and if so, could result in underestimating consequences by approximately two orders of magnitude.

3.3.3 TSPA 93

In TSPA 93 (Wilson, et al., 1994), there was no new analysis beyond what was performed in TSPA 91 with respect to the effects of a direct volcanic eruption through a repository. TSPA 93 concentrated on the indirect effects caused by the intrusion of a dike into the repository. The analysis was such that the dike was constrained from intersecting waste canisters. Therefore, the consequence analysis was only concerned with the effects of temperature and magmatic gases on repository performance. In the analysis, probability values from 1.0 to 1.8×10^{-4} per 10,000 years were used. These values are at the extreme low end of those values that NRC considers reasonable for direct volcanic disruption.

As discussed in Section 4.1.6.3, the probability of indirect disruption by the intrusion of a dike into the repository is necessarily higher than the probability of direct volcanic disruption. Therefore, the probability values used in TSPA 93 are low. According to Conway, et al., 1997, the probability of dike intrusion into the repository is two to five times the probability of direct volcanic eruption through a repository. While NRC considers this probability value low, the results of TSPA 93 suggest that the releases due to these indirect effects would be much less than releases from direct effects.

3.3.4 NRC Iterative Performance Assessment Phase 2 - 1995

In the NRC Iterative Performance Assessment Phase 2 (IPA Phase 2), volcanism was modeled as a dike intersecting the repository. To simulate the effects of direct disruption, 4 percent of the material intersected by a dike was assumed to be released to the atmosphere. While the methodology was extremely simplistic, the results did suggest that: (i) the effects of direct release through volcanism could make a discernable difference in the expected releases in the tails (low probability) portion of the distribution function, and (ii) the effects of igneous processes other than direct volcanic release will probably have a very minor effect on overall dose or risk.

These calculations have been used to revise NRC's TSPA code (i.e., TPA-3, Manteufel, et al., 1997) and evaluate dose sensitivity to variations in key igneous activity parameters.

3.4 NRC/CNWRA SENSITIVITY STUDIES

Dose calculations for basaltic volcanic activity are in progress and will be completed in FY98. These calculations have been used to revise NRC's TSPA code (i.e., TPA-3, Manteufel, et al., 1997) and evaluate dose sensitivity to variations in key igneous activity parameters. Preliminary dose calculations were performed in early FY96, however, to evaluate the possible impacts on repository performance associated with basaltic volcanism (Jarzempa and LaPlante, 1996; Jarzempa, et al., 1997; Hill, 1997). More recently, as a result of ongoing sensitivity analysis, more detailed calculations have been performed. The results of these calculations are presented in Figure 2. These calculations had the following basic assumptions:

- Critical group located 20 km south of repository
- Volcanic eruption occurs through repository between +200 and +10,000 yr post-closure
- One to 10 canisters fail and all waste (10-100 MTU) is available for magmatic transport
- Wind blows to south towards critical group 14 percent of the time
- Waste particle diameters are between 0.01–10 mm
- NRC TPA 3.0 approach (Manteufel, et al., 1997) used for dose calculations
- Eruption power and duration (column height, eruption rate, mass), column shape, time, wind speed, and tephra diameter are uncorrelated random variables.

Using these parameters and 100 simulations, mean annual peak dose at 20 km south of the proposed repository site due solely to basaltic volcanism via an air pathway, assuming volcanism occurs, results in a conditional mean dose of 3.6 rem yr⁻¹ (See Figure 2).

Although this analysis is ongoing, preliminary indications are that dose is most sensitive to ash diameter, wind direction, conduit diameter, and wind speed. One of the more interesting results of this analysis is that, within the range of eruptive energies considered reasonable for the YMR, relatively low energy eruptions result in higher doses than more energetic eruptions if a dose to a critical group is the basis for the standard. While this at first seems counter-intuitive, it must be realized that although more energetic eruptions may result in release of more waste material, the wider dispersion of material would dilute the dose to a critical group. An additional finding is that the resuspension factor assumed in the dose conversion model appears very important, as there is almost a direct relationship between dose and resuspension factor. Therefore, while dose conversion factors are analyzed outside the IA KTI, additional work is being performed on resuspension and mass loading factors to ensure a reasonable range is being assumed in the various models.

The additional effects of intrusion on repository performance have not been evaluated in detail. These effects, however, will likely result in early failure of some fraction of the waste package inventory (e.g., Wilson, et al., 1994). Dose to affected individuals related to intrusive effects will occur through normal hydrologic flow and transport processes. The risk associated with

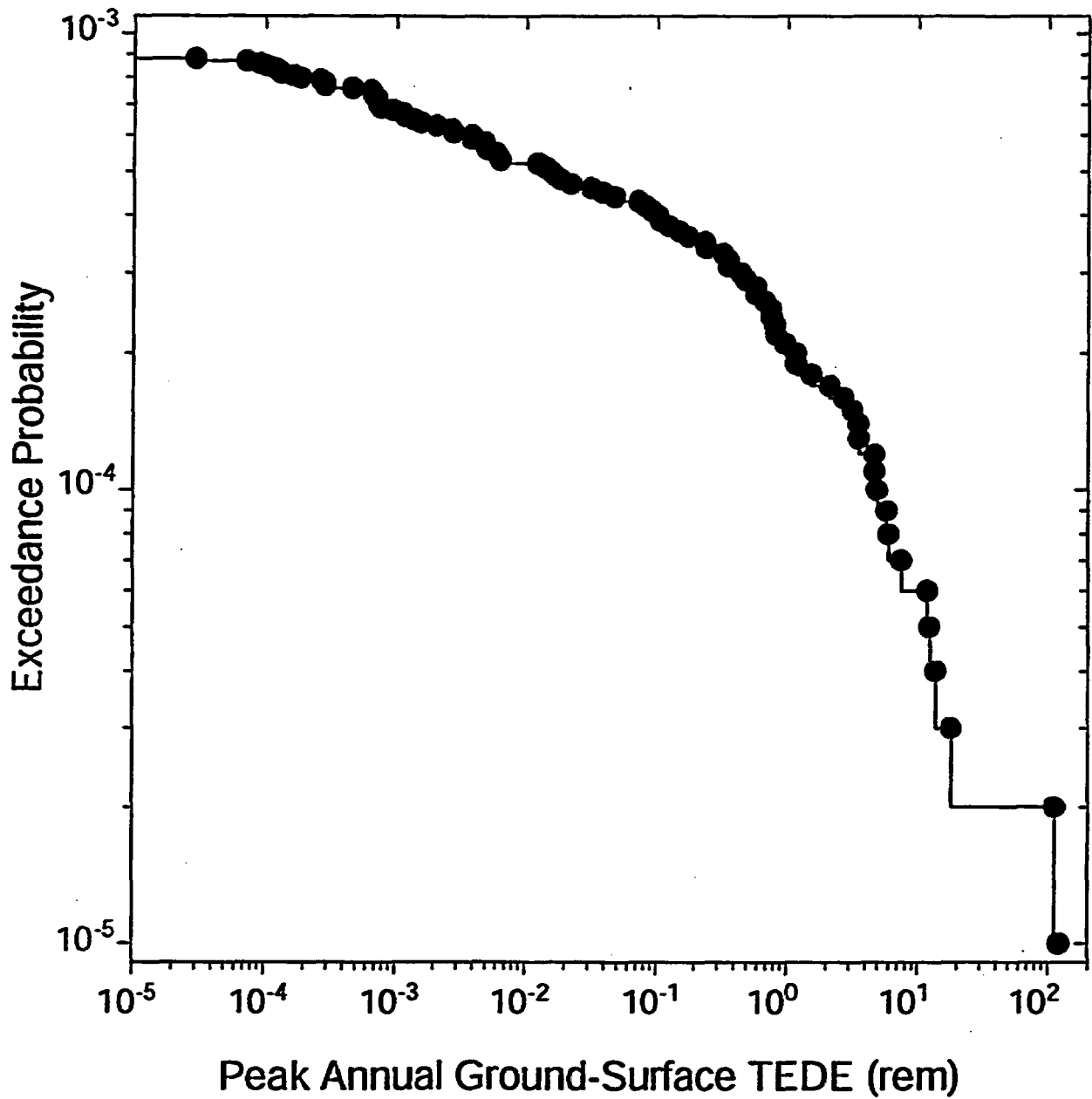


Figure 2. CCDF for volcanism disruptive scenario, all parameters sampled from ranges, receptor location 20 km south of repository, 10,000 yr performance period.

basaltic volcanic activity is calculated by simply multiplying the probability of occurrence times the conditional preliminary dose. Using this methodology with a 10^{-3} probability of volcanic disruption over 10,000 yr, the mean risk from basaltic volcanic activity from this preliminary calculation is estimated at 3.6 mrem. It must be re-emphasized that this preliminary value solely results from the contribution of the air transport pathway. It does not include any contribution from the groundwater pathway as a result of igneous activity disrupting the repository, resulting in premature failure of some portion of the waste packages, or the other potential thermal, mechanical, and chemical effects on the repository. In addition, contributions to the dose from leaching of radionuclides from volcanic materials that were brought to the surface through volcanic activity and then transported down to the groundwater have not been included. The total dose that would occur during a volcanism scenario would, thus, be the summation of the direct air dose, the secondary contribution from such things as leaching of surface materials, and the dose expected via normal groundwater pathways.

To date, NRC has only analyzed the probability of volcanic activity affecting the repository. As is stated later (for example, Section 4.1.6.3.3), available information allows only a crude approximation of probability values for the other igneous scenarios. By the same token, preliminary consequence analysis has been performed only for the ash fall portion of this scenario. During FY98, the staff will be continuing to work on the consequences of direct volcanic disruption of the repository. Effort in future years will first be directed on determining the consequences of an intrusion in the repository to determine if the preliminary indications that these effects are minor are correct. If so, NRC does not consider that additional effort on the probability of intrusion is necessary. As discussed in Section 4.1.6.3, NRC will be using an interim probability value of 2 to 5 times the probability of volcanic disruption (Conway, et al., 1997) to evaluate intrusive effects at the repository.

4.0 REVIEW METHODS AND ACCEPTANCE CRITERIA

Review methods and acceptance criteria are listed for the probability subissue. Detailed technical bases are presented in subsequent subsections to support these acceptance criteria and review methods. These technical bases address the most significant topics for resolution of the probability subissue, including reviews of relevant work and newly-developed models that provide an independent technical basis for resolution.

4.1 PROBABILITY

DOE will need to estimate the probability of future volcanic eruptions and igneous intrusions affecting the performance of the proposed repository. Staff will review DOE assumptions made in estimation of the probability of volcanic eruptions and igneous intrusions for consistency with known past igneous activity in the YMR and to determine if the analysis and assumptions do not underestimate effects. The following nine acceptance criteria apply to the probabilistic assessment of igneous hazards.

Estimates of the probability of future igneous activity in the YMR will be acceptable provided that:

- (1) The estimates are based on past patterns of igneous activity in the YMR,
- (2) The definitions of igneous events are used consistently. Intrusive and extrusive events should be distinguished and their probabilities estimated separately.
- (3) The models are consistent with observed patterns of volcanic vents and related igneous features in the YMR.
- (4) Parameters used in probabilistic volcanic hazard assessments, related to recurrence rate of igneous activity in the YMR, spatial variation in frequency of igneous events, and area affected by igneous events are technically justified and documented by DOE.
- (5) The models are consistent with tectonic models proposed by NRC and DOE for the YMR.
- (6) The probability values used by DOE in performance assessments reflect the uncertainty in DOE's probabilistic volcanic hazard estimates.
- (7) The values used (single values, distributions, or bounds on probabilities) are technically justified and account for uncertainties in probability estimates.
- (8) If used, expert elicitations were conducted and documented, using the guidance in the Branch Technical Position on Expert Elicitation (NRC, 1996), or other acceptable approaches.

- (9) The collection, documentation, and development of data and models have been performed under acceptable QA procedures, or if data was not collected under an established QA program, it has been qualified under appropriate QA procedures.

The following sections present the review methods, technical basis, and status of resolution of these criteria. These technical bases represent a summary of relevant information used to evaluate the status of the subissue.

4.1.1 Probability Criterion 1

4.1.1.1 Acceptance Criterion

Estimates of the probability of future igneous activity in the YMR will be acceptable provided that:

- The estimates are based on past patterns of Igneous Activity in the YMR.

4.1.1.2 Review Method

During its review, staff should ascertain the adequacy and sufficiency of DOE characterization and documentation of past igneous activity, including the remaining uncertainties about the distribution, timing and nature of this past igneous activity. At a minimum, documentation of past volcanic activity should encompass the Yucca Mountain-Death Valley isotopic province of Yogodzinski and Smith (1995) since the cessation of large-volume silicic volcanism in the region at approximately 11 Ma. Particular attention should be given to assuring that the locations, ages, volumes, geochemistry, and geologic settings of <6-Ma basaltic igneous features, such as cinder cones, lava flows, igneous dikes, and sills, are adequately documented. Staff should determine that DOE used geological and geophysical information relevant to past volcanic activity contained in the literature (e.g., references in Appendix A).

4.1.1.3 Technical Basis

Acceptable probability models use past patterns of YMR igneous activity to estimate probabilities of future igneous events. Current models in the available literature for the spatial and temporal recurrence of basaltic volcanism rely on probabilistic methods (e.g., Ho, 1991; Kuntz, et al., 1986; McBirney, 1992; Wadge, et al., 1994; Connor and Hill, 1995). In these models, patterns of future activity are primarily estimated from patterns of past volcanic activity, including eruption location, frequency, volume, and chemistry. In addition, geologic processes, particularly structural deformation, have been investigated as partially controlling the distribution and timing of volcanism (Bacon, 1982; Parsons and Thompson, 1991; Connor, et al., 1992; Lutz and Gutmann, 1995; Conway, et al., 1997). Probabilistic models of volcanism at the proposed repository site should be consistent with rates and timing of past volcanism and with observations made in the YMR and other volcanic fields, regarding the relationship between igneous activity and other tectonic processes.

Basaltic igneous activity has been a characteristic of the Western Great Basin (WGB) in Nevada and California since about 12 Ma (e.g., Luedke and Smith, 1981). Although much of

this activity has occurred near the boundaries of the WGB since 10 Ma (Figure 3), distributed volcanism between Death Valley, Yucca Mountain, and the Reville Range is a well-recognized feature of the WGB (e.g., Carr, 1982). Basaltic volcanism, however, is localized in specific areas of the WGB and often shows regular spatial shifts through time (Connor and Hill, 1994). Many of the WGB basaltic volcanic fields exhibit clear spatial and temporal boundaries to igneous activity. In contrast, diffuse basaltic volcanism in the YMR is distributed over a relatively large area with often ambiguous spatial and temporal bounds (Figure 3).

Defining the spatial and temporal extent of the YMR magma system is the first step in quantifying patterns of igneous activity for use in probability models. Quantitative criteria, however, do not clearly define the extent of the YMR basaltic volcanic system in space and time. For example, to date, petrogenetic relationships between <6-Ma and 6–11-Ma basalts are ambiguous, as similar composition basalts occur within each interval of time. Isotopic geochemical characteristics are distinct for \leq 6-Ma basalts located within 40 km of the proposed repository site, which is a distance that encompasses the main YMR system. Some \leq 6-Ma basalts within 90 km south and west of the proposed repository site, however, have the same distinct compositional characteristics and, thus, may be part of the YMR volcanic system.

Numerous attempts to define the extent of the YMR basaltic volcanic system have been based on qualitative to semi-quantitative criteria. Early workers (Vaniman, et al., 1982; Crowe, et al., 1982) concluded that basalts younger than about 9 Ma were petrologically distinct from 9- to 11-Ma basalts and, thus, constitute the igneous system of interest. Subsequent work (Crowe, et al., 1983; 1986) generally confirmed this interpretation; however, many analyzed Plio-Quaternary basalts have petrogenetic characteristics similar to some 9- to 11-Ma basalts (i.e., Crowe, et al., 1986). Crowe and Perry (1989) used similar petrogenetic arguments to define the Crater Flat Volcanic Zone (CFVZ), which is a northwest-trending zone based on the occurrence of <5-Ma volcanoes between Sleeping Butte and buried volcanoes in the Amargosa Desert (Figure 4). Smith, et al., (1990) expanded the CFVZ to include Buckboard Mesa. Numerous other subdivisions are possible, based on the pattern of <5-Ma basaltic volcanoes (e.g., Crowe, et al., 1995; Geomatrix, 1996).

Isotopic geochemical characteristics commonly are used to define the extent of basaltic igneous systems (e.g., Leeman, 1970; Farmer, et al., 1989). Isotopes of Sr and Nd are distinct for \leq 6-Ma basalts located within 50 km of the proposed repository site (Farmer, et al., 1989; Yogodzinski and Smith, 1995; Hill, et al., 1996). In addition, Pliocene basalts in the Grapevine Mountains, Funeral Formation, and southern Death Valley (Figure 4) also share these distinctive isotopic characteristics. These more distal basalts, however, are located in significantly different tectonic regimes than the YMR. Crustal tectonics likely influence magma ascent and eruption rates (e.g., McKenzie and Bickle, 1988). Although the distal basalts may have originated from a compositionally-similar mantle, differences in tectonic history or crustal lithologies may have resulted in spatial and temporal controls on basaltic volcanism that are significantly different from the YMR. Figure 4 shows the extent of basalts that are potentially part of the YMR igneous system, based on temporal, spatial, and geochemical affinities. Although a range of geochronological techniques has been utilized in the YMR to date Quaternary basaltic features, most basalts older than about 1 Ma have been dated using standard K-Ar and $^{40}\text{Ar}/^{39}\text{Ar}$ methods (Hill, et al., 1993). These data are compiled in Appendix A and are used in subsequent probability analyses.

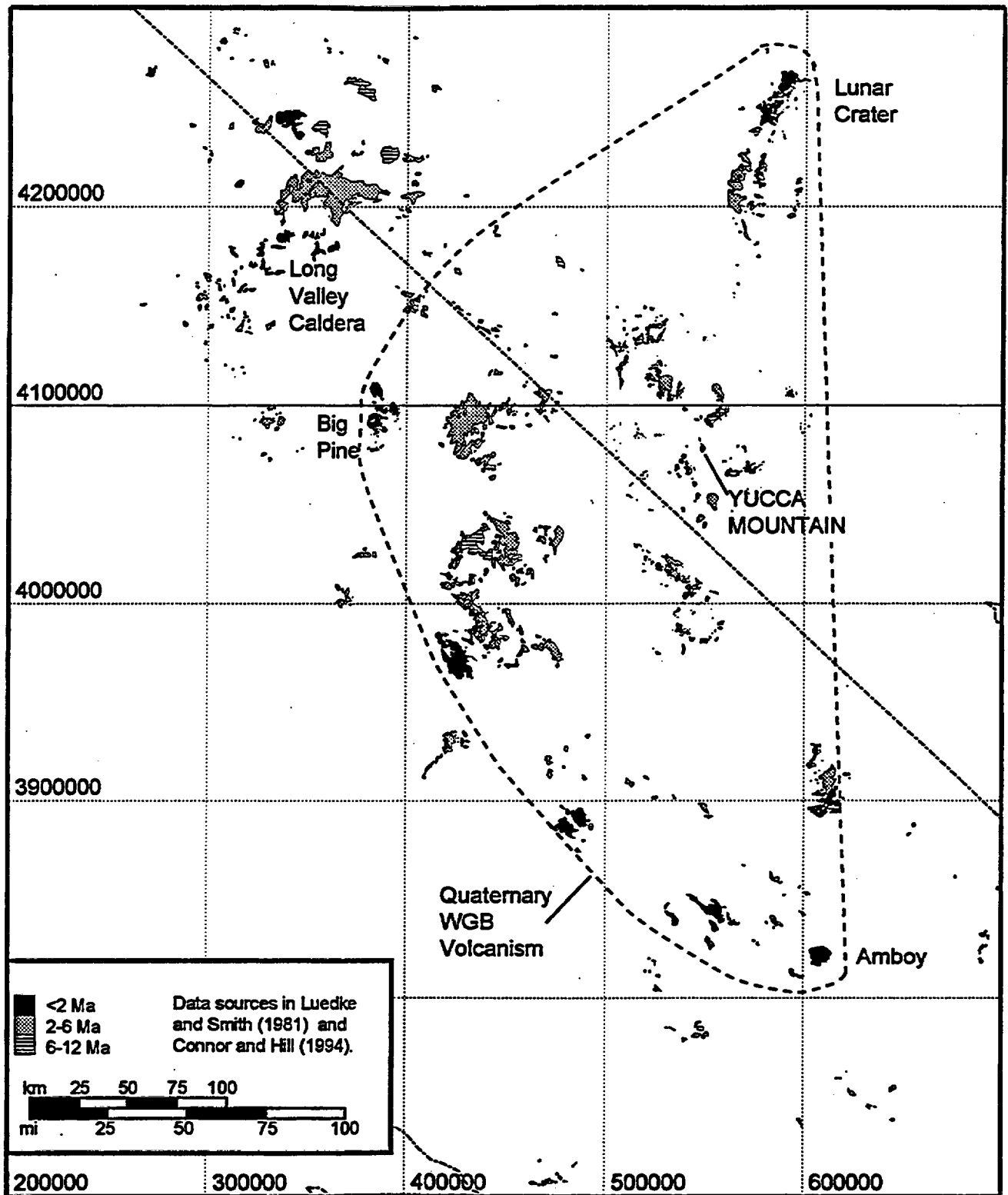


Figure 3. Basaltic volcanic rocks of the Western Great Basin since about 12 Ma, from Luedke and Smith (1981) and references in Connor and Hill (1994) and Appendix A. Dashed area represents zone used to calculate background Quaternary volcano recurrence rates, which does not encompass the Long Valley Caldera magmatic system. Coordinates in Universal Transverse Mercator meters, Zone 11, NAD27.

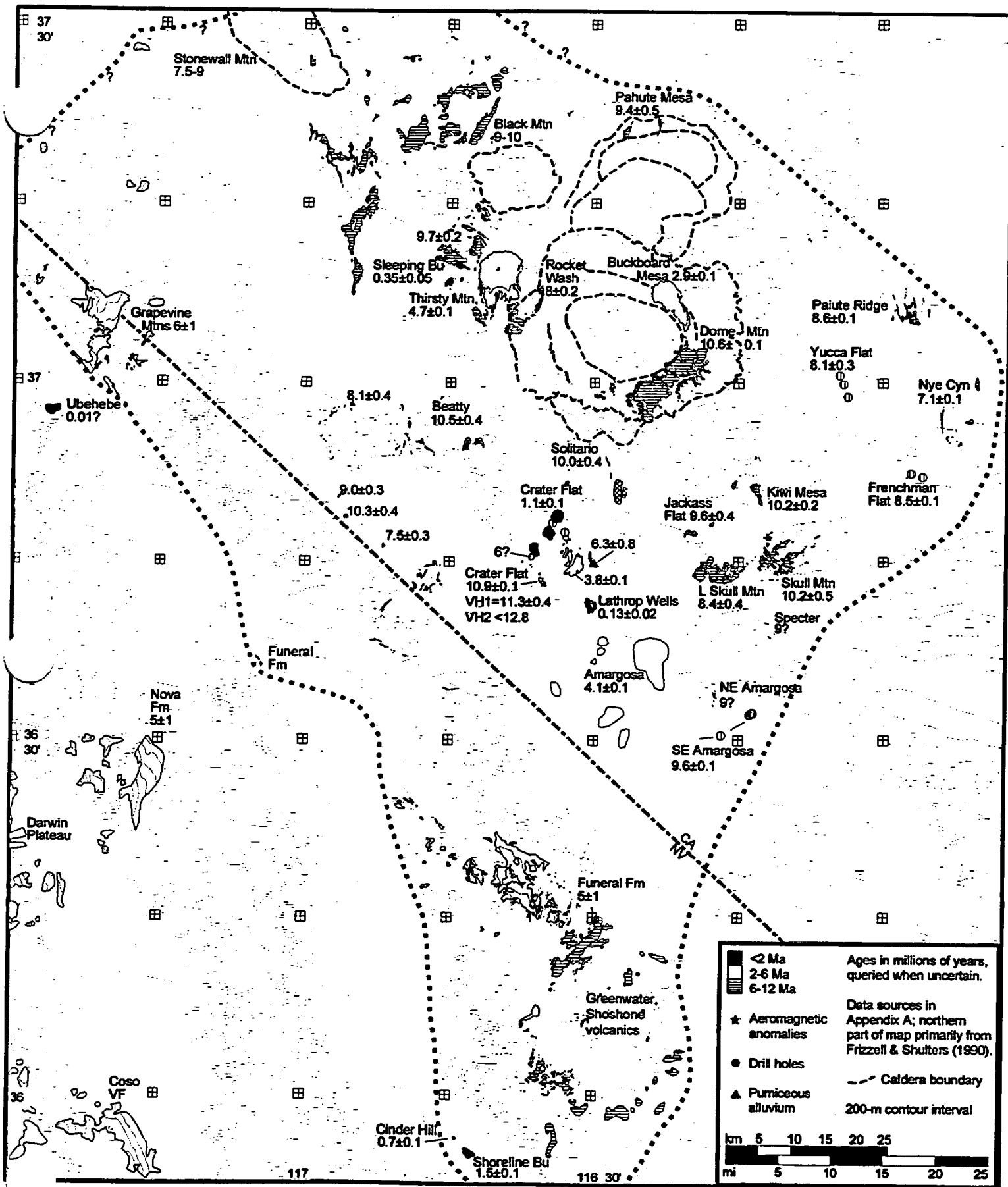


Figure 4. Basaltic volcanic rocks of the Yucca Mountain region since about 11 Ma. Data sources listed in Appendix A. Dotted line represents the extent of basaltic volcanic rocks that potentially constitute the Yucca Mountain region magma system.

The extent of the YMR magmatic system was also considered during the DOE-sponsored formal expert elicitation (Geomatrix, 1996). This report utilized areas that generally encompassed about the same general region as that shown on Figure 4. However, more extensive regions were often included in the background or regional recurrence rate estimates. In general, the report concluded that the <5 Ma basalts were most important to define temporal recurrence rates for the YMR. However, it appears from Geomatrix, 1996, that petrographic data and models were not used to define spatial patterns or process models. It also is not clear why the 5-11 MA volcanics were not considered by all experts to define spatial patterns or derive process models. As a result, the areas used for the regional recurrence rate estimates do not appear to be well supported by the petrographic data and models.

The significance of basaltic centers >40 km from the site to probability issues depends on the model being evaluated. Probability models that depend heavily on the timing of past events (e.g., Ho, 1992) are strongly affected by inclusion of these centers in the YMR system. Depending on the time used to calculate future volcano recurrence rates, inclusion of the distal centers may substantially elevate or decrease the probability of future eruptions at the proposed repository site. In contrast, models that spatially define the extent of the system and evaluate the area of the system to the area of the proposed repository (e.g., Crowe, et al., 1982; Geomatrix, 1996) may exhibit a marked decrease in probability at the site due to expansion of the YMR system to accommodate distal volcanoes. Finally, the presence of the distal volcanic centers has little effect on spatio-temporal recurrence models (e.g., Connor and Hill, 1995), as distal centers are too old and too far away from the proposed repository site to strongly influence the locus of volcanism in Crater Flat basin.

4.1.1.4 Summary

Sufficient information exists on the spatial and temporal extent of the YMR basaltic system to support spatio-temporal probability models (e.g., Connor and Hill, 1995). Evaluation and acceptance of other models, however, requires assessment of the petrogenesis of 0.1–11-Ma basalt of the YMR. A reasonably conservative working hypothesis for these assessments is that all ≤ 6 -Ma basalt within the dashed boundaries of Figure 4 is part of the YMR igneous system. Relevant data for these volcanic centers are summarized in Appendix A. In addition, some 6–11-Ma basalt within these boundaries has the same petrogenesis as ≤ 6 -Ma basalt and, thus, may be part of the YMR igneous system of interest.

All current probability estimates for future igneous activity at the proposed repository site are based on past patterns of igneous activity in the YMR. These models are, thus, acceptable to NRC. Some parameter values or ranges used in these probability models, however, are dependent on definitions of the spatial or temporal extent of the YMR igneous system. Models that may be developed by DOE subsequent to those discussed in this report will need to be evaluated independently by NRC to assure that the parameters and definitions are internally consistent.

4.1.2 Probability Criterion 2

4.1.2.1 Acceptance Criterion

Estimates of the probability of future igneous activity in the YMR will be acceptable provided that:

- The definitions of igneous events are used consistently. Intrusive and extrusive events should be distinguished and their probabilities estimated separately.

4.1.2.2 Review Method

Staff should determine that igneous events are defined consistently by DOE and that probabilities of intrusive and extrusive igneous events are calculated separately. Definitions in current use for extrusive volcanic events include formation of a new volcano (Crowe, et al., 1982; Connor and Hill, 1995); an episode of eruptive activity at a new or existing volcano following an extended period of quiescence (Ho, et al., 1991; Bradshaw and Smith, 1994); and mappable eruptive units, each being an assemblage of volcanic products with internal stratigraphic features that indicate a cogenetic origin and eruption from a common vent (Condit and Connor, 1996). Definitions of intrusive events include injection of single, igneous dikes and formation of dike swarms (Delaney and Gartner, 1995).

4.1.2.3 Technical Basis

Although all volcanic events are associated with an intrusive event, basaltic intrusions may reach subsurface depths of less than 300 m without forming a volcano (Gudmundsson, 1984, Carter Krogh and Valentine, 1995, Ratcliff, et al., 1994). Therefore, probability calculations must distinguish between volcanic (i.e., extrusive) and intrusive events in order to be applicable in repository performance and risk assessment models.

Because recurrence rates used in many probability models are sensitive to the size, duration, and area affected by igneous events, igneous event definitions must be used consistently throughout an acceptable analysis. Furthermore, differences in igneous event definitions must be considered when comparing the results of different probabilistic hazard analyses (See Criterion 6). In addition, the method used to count igneous events affects the outcome of the probability analysis. Definitions of volcanic and intrusive igneous events commonly found in the geologic literature include:

- Individual, mappable eruptive units
- Episodes of vent or vent-alignment formation
- Emplacement of an igneous intrusion
- Volcanic eruption and accompanying dike injection

As discussed in the following section, igneous activity in the YMR can be categorized using each of these definitions with varying degrees of confidence.

4.1.2.3.1 Individual Eruptive Units

Definitions of volcanic events vary widely in the literature (Condit, et al., 1989; Bemis and Smith, 1993; Delaney and Gartner, 1995; Lutz and Gutmann, 1995; Connor and Hill, 1995). Ideally, volcanic events would correspond to eruptions. Unfortunately, subsequent geologic processes often obliterate evidence of previous eruptions from the geologic record (e.g., Walker, 1993). Consequently, volcanic events often have been defined as mappable eruptive units, each unit being an assemblage of volcanic products having internal stratigraphic features that indicate a cogenetic origin and eruption from a common vent (Condit and Connor, 1996). A simple definition that can be applied to young cinder cones, spatter mounds, and maars is based on morphology: an individual edifice represents an individual volcanic event (Connor and Hill, 1995). In older, eroded systems, such as Pliocene Crater Flat, evidence of vent occurrence, such as near-vent breccias or radial dikes, is required. One important advantage of this definition of volcanic events is its reliance on geological and geophysical mapping, with no requirement for geochronological data. Therefore, this definition can be applied with greater confidence than the other definitions, which require relatively precise geochronological data. Volcanic hazard analyses using the individual vent definition for volcanic events assume all mapped volcanic units occur as independent events. The resulting probability estimate is for direct disruption of the proposed repository by a single vent-forming volcanic eruption (e.g., Connor and Hill, 1995).

However, it should be noted that several edifices can form during an essentially-continuous basaltic, eruptive episode. For example, three closely-spaced cinder cones formed during the 1975 Tolbachik eruption (Tokarev, 1983; Magus'kin, et al., 1983). In this case, the three cinder cones represent a single, eruptive event that is distributed over a larger area than represented by a single cinder cone. The three 1975 Tolbachik cinder cones have very different morphologies and erupted adjacent to three older (Holocene) cinder cones (Braytseva, et al., 1983). Together, this group of six cinder cones forms a 5-km-long, north-trending alignment. Without observing the formation of this alignment, it likely would be difficult to resolve the number of volcanic events represented by these six cinder cones if the number of volcanic events was defined as the number of eruptions. This type of eruptive activity raises uncertainties about how a number of volcanic events represented by individual volcanoes should be assessed, even where these volcanoes are well-preserved.

Geochemical and apparent geochronological variations present at some YMR Quaternary volcanoes have been interpreted as reactivation of individual volcanoes after more than 10,000-yr quiescence (Wells, et al., 1990; Crowe, et al., 1992; Bradshaw and Smith, 1994). Results from paleomagnetic studies, however, appear to contradict this interpretation (Champion, 1991; Turrin, et al., 1991) and cast doubt on the likelihood that cinder cones in the YMR have reactivated long after their original formation (Whitney and Shroba, 1991; Wells, et al., 1990, 1992; Turrin, et al., 1992; Geomatrix, 1996). Given the possibility of cinder cone reactivation, the number of volcanoes present in the YMR may underestimate the rate of future YMR volcanic eruptions. In the context of volcanic hazards for the proposed repository, however, the spatially dispersed character of volcanism is extremely important in calculating the probability of occurrence, whereas the reactivation of an existing cinder cone is more important in determining consequence of the activity. Thus, reactivation of cinder cones is interesting as a

gauge of overall activity in the volcanic system, but is not easily related to rates of new volcano formation.

4.1.2.3.2 Episodes of Vent or Vent-Alignment Formation

Additional investigations in other volcanic fields have demonstrated that some cinder cone alignments develop over long periods of time during multiple episodes of volcanic eruption (Connor, et al., 1992; Conway, et al., 1997), particularly where a large fault controls the locations of basaltic vents. For example, Conway, et al. (1997) found that the northern segment of the Mesa Butte fault zone in the San Francisco volcanic field, Arizona, repeatedly served as a pathway for magma ascent for at least 1 m.y. and formed a 20-km-long cinder cone alignment (Figure 5). Isochron dates reported in Conway, et al. (1997) indicate volcanism along the northern Mesa Butte fault was episodic, and successive episodes were separated in time by as much as 400 k.y. (Figure 6). Spatial patterns of volcanism along the Mesa Butte alignment apparently were independent of field-wide trends, indicated by the large lateral shifts in volcanic loci between successive episodes (Conway, et al., 1997). These observations help clarify trends observed in the development of young, potentially active volcanic alignments. For example, the largely Holocene Craters of the Moon volcanic field, Idaho, shows similar eruption patterns characterized by multiple episodes of magmatism and frequently-shifting loci of volcanism along the Great Rift (Kuntz, et al., 1986), albeit on a time scale of thousands of years. This behavior contrasts sharply with eruption patterns of other short-lived fissure eruptions, such as the Laki fissure eruption (Thordarson and Self, 1993) or the Tolbachik eruption of 1975 (Tokarev, 1983). Evidence of episodic volcanism along the Mesa Butte fault indicates independent magmatic episodes may recur along geologic structures even following periods of quiescence lasting 100 k.y. or more. Volcano alignments in the YMR, such as the Amargosa Aeromagnetic Anomaly A alignment (Connor, et al., 1997), thus, may constitute multiple volcanic events.

Paleomagnetic (Champion, 1991) and radiometric dating (Appendix A) of the Quaternary Crater Flat cinder cones (Figure 7) suggests these cinder cones may have formed during a relatively brief period of time (<100,000 yr) and, therefore, may represent a single, eruptive event like the Tolbachik alignment. Evidence from aeromagnetic and ground magnetic surveys (Langenheim, et al., 1993; Connor, et al., 1997) suggests that older buried volcanoes exist in southern Crater Flat along this alignment. Therefore, the alignment may have reactivated through time, in a manner similar to the Mesa Butte volcano alignment.

Defining aligned volcanoes of similar ages as single volcanic events effectively reduces both the total number of volcanic events in the region and the regional recurrence rate. The area affected by the entire cone alignment, however, is much greater than the areas impacted by individual cinder cones. This variation in disruption area must be propagated through the volcanic hazard analysis.

Hazard analyses defining vents and vent alignments as volcanic events are used to estimate the probability of direct disruption of the proposed repository. Primary uncertainties in those probability estimates result from uncertainty in the number and distribution of volcanic vents along alignments.

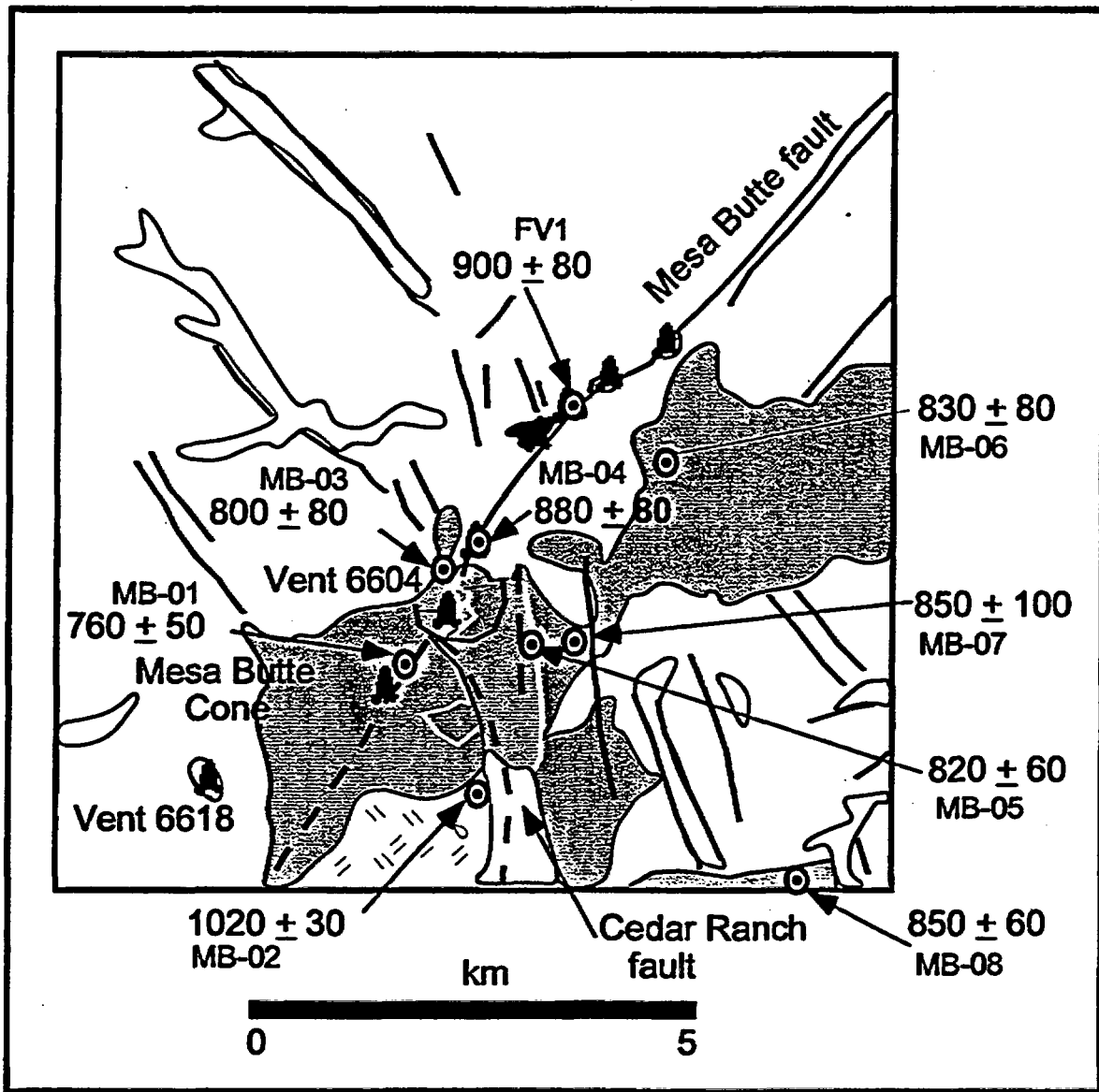


Figure 5. Development of multiple vent alignments along a fault is illustrated by the Mesa Butte alignment in the San Francisco volcanic field, Arizona. Dated cones and associated lava flows show that this 20-km-long alignment developed by repeated injection of magma along the Mesa Butte fault. Figure from Conway, et al. (1997).

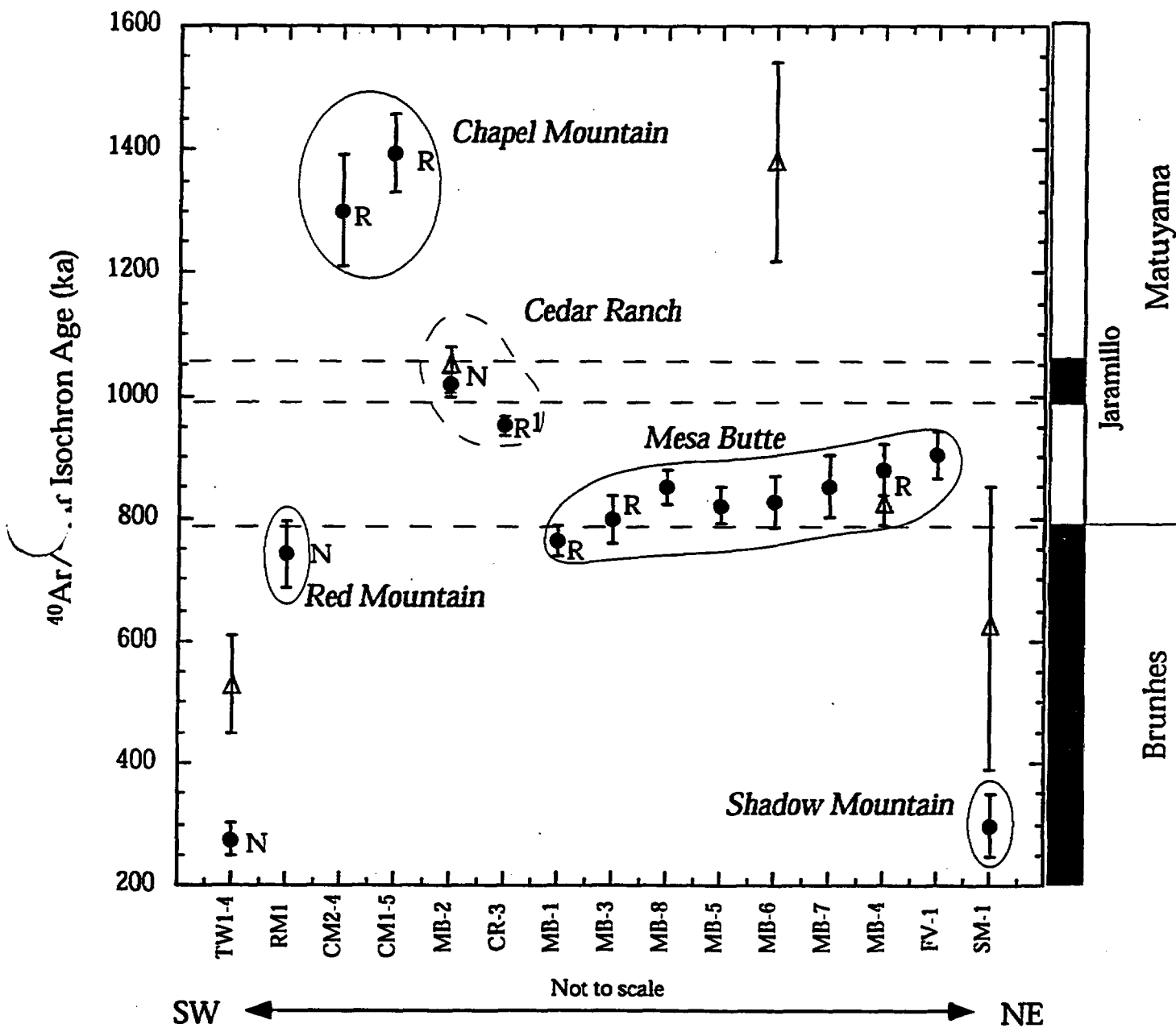


Figure 6. Detailed geochronology shows that the Mesa Butte alignment formed over a period of more than 1 m.y. through several distinct episodes of volcanism. Figure from Conway, et al. (1997).

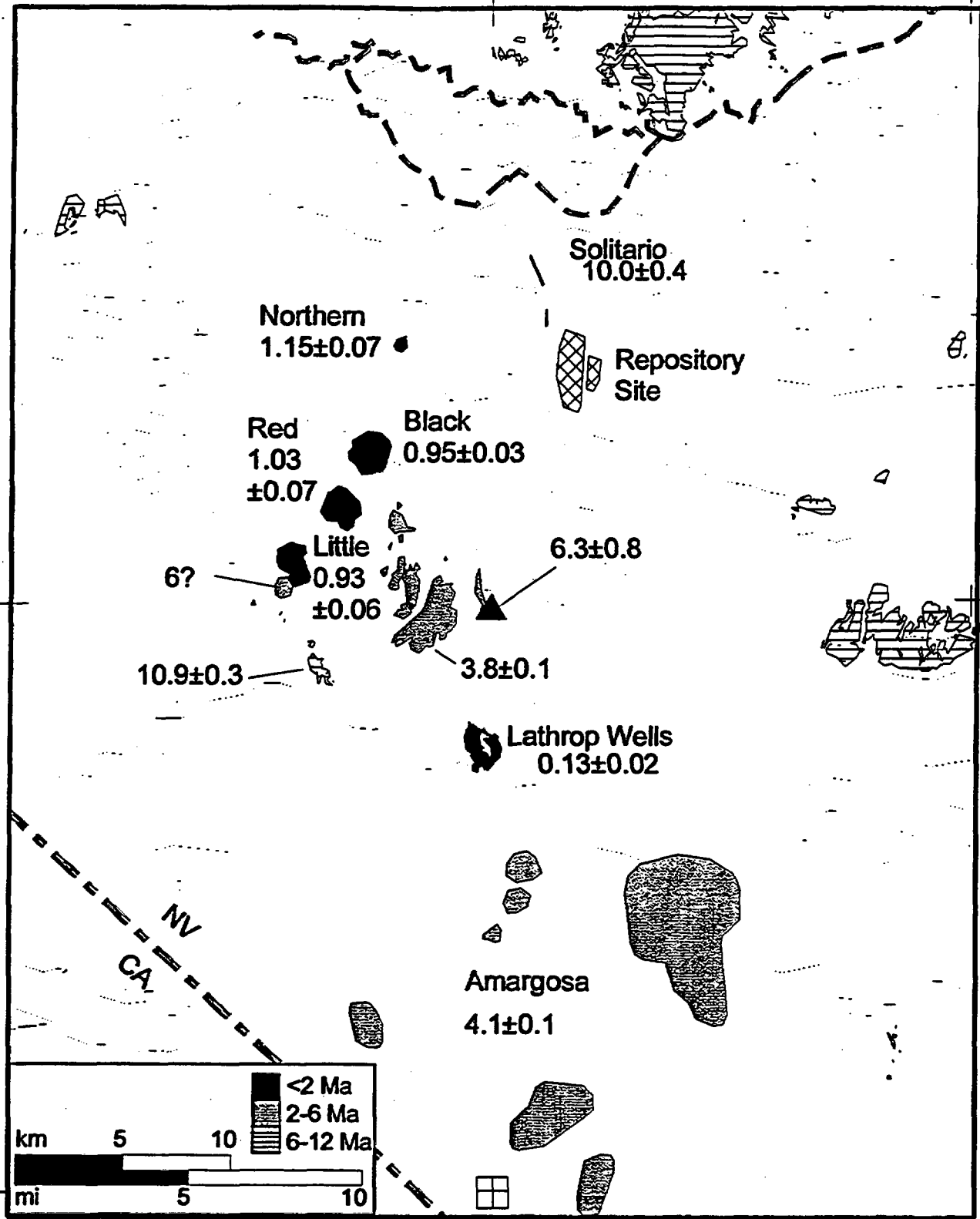


Figure 7. Basaltic volcanic rocks of the Crater Flat area, Nevada. Data sources listed in Appendix A. Extent of Amargosa Desert basalt interpreted from aeromagnetic data in Langenheim, et al. (1993) and Connor, et al. (1997).

4.1.2.3.3 Emplacement of an Igneous Intrusion

Igneous events are a broader class than volcanic events in that igneous events must encompass the intrusive and extrusive components of igneous activity. The number of mapped, igneous dikes generally is not considered a reasonable definition of an igneous event because multiple dikes often are injected into the shallow crust during single episodes of igneous intrusion. Furthermore, individual dikes frequently coalesce at lower stratigraphic levels. As a result, several mapped dikes may represent a single, igneous event. For example, Delaney and Gartner (1995) mapped approximately 1,700 individual dikes in the Pliocene San Rafael volcanic field, Utah (Figure 8). These dikes are associated with approximately 60 breccia zones and volcanic buds, which are interpreted as the roots of eroded, volcanic vents. Based on their mapping, Delaney and Gartner (1995) suggested that approximately 175 episodes of intrusion resulted in the emplacement of the 1,700 dikes and 60 volcanic vents, but also indicated that this grouping of mapped units was a subjective process.

In the YMR, the number of Plio-Quaternary igneous events is unknown. Based on analogy with the San Rafael volcanic field, YMR intrusive events may be a factor of two or more greater than the number of volcanic events (Conway, 1997). Studies in the YMR by Ratcliff, et al. (1994) and Carter Krough and Valentine (1995) have demonstrated that some Miocene basaltic, igneous intrusions stagnated within several hundred meters of the surface without erupting. These basaltic dikes and sills are mapped in Miocene tuffs, similar in character and composition to those underlying Yucca Mountain. Thus, probability estimates based on the number of igneous events characterized by this approach would encompass both direct disruption of the repository with transport of waste into the accessible environment during a volcanic eruption, and the indirect effects, such as canister failure during dike or sill intrusion. Additional complications arise with this definition based on the limited ability of a shallow dike to laterally transport entrained material into the volcanic conduit (e.g., Spence and Turcotte, 1985). A volcano may form outside of the repository boundary, with an associated subsurface dike that penetrates the repository directly. Although an intrusive, igneous event definition would indicate disruption of the repository, the ability of the waste to be transported laterally by the dike and dispersed into the accessible environment by the volcano would be extremely limited. The definition of an igneous event as encompassing both volcanic and intrusive components, while strictly correct from a geologic perspective, is unsuitable for application in risk assessments because of the dramatically-different consequences of intrusive and extrusive igneous activity. Therefore, it is best to consider only the intrusive component of igneous events under this definition, reserving extrusive components for definitions based on vents and vent alignments.

4.1.2.3.4 Volcanic Eruptions with Accompanying Dike Injection

An igneous event can be similarly defined in terms of the subsurface area disrupted by the intrusion of magma during a volcanic event. For example, numerous dikes in the San Rafael volcanic field were injected laterally through the shallow subsurface for hundreds of meters away from volcanic vents during volcanic eruptions (Delaney and Gartner, 1995). Uncertainties resulting from this definition of an igneous event include estimates of probable lengths and widths of dike zones associated with the formation of vents and the locations of vents along these dike zones (e.g., Hill, 1996). The effects of these laterally-injected dikes on performance,

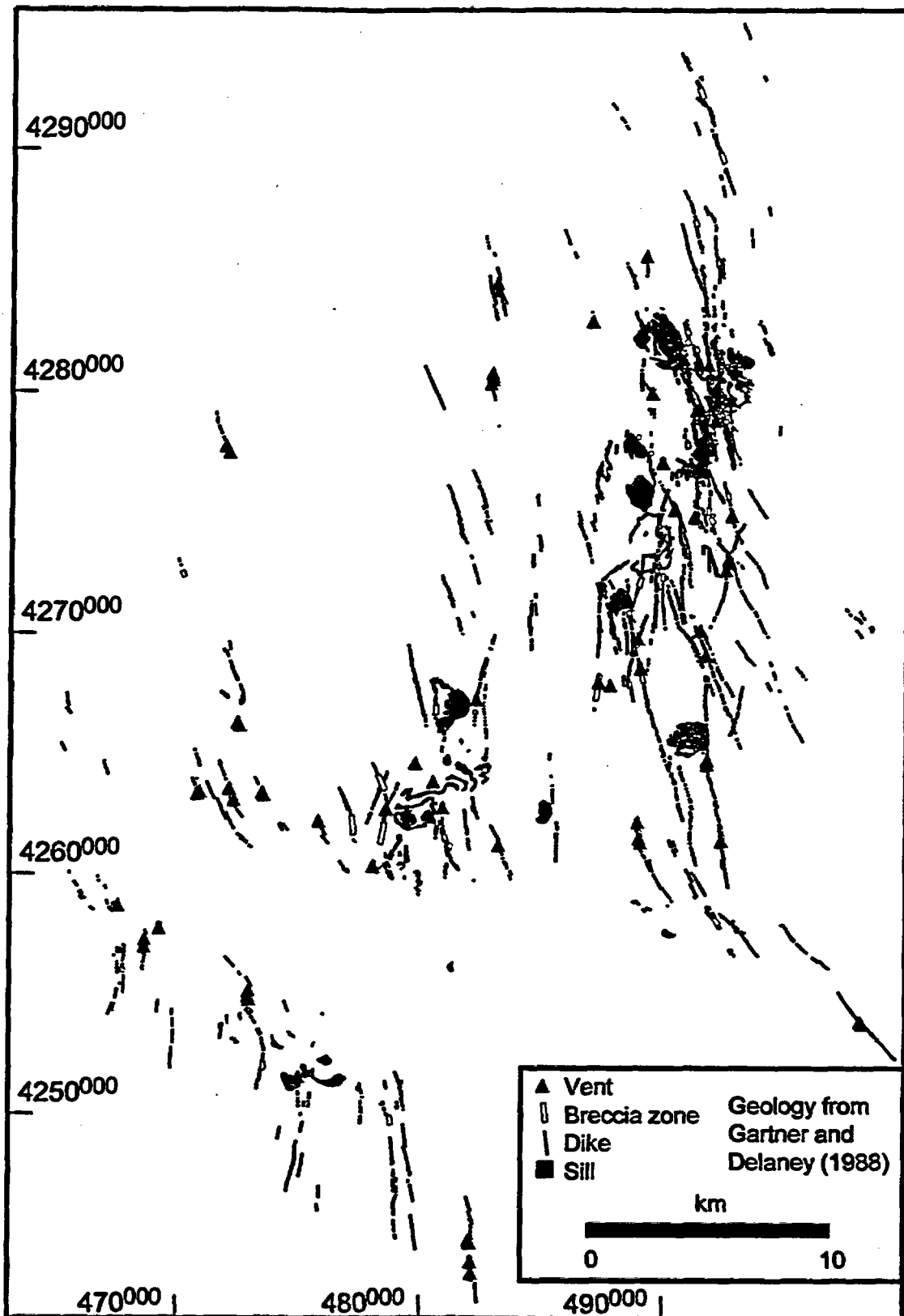


Figure 8. Distribution of dikes, breccia zones, sills, and vents in the San Rafael volcanic field, Utah. Figure from map by Gartner and Delaney (1988).

however, are substantially less than the direct effects of vent formation, because of the limited ability of the waste to be directly transported to the surface along nearly the length of the dikes when compared to the transportation ability of the volcanic vent itself.

4.1.2.4 Summary

There is no one generally-accepted criterion to singularly define an igneous event. Probability models are acceptable, provided igneous events are explicitly defined and the definition is applied consistently throughout the model. Therefore, all the above definitions can be considered acceptable. Repository performance considerations, however, require that the probability of volcanic disruption is calculated discretely from the probability of intrusive disruption. All volcanic events that may penetrate the proposed repository are accompanied by a subsurface intrusion. However, intrusive events may occur without direct volcanic disruption, either because a volcano does not form at the surface or the location of the volcano is at a distance greater than the lateral transport ability of a shallow dike. Therefore, the probability of intrusive igneous events affecting the proposed repository is at least as large as, and could be significantly larger than, the probability of volcanic disruption.

Potential intrusive and extrusive events must be considered separately because the effects on repository performance are significantly different for extrusive and intrusive processes. A volcanic, igneous event that penetrates the repository has the potential to entrain, fragment, and transport radioactive material into the subaerial accessible environment. In contrast, an intrusive, igneous event that penetrates the repository would produce thermal, mechanical, and chemical loads on engineered systems, which could impact waste-package degradation. Radioactive release associated with intrusive, igneous events is through hydrologic flow and transport, rather than through direct transport by volcanic processes. Therefore, probability calculations must distinguish between volcanic and intrusive, igneous events in order to be applicable in repository performance and risk assessment models.

4.1.3 Probability Criterion 3

4.1.3.1 Acceptance Criterion

Estimates of the probability of future igneous activity in the YMR will be acceptable provided that:

- The models are consistent with observed patterns of volcanic vents and related igneous features in the YMR.

4.1.3.2 Review Method

Staff should determine if DOE probability models are consistent with known Pliocene and Quaternary igneous events in the Yucca Mountain-Death Valley magmatic system and that the proposed probability models are consistent with patterns of igneous activity in other, comparable volcanic fields. Current interpretations indicate these patterns include a tendency for basaltic volcanic vents to cluster and form northeast-trending vent alignments in the YMR. Structural control of the locations of individual volcanoes by faults also is prevalent. Other interpretations that lead to reasonably conservative estimates of probability will be acceptable.

4.1.3.3 Technical Basis

Previous studies of volcanism in the YMR, and elsewhere, cumulatively indicate that models describing the recurrence rate, or probability of basaltic volcanism should reflect the clustered nature of basaltic volcanism and shifts in the locus of basaltic volcanism through time. Models also should be amenable to comparison with basic geological data, such as fault patterns and neotectonic stress information, that affect vent distributions on a comparatively more detailed scale. The models used to estimate future igneous activity in the YMR should either explicitly account for the following or obtain bounding estimates:

- Shifts in the locus of volcanic activity through time
- Vent clusters
- Vent alignments and correlation of vents and faults

Data from other basaltic volcanic fields may be used to test the models. Each of these spatial patterns is reviewed in this section, with emphasis on the nature of these spatial patterns in the YMR and how these compare with spatial patterns in cinder cone volcanism observed in other basaltic volcanic fields. This comparison is followed by a discussion in Section 4.1.4.3 of how these spatial patterns in volcanic activity can be used to calibrate and test probabilistic volcanic hazard models for disruption of the proposed repository.

4.1.3.3.1 Shifts in the Location of Basaltic Volcanism

Spatial variation in recurrence rate of volcanism in the YMR has been suggested based on apparent shifts in the locus of basaltic volcanism from east-to-west since the cessation of caldera-forming volcanism in the Miocene Southern Nevada Volcanic Field (Crowe and Perry, 1989). Well-defined shifts in volcanism have occurred in many other basaltic volcanic fields. In the Coso volcanic field, California, Duffield, et al. (1980) found that basaltic volcanism occurred in essentially two stages. Eruption of basalts occurred over a broad area in what is now the northern and western portions of the Coso volcanic field from approximately 4 to 2.5 Ma. In the Quaternary, the locus of volcanism shifted to the southern portion of the Coso volcanic field. Condit, et al. (1989) noted the tendency for basaltic volcanism to gradually migrate from west to east in the Springerville volcanic field between 2.5 and 0.3 Ma. Other examples of continental basaltic volcanic fields in which the location of cinder cone volcanism has migrated include the San Francisco volcanic field, Arizona, (Tanaka, et al., 1986), the Lunar Crater volcanic field, Nevada, (Foland and Bergman, 1992), the Michoacán-Guanajuato volcanic field, Mexico, (Hasenaka and Carmichael, 1985), and the Cima volcanic field, California, (Dohrenwend, et al., 1984; Turrin, et al., 1985). In some areas, such as the San Francisco and Springerville volcanic fields, migration is readily explained by plate movement (Tanaka, et al., 1986; Condit, et al., 1989; Connor, et al., 1992). In other areas, the direction of migration or shifts in the locus of volcanism does not correlate with the direction of plate movement. In either case, models developed to describe recurrence rate of volcanism or to predict the locations of future eruptions in volcanic fields need to be sensitive to these shifts in the location of volcanic activity.

Sensitivity to shifts in the locus of volcanism can be accomplished by weighing more recent (e.g., Pliocene and Quaternary) volcanic events more heavily than older (e.g., Miocene) volcanic events. Shifts in the locus of volcanism, however, also introduce uncertainty into the probabilistic hazard assessment. For example, in the Cima volcanic field, <1.2-Ma basaltic vents are located south of significantly older volcanic vents (Dohrenwend, et al., 1984; Turrin, et al., 1985). This suggests that probability models based on the distribution of older vents would not have forecast the location of subsequent (<1.2 Ma) eruptions adequately. In the Springerville volcanic field, large-scale shifts in the locus of volcanism accompanied a major geochemical change in the basalts from tholeiitic to more alkalic, suggesting that a fundamental change in petrogenesis may have affected shifts in the locus of volcanism (Condit and Connor, 1996).

As the period required for large-scale shifts in the locus of volcanism is much greater than the period of performance of a repository, the effects of these shifts can be effectively mitigated in the probability models by simply applying a more heavy weight to the distribution of Quaternary volcanic events than older volcanic events in the probability analysis.

4.1.3.3.2 Vent Clustering

Crowe, et al. (1992) and Sheridan (1992) noted that basaltic vents appear to cluster in the YMR. Connor and Hill (1995) performed a series of analyses of volcano distribution that yielded several useful observations about the nature of volcano clustering in the region. First, vents form statistically-significant clusters in the YMR. Spatially, volcanoes less than 5 Ma form four clusters: Sleeping Butte, Crater Flat, Amargosa Desert, and Buckboard Mesa. The Crater Flat and Amargosa Desert Clusters overlap somewhat due to the position of Lathrop Wells volcano and the three Amargosa Aeromagnetic Anomaly A vents (Figure 9). Second, a volcanic event located at the repository would be spatially part of, albeit near the edge of, the Crater Flat Cluster, rather than forming between or far from clusters in the YMR. Third, three of the four clusters reactivated in the Quaternary, indicating these clusters are long-lived and, thus, provide some constraints on the areas of future volcanism.

Cinder cones are known to cluster within many volcanic fields (Heming, 1980; Hasenaka and Carmichael, 1985; Tanaka, et al., 1986; Condit and Connor, 1996). Spatial clustering can be recognized through field observation or through the use of exploratory data analysis or cluster analysis techniques (Connor, 1990). Clusters identified using the latter approach in the Michoacán-Guanajuato and the Springerville volcanic fields were found to consist of 10 to 100 individual cinder cones. Clusters in these fields are roughly circular to elongate in shape with diameters of 10 to 50 km. The simplest explanation for the occurrence, size, and geochemical differences between many of these clusters is that these areas have higher magma supply rates from the mantle. Factors affecting magma pathways through the upper crust, such as fault distribution, appear to have little influence on cluster formation (Connor, 1990; Condit and Connor, 1996). In some volcanic fields, such as Coso, the presence of silicic magma bodies in the crust may influence cinder cone distribution by impeding the rise of denser mafic magma (Eichelberger and Gooley, 1977; Bacon, 1982), resulting in the formation of mafic volcano clusters peripheral to the silicic magma bodies.

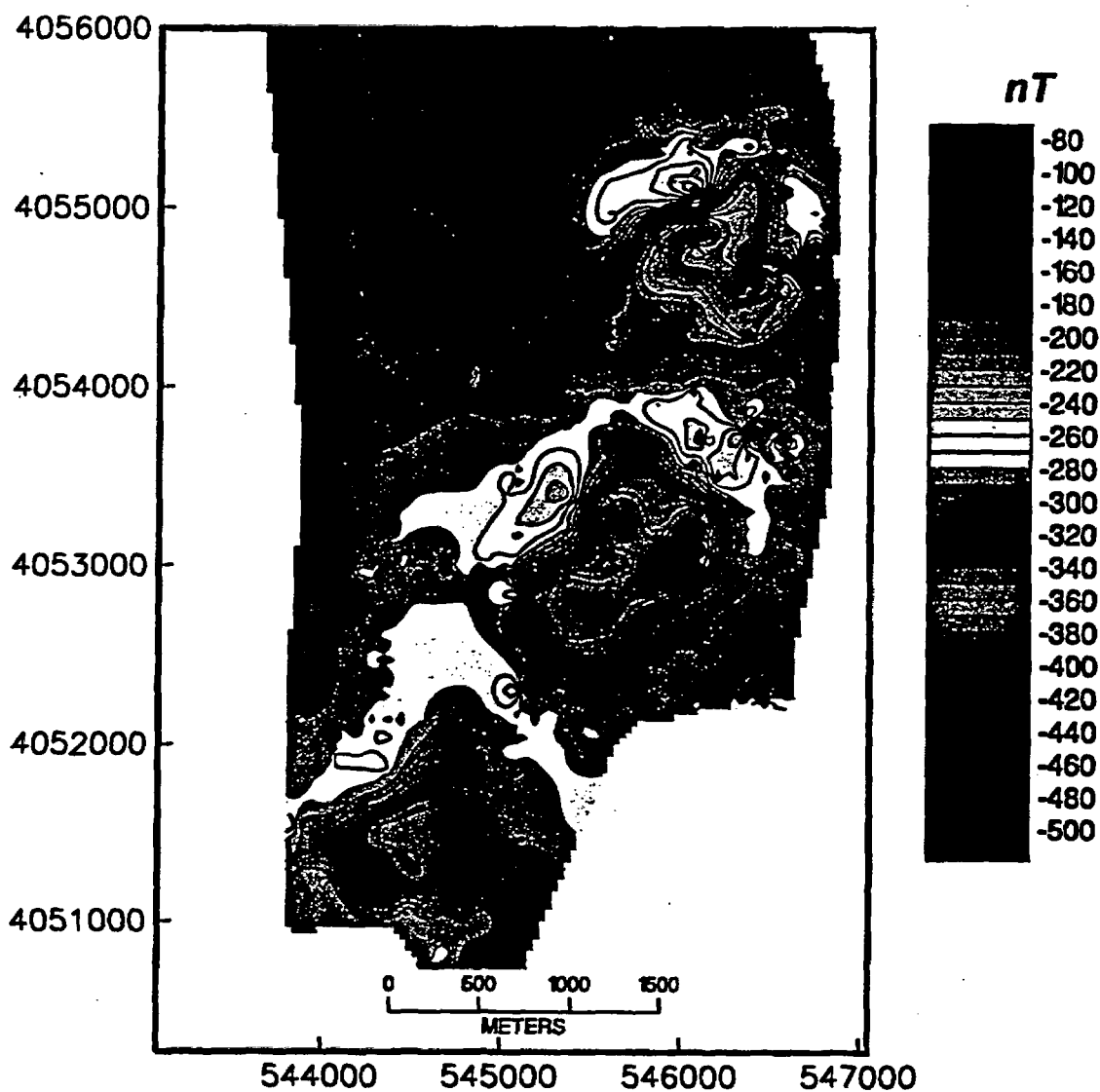


Figure 9. Ground magnetic map of Amargosa Aeromagnetic Anomaly A showing three aligned anomalies, interpreted to be produced by a buried alignment of three basaltic volcanoes. Contour interval is 10 nT. Figure from Connor, et al. (1997).

Basaltic vent clustering has a profound effect on estimates of recurrence rate of basaltic volcanism. For example, Condit and Connor (1996) found that recurrence rate varies by more than two orders of magnitude across the Springerville volcanic field due to spatio-temporal clustering of volcanic eruptions. In the YMR, Connor and Hill (1995) identified variations in recurrence rate of more than one order of magnitude from the Amargosa Desert to southern Crater Flat due to the clustering Quaternary volcanism. In contrast, probability models based on a homogeneous Poisson density distribution that ignores clustering will overestimate the likelihood of future igneous activity in parts of the YMR far from Quaternary centers and underestimate the likelihood of future igneous activity within and close to Quaternary volcano clusters.

4.1.3.3.3 Vent Alignments and Correlation of Vent Alignments and Faults

Tectonic setting, strain-rate and fault distribution all may influence the distribution of basaltic vents within clusters, and sometimes across whole volcanic fields (Nakamura, 1977; Smith, et al., 1990; Parsons and Thompson, 1991; Takada, 1994). Kear (1964) discussed local vent alignments, in which vents are the same age and easily explained by a single episode of dike injection, and regional alignments, in which vents of varying age and composition are aligned over distances of 20 to 50 km or more. For example, by Kear's (1964) definition, the Mesa Butte alignment (Figure 5) would be a regional alignment that is more likely to reactivate after a long period of quiescence than a local alignment. Thus, this distinction between local and regional alignments can potentially alter probability estimates.

Numerous mathematical techniques have been developed to identify and map vent alignments on different scales, including the Hough transform (Wadge and Cross, 1988), two-point azimuth analysis (Lutz, 1986), frequency-domain map filtering techniques (Connor, 1990), and application of kernel functions (Lutz and Gutmann, 1995). Regional alignments identified using these techniques are commonly colinear or parallel to mapped regional structures. For example, Draper, et al. (1994) and Conway, et al. (1997) mapped vent alignments in the San Francisco volcanic field that are parallel to, or colinear with, segments of major fault systems in the area. About 30 percent of the cinder cones and maars in the San Francisco volcanic field are located along these regional alignments (Draper, et al., 1994). Lutz and Gutmann (1995) identified similar patterns in the Panicked volcanic field, Mexico. Although alignments clearly can form as a result of single episodes of dike injection (Nakamura, 1977) and, therefore, are sensitive to stress orientation (Zoback, 1989), there are also examples of injection along pre-existing faults (e.g., Kear, 1964; Draper, et al., 1994; Conway, et al., 1997). Therefore, stress orientation in the crust and orientations of faults are indicators of possible vent-alignment orientations.

In the YMR, Smith, et al. (1990) and Ho (1992) define north-northeast-trending zones within which average recurrence rates exceed that of the surrounding region. The trend of these zones corresponds to cinder cone alignment orientations, including Quaternary Crater Flat and Sleeping Butte, that Smith, et al. (1990) and Ho (1992) hypothesize may occur as a result of structural control. Recent geophysical surveys of Amargosa Aeromagnetic Anomaly A provide further evidence of the significance of northeast-trending alignments in the YMR (Connor, et al., 1997). The ground magnetic map of data collected over Amargosa Aeromagnetic Anomaly A delineates three separate anomalies associated with shallowly buried basalt with a strong reversed polarity remanent magnetization (Figure 9). These anomalies are distributed over 4.5

km on a northeast trend, each having an amplitude of 70–150 nT. Although these features can be partially resolved with aeromagnetic data (Langenheim, et al., 1993), trenchant details emerge from the ground magnetic survey that are important to probabilistic volcanic hazard analyses and tectonic studies of the region. The southernmost anomaly, which has a smaller amplitude than those to the north but is nonetheless distinctive, and the northeast-trending structure within the negative portion of the central anomaly, which mimics the overall trend of the alignment (Figure 9), are important characteristics. The ground magnetic data also enhance the small positive anomalies north of each of the three larger-amplitude negative anomalies, reinforcing the interpretation that Amargosa Aeromagnetic Anomaly A is produced by coherent basaltic vents with strongly-reversed remanent magnetizations.

A key result of this ground magnetic survey is identification of the northeast trend of the anomalies, which is quite similar to the alignment of five Quaternary cinder cones in Crater Flat (Figure 7), and to the Sleeping Butte cinder cones, a Quaternary vent alignment 40 km to the northwest of Crater Flat. Although the age of the Amargosa Aeromagnetic Anomaly A alignment is at present uncertain, it suggests that development of northeast-trending cone alignments is a pattern of volcanism that has persisted through time in the YMR and supports the idea that future volcanism may exhibit a similar pattern (Smith, et al., 1990).

Other ground magnetic surveys provide further evidence of cinder cone localization along faults (Stamatakos, et al., 1997a; Connor, et al., 1997). Northern Cone is located approximately 8 km from the repository site in Crater Flat and is the closest Quaternary volcano to Yucca Mountain. Its proximity to the site of the proposed repository makes the structural setting of Northern Cone of particular interest to volcanic hazard assessment. Northern Cone consists of approximately 0.4 km² of highly magnetized (10–20 A m⁻¹) lava flows, near-vent agglutinate, and scoria aprons resting on a thin alluvial fan. Large-amplitude, short-wavelength magnetic anomalies were observed over the lavas. No evidence of northeast-trending structures was discovered that could directly relate Northern Cone to the rest of the Quaternary Crater Flat cinder cone alignment. Instead, prominent linear anomalies surrounding Northern Cone trend nearly north-south and have amplitudes of up to 400 nT (Figure 10). These anomalies likely result from offsets in underlying tuff across faults extending beneath the alluvium (cf. Faulds, et al., 1994).

The relationship between faults and Northern Cone is clarified when the ground magnetic map is compared with topographic and fault maps (Frizzell and Schulters, 1990; Faulds, et al., 1994). The north-trending anomalies at Northern Cone roughly coincide with mapped faults immediately north of the survey area that have topographic expression resulting from large vertical displacements. These mapped faults and faults inferred from the magnetic map are all oriented north to north-northeast, which are trends favorable for dilation and dike injection in the current stress state of the crust (e.g., Morris, et al., 1996). Thus, the Northern Cone magnetic survey provides further support for the concept that volcanism on the eastern margin of Crater Flat was localized along faults.

Thus, there is ample evidence to suggest patterns in YMR basaltic volcanic activity are influenced by the stress state of the crust and by fault patterns. This influence includes the development of northeast-trending volcanic alignments and the localization of vents along faults. Smith, et al. (1990) noted that the occurrence of northeast-trending alignments is particularly important because much of the Quaternary volcanic activity in the region has

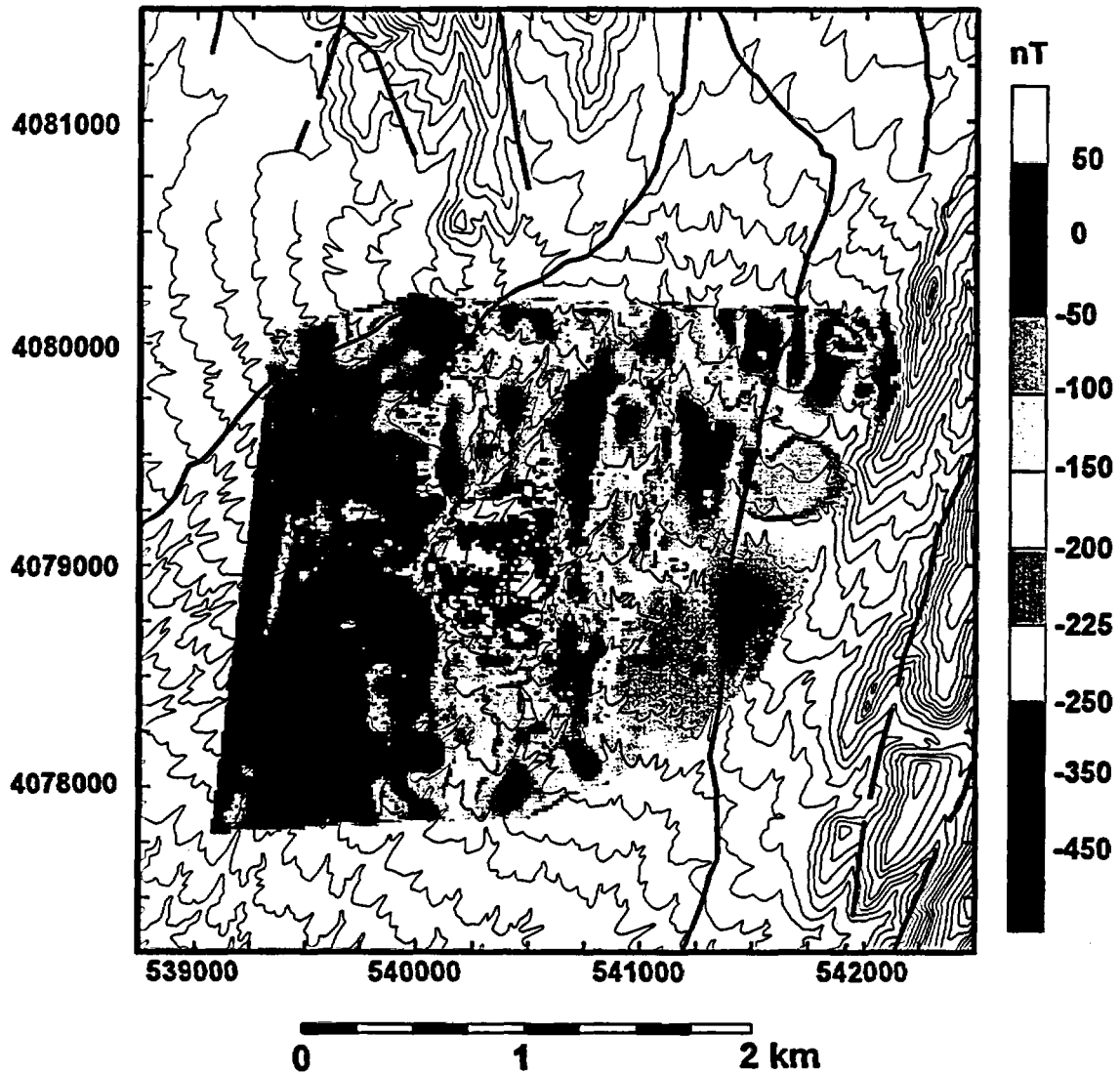


Figure 10. Ground magnetic map of the Northern Cone area, Crater Flat, Nevada. Northern Cone is located in the central part of the map, as indicated by high-amplitude, short-wavelength anomalies. North-south trending anomalies are interpreted to be produced by faults that displace tuff beneath the thin alluvial cover. Figure from Connor, et al., 1997.

occurred southwest of the proposed repository site. Furthermore, faults that bound and penetrate the repository block have a map pattern similar to those faults that have hosted volcanism at Northern Cone and Lathrop Wells. Given these observations, probability models for igneous disruption of the proposed repository need to account for these trends because they tend to increase the probability of igneous activity at the site relative to spatially-homogenous models.

4.1.3.4 Summary

Good agreement exists on the basic patterns of basaltic volcanism in the YMR. These patterns include changes in the locus of volcanism with time, recurring volcanic activity within vent clusters, formation of vent alignments, and structural controls on the locations of cinder cones. Each of these patterns in vent distribution has an important impact on volcanic probability models and is considered in current NRC, DOE, and State of Nevada probability models.

4.1.4 Probability Criterion 4

4.1.4.1 Acceptance Criterion

Estimates of the probability of future igneous activity in the YMR will be acceptable provided that:

- The parameters used in probabilistic volcanic hazard assessments, related to recurrence rate of igneous activity in the YMR, spatial variation in frequency of igneous events, and area affected by igneous events, are technically justified and documented by DOE.

4.1.4.2 Review Method

Staff should ascertain whether parameters used in volcanic hazard assessments are reasonable, based on data from the YMR and comparable volcanic systems.

4.1.4.3 Technical Basis

Models to estimate the probability of volcanic disruption of the proposed repository are likely to rely on a set of parameters. Use of values or ranges for these parameters must be justified using geologic data and analyses. In the following, current understanding of parameters related to:

- Temporal recurrence rate of volcanism
 - Spatial recurrence rate of volcanism
 - Area affected by volcanic and igneous events
- are discussed and evaluated.

4.1.4.3.1 Temporal Recurrence Rate

Probability models use estimates of the expected regional recurrence rate of volcanism in the YMR in order to calculate the probability of future disruptive volcanic activity. Previous estimates have relied on past recurrence rates of volcanism as a guide to future rates of volcanic activity. This approach has yielded estimates of regional recurrence rate between 1 and 12 volcanic events per million years (v/m.y.) (e.g., Ho, 1991; Ho, et al., 1991; Crowe, et al., 1992; Margulies, et al., 1992; Connor and Hill, 1995), with the various definitions of what constitutes a volcanic event accounting for at least part of this range.

The simplest approach to estimate regional recurrence rate is to average the number of volcanic events that have occurred during some time period of arbitrary length. For instance, Ho, et al. (1991) average the number of volcanoes that have formed during the Quaternary (1.6 m.y.) to calculate recurrence rate. Through this approach, they estimate an expected recurrence rate of 5 v/m.y. Crowe, et al. (1982) averaged the number of new volcanoes over a 1.8-m.y. period. Crowe, et al. (1992) considered the two Little Cones to represent a single volcanic event, and, therefore, concluded that there are seven Quaternary volcanic events in the YMR. This lowers the estimated recurrence rate to approximately 4 v/m.y. The probability of a new volcano forming in the YMR during the next 10,000 yr is 4-5 percent, assuming a recurrence rate of between 4 and 5 v/m.y.

An alternative approach is the repose time method (Ho, et al., 1991). In this method, a recurrence rate is defined using a maximum likelihood estimator (Hogg and Tanis, 1988) that averages events over a specific period of volcanic activity:

$$\lambda_t = \frac{(N-1)}{(T_o - T_y)} \quad (1)$$

where N is the number of events, T_o is the age of the first event, T_y is the age of the most recent event, and λ_t is the estimated recurrence rate. Using eight Quaternary volcanoes as the number of events, N , and 0.1 Ma for the formation of Lathrop Wells (Appendix A), the estimated recurrence rate depends on the age of the first Quaternary volcanic eruption in Crater Flat. Using a mean age of 1.0 Ma (Appendix A) yields an expected recurrence rate of approximately 8 v/m.y. The ages of Crater Flat volcanoes, however, are currently estimated at approximately 1.0 ± 0.2 Ma (Appendix A). Within the limits of this uncertainty, the expected recurrence rate is between approximately 7 and 10 v/m.y. Of course, using different definitions of volcanic events leads to different estimates of recurrence rate. For example, using the formation of vents and vent alignments during the Quaternary, $N = 3$ and the recurrence rate is 2-3 v/m.y. The repose-time method has distinct advantages over techniques that average over an arbitrary period of time because it restricts the analysis to a time period that is meaningful in terms of volcanic activity. In this sense, it is similar to methods applied previously to estimate time-dependent relationships in active volcanic fields (Kuntz, et al., 1986). Application of these methods has shown that steady-state recurrence rates characterize many basaltic volcanic fields.

Ho (1991) applied a Weibull-Poisson technique (Crow, 1982) to estimate the recurrence rate of new volcano formation in the YMR as a function of time. Ho (1991) estimates $\lambda(t)$ as:

$$\lambda(t) = \left(\frac{\beta}{\theta} \right) \left(\frac{t}{\theta} \right)^{\beta-1} \quad (2)$$

where t is the total time interval under consideration (such as the Quaternary), and β and θ are intensity parameters in the Weibull distribution that depend on the frequency of new volcano formation within the time period, t . In a time-truncated series, β and θ are estimated from the distribution of past events. In this case, there are $N = 8$ new volcanoes formed in the YMR during the Quaternary. β and θ are given by (Ho, 1991):

$$\beta = \frac{N}{\sum_{i=1}^n \ln \left(\frac{t}{t_i} \right)} \quad (3)$$

and

$$\theta = \frac{t}{N^{1/\beta}} \quad (4)$$

where t_i refers to the time of the i^{th} volcanic event. If β is approximately equal to unity, there is little or no change in the recurrence rate as a function of time, and a homogeneous nonstationary Poisson model would provide an estimate of regional recurrence rate quite similar to the nonhomogeneous Weibull-Poisson model. If $\beta > 1$, then a temporal trend exists in the recurrence rate and the system is waxing; new volcanoes form more frequently with time. If $\beta < 1$, new volcanoes form less frequently over time, and the magmatic system may be waning.

Where few data are available, such as in analysis of volcanism in the YMR, the value of β can be strongly dependent on the period t and the timing of individual eruptions. This independence strongly reduces the confidence with which β can be determined. Ho (1991) analyzed volcanism from 6 Ma, 3.7 Ma, and 1.6 Ma to the present and concluded that volcanism is developing in the YMR on time scales of $t = 6$ Ma and 3.7 Ma, and has been relatively steady, $\beta = 1.1$, during the Quaternary.

Uncertainty in the ages of Quaternary volcanoes has a strong impact on recurrence rate estimates calculated using a Weibull-Poisson model. For example, if mean ages of Quaternary volcanoes are used (Appendix A) and $t = 1.6$ Ma then, as Ho (1991) calculated, $\beta = 1.1$, and the probability of a new volcano forming in the region within the next 10,000 yr is approximately 5 percent. This agrees well with recurrence rate calculations based on simple averaging of the number of new volcanoes that have formed since 1.6 Ma.

Crowe, et al. (1995), however, concluded that the Weibull-Poisson model is strongly dependent on the value of t and suggested that t should be limited to the time since the initiation of a particular episode of volcanic activity. This has an important effect on Weibull-Poisson probability models. If mean ages of Quaternary volcanoes are used and $t = 1.2$ Ma, the probability of a new volcano forming in the next 10,000 yr drops from 5 percent to 2 percent, and $\beta < 1$, indicating waning activity. Alternatively, if volcanism was initiated along the alignment approximately 1.2 Ma, but continued through 0.8 Ma, the expected recurrence rate is again

close to 5 v/m.y., and the probability of new volcanism in the YMR within the next 10,000 yr is about 5 percent ($t = 1.2$ Ma). The confidence intervals calculated on $\lambda(t)$ are quite large in all of these examples due to the few volcanic events ($N = 8$) on which the calculations are based (Connor and Hill, 1993).

Cumulatively, these analyses indicate a broad range of recurrence rates should be considered, this range varying with the definition of igneous event used. Many recurrence rate models depend on additional information to estimate recurrence rates of volcanism. Bacon (1982) observed that cumulative erupted volume in the Coso volcanic field since about 0.4 Ma is remarkably linear in time. Successive eruptions occur at time intervals that depend on the cumulative volume of the previous eruptions. This linear relationship was used by Bacon (1982) to forecast future eruptions and to speculate about processes, such as strain rate, that may govern magma supply and output in the Coso volcanic field. Kuntz, et al. (1986) successfully applied a volume-predictable model to several areas on the Snake River Plain, where recurrence rates of late Quaternary volcanism are much higher than in the Coso volcanic field but the cumulative volumetric rate of basaltic magmatism is nonetheless linear in time. Condit and Connor (1996) discovered volume eruption rates were relatively constant in the Springerville volcanic field between 1.2 and 0.3 Ma, but the number of cone-forming eruptions varied in time, in conjunction with changes in petrogenesis. These relationships between eruption volume, petrogenesis, strain rate, and frequency of volcanic events observed in other volcanic fields suggest that recurrence rate estimates in the YMR can be further refined by considering fault location, magma generation, and strain rate.

4.1.4.3.2 Spatial Recurrence Rate

Early models assessing the probability of future volcanism in the YMR and the likelihood of a repository-disrupting igneous event relied on the assumption that Plio-Quaternary basaltic volcanoes are distributed in a spatially uniform random manner over some bounded area (e.g., Crowe, et al., 1982; Crowe, et al., 1992; Ho, et al., 1991; Margulies, et al., 1992). However, as discussed in Section 4.1.4, patterns in the distribution and age of basaltic volcanoes in the YMR make the choice of these bounded areas subjective. For example, Smith, et al. (1990) and Ho (1992) define north-northeast-trending zones within which average recurrence rates exceed that of the surrounding region. These zones correspond to cinder cone alignment orientations that Smith, et al. (1990) and Ho (1992) hypothesize may result from structural control. These narrow zones lead to comparatively high estimates of spatial recurrence rate and probability of volcanic disruption of the proposed repository site. Utilizing bounded areas that are large compared to the current distributions of cinder cone clusters, however, results in relatively low estimates of spatial recurrence rate. Ho (1992) argued that, under these circumstances, using narrow bounding areas that include the proposed repository gives conservative estimates of probability of volcanic disruption.

Alternatively, spatial recurrence rate can be estimated using models that explicitly account for volcano clustering (Connor and Hill, 1995). This approach features several characteristics of nearest-neighbor methods that make them amenable to volcano distribution studies and hazard analysis in areal volcanic fields. First, volcanic eruptions, such as the formation of a new cinder cone, are discrete in time and space. Using nearest-neighbor methods, the probability surface

is estimated directly from the location and timing of these past, discrete volcanic events. As a result, nearest-neighbor models are sensitive to patterns generally recognized in cinder cone distributions. Resulting probability surfaces also are continuous, rather than consisting of abrupt changes in probability that must be introduced in spatially homogeneous models. Continuous probability surfaces can be readily compared to other geologic data, such as fault locations, that may influence volcano distribution. Nearest-neighbor methods also eliminate the need to define areas or zones of volcanic activity, as is required by all spatially homogeneous Poisson models.

Past volcanic activity can be used to estimate parameters used in these spatially nonhomogeneous Poisson probability models for disruption of the proposed repository. This is particularly important in modeling the distribution of volcanism in the YMR because of vent clustering. As discussed previously (Section 4.1.2.3), vent clustering results in dramatic changes in spatial recurrence rate across the YMR. In order to model clustering and use these models in probabilistic volcanic hazard analysis, it is necessary to estimate parameters used in the models. One approach to parameter estimation is to use observed volcano distributions as a basis for comparison. This parameter estimation can be done formally, if appropriate models are used.

One estimation method for the spatial recurrence rate of volcanic events in the YMR and the probability of future volcanic events uses kernel functions (Silverman, 1986; Lutz and Gutmann, 1995; Connor and Hill, 1995; Condit and Connor, 1996). In volcanic hazard analysis, the kernel function must be estimated and used to deduce a probability density function for spatial recurrence rate of volcanism. Several types of kernels, including Gaussian and Epanechnikov kernels, are discussed by Silverman (1986). All multivariate kernels have the property:

$$\int_{\mathbb{R}} K(\mathbf{x}) d\mathbf{x} = 1 \quad (5)$$

where $K(\mathbf{x})$ is the kernel function, and \mathbf{x} is an n -dimensional vector in real space \mathbb{R} . A Gaussian kernel function for 2D spatial data is:

$$K(x,y) = \frac{1}{2\pi} \exp \left\{ -\frac{1}{2} \left[(x - x_v)^2 + (y - y_v)^2 \right] \right\} \quad (6)$$

where the kernel is calculated for a point x, y and the center of the kernel, in this case the volcano location, is x_v, y_v . If the kernel is normalized using the smoothing parameter, h , then the kernel function is a Gaussian function, and h is equivalent to the standard deviation of the distribution:

$$K(x,y) = \frac{1}{2\pi h^2} \exp \left\{ -\frac{1}{2} \left[\left(\frac{x - x_v}{h} \right)^2 + \left(\frac{y - y_v}{h} \right)^2 \right] \right\} \quad (7)$$

If x and y locations are on a rectangular grid, the probability density function based on the distribution of N volcanoes is:

$$\hat{f}(x,y) = \frac{\Delta x \Delta y}{N} \sum_{i=1}^N K(x,y) \quad (8)$$

where Δx and Δy are grid spacing in the x and y directions, respectively. The above equations can be used to estimate spatial recurrence rate of volcanism, or the probability of volcanic disruption of the proposed repository site, given a volcanic eruption in the region. The results of this probability estimate depend on h . The approach to bounding uncertainty in the probability estimates resulting from this calculation is to evaluate probability using a wide range of h (Connor and Hill, 1995). Alternatively, the effectiveness of the kernel model and optimal values of h can be deduced from the distribution of nearest-neighbor distances between existing volcanoes. For example, the 2D-Gaussian kernel model can be compared with the distribution of nearest-neighbor distances between existing volcanoes by recasting the kernel function (Eq. 7) in polar coordinates:

$$K(r,\theta) = \frac{2}{h(2\pi)^{3/2}} \exp\left[-\frac{1}{2}\left(\frac{r^2}{h^2}\right)\right] \quad (9)$$

where r, θ is distance and direction from the nearest-neighbor volcanic event. The cumulative probability density function then becomes

$$\hat{F}(R) = \int_0^{2\pi} \int_0^R \frac{2}{h(2\pi)^{3/2}} \exp\left[-\frac{1}{2}\left(\frac{r^2}{h^2}\right)\right] dr d\theta \quad (10)$$

where $\hat{F}(R)$ is the expected fraction of volcanic events within a distance R of their nearest-neighbor volcanic event.

Distance to nearest-neighbor volcanic event in the YMR varies depending on the definition used for a volcanic event. Treating all vents as individual volcanic events, the mean distance to nearest-neighbor volcanic event is 3.8 km with a standard deviation of 5.8 km. Some vents such as southwest and northeast Little Cones, however, are quite closely spaced and may be treated as single volcanic events. Treating vents spaced more closely than 1 km as single volcanic events, the mean distance to nearest-neighbor volcanic event increases to 5.0 km and the standard deviation to 5.9 km. Alternatively, volcanic events can be defined in terms of vents and vent alignments. In this definition, Quaternary Crater Flat volcanoes are taken as a single event, as is Pliocene Crater Flat. Using this definition, mean distance to nearest-neighbor volcanic event increases to 7.0 km with a standard deviation of 6.4 km.

The observed fraction of volcanoes erupted at a given nearest-neighbor distance or less is compared with a Gaussian kernel model with standard deviations of 3–7 km in Figure 11. A Gaussian kernel model with $h = 5$ km reasonably describes the expected distance to nearest-neighbor volcano, particularly between 5 and 10 km. Smaller values, such as $h = 3$ km, model the distribution of individual vents at distances less than 4 km, but do not compare well with vent distributions at distances greater than 4 km. For instance, the $h = 3$ km model predicts that 95 percent of all volcanoes will be located at nearest-neighbor distances less than 6 km, but actually 15 to 40 percent of all volcanoes in the YMR are located at greater distances than this, depending on the definition of volcanic events used. The $h = 7$ km model tends to slightly

overestimate the number of volcanoes at nearest-neighbor distances greater than 8 km. Thus, the $h = 5$ km model best describes the overall distribution of YMR vents and vent pairs for use in evaluation of hazards at the repository, located approximately 8 km from the nearest Quaternary volcano. This is slightly less than the standard deviation of the observed distribution because Buckboard Mesa, located 25 km from its nearest-neighbor, is an outlier in the observed volcano distribution and increases the variance.

Vents and vent alignments have fewer nearest-neighbors than expected at distances less 4 km if this distribution is modeled using a Gaussian kernel (Figure 11). Rather, this distribution can be modeled using a simple modification of the Gaussian kernel to account for a mean offset of the probability density function from zero:

$$\hat{F}(R) = \int_0^{2\pi R} \int_0^{\frac{3}{2}} \frac{2}{h(2\pi)^{\frac{3}{2}}} \exp\left[-\frac{1}{2}\left(\frac{r-\bar{x}}{h}\right)^2\right] dr d\theta \quad (11)$$

where \bar{x} is the mean offset. Incorporating a mean offset of 5–7 km and $h = 3$ km results in an improved fit between the observed distribution of distance to nearest-neighbor volcanic events and the Gaussian kernel model (Figure 12). The need for this mean offset arises because vent alignments are more widely spaced than individual vents. Variance does not increase significantly as a result of this increased spacing, however, when vent alignments are considered as single volcanic events. This comparatively low variance suggests there is a characteristic nearest-neighbor distance of 5–10 km in the YMR for volcanic events defined as vents or vent alignments.

This analysis indicates volcanic event distribution can be modeled using a Gaussian kernel with $h \geq 5$ km provided volcanic events are defined as individual vents or vent pairs. When vent alignments are considered as individual volcanic events the value of h must increase to $h \geq 7$ km, or the Gaussian kernel needs to be modified to include an offset distance. Thus, model testing indicates the types of kernels and parameters used within each kernel to evaluate probability should vary with the definition of volcanic event.

The Epanechnikov kernel function is widely used to estimate spatial recurrence rate in basaltic volcanic fields (Lutz and Gutmann, 1995; Connor and Hill, 1995; Condit and Connor, 1996) and may be tested in a similar manner as the Gaussian kernel function. The Epanechnikov kernel in 2D-Cartesian coordinates is:

$$K_e(x,y) = \frac{2}{\pi h^2} \left\{ 1 - \left[\left(\frac{x - x_v}{h} \right)^2 + \left(\frac{y - y_v}{h} \right)^2 \right] \right\} \quad (12)$$

where

$$\sqrt{(x-x_v)^2 + (y-y_v)^2} \leq h$$

otherwise

$$K_e(x,y) = 0$$

In polar coordinates this kernel function becomes

$$K_e(r,\theta) = \frac{3}{4\pi h} \left[1 - \left(\frac{r^2}{h^2} \right) \right] \quad r \leq h \quad (13)$$

where r is distance from the volcano and θ is direction. The cumulative probability density

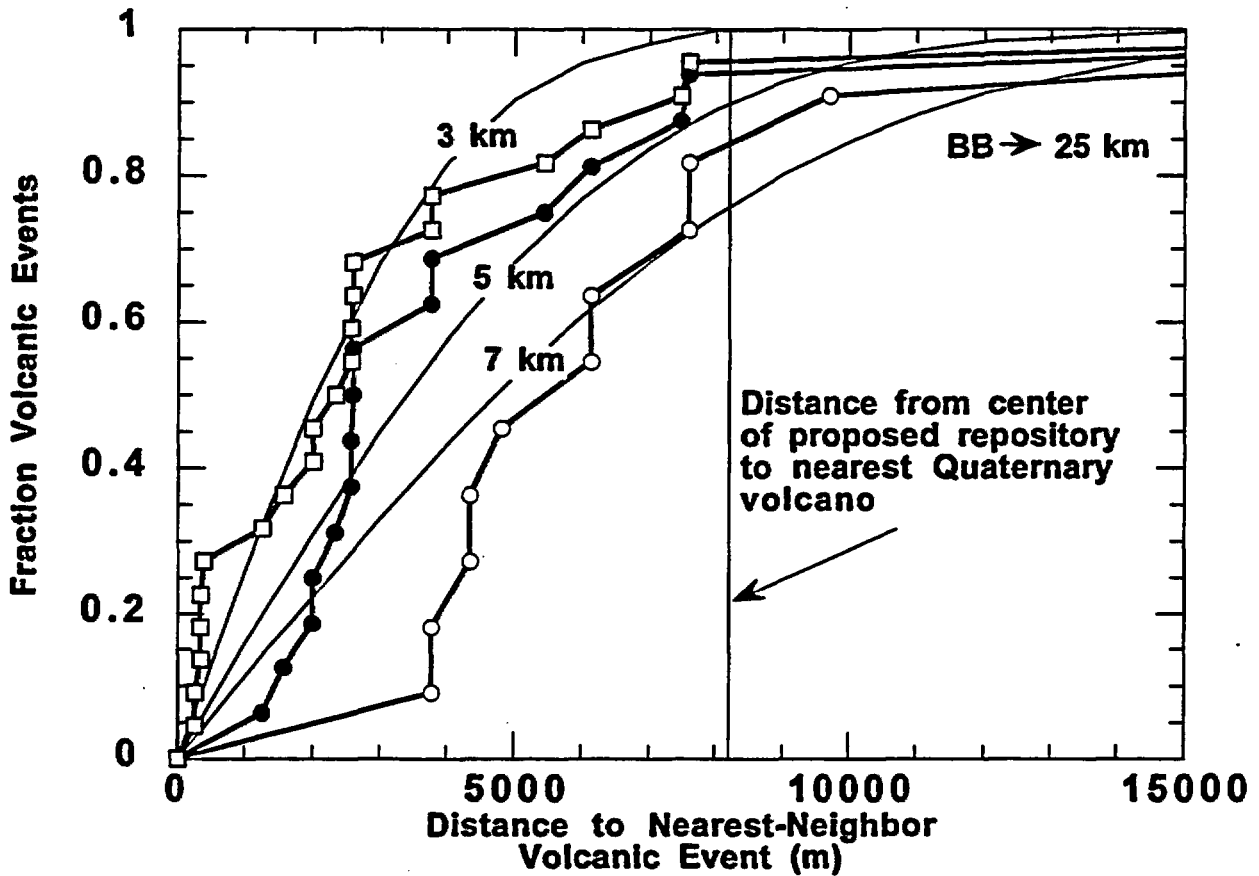


Figure 11. Comparison of observed fraction of volcanoes within a given distance of their nearest-neighbor volcano with Gaussian kernel models calculated using $h = 3$ km, 5 km, and 7 km. Observed curves include all vents (open squares), all vents or vent pairs more closely spaced than 1 km (solid circles), and vents and vent alignments (open circles). Buckboard Mesa (BB) is an outlier in the distribution as it is approximately 25 km from its nearest neighbor. The center of the repository site is located 8.2 km from Northern Cone, the nearest Quaternary volcano.

function is then:

$$\hat{F}(R) = \int_0^{2\pi} \int_0^R \frac{3}{4\pi h} \left[1 - \left(\frac{r^2}{h^2} \right) \right] dr d\theta, R \leq h \quad (14)$$

As was accomplished with the Gaussian kernel, the cumulative probability density function for the Epanechnikov kernel can be compared with the observed fraction of volcanoes erupted at a given nearest-neighbor distance or less for various values of h (Figure 13). This comparison indicates an Epanechnikov kernel function with $h = 10$ km best models the distribution of distance to nearest-neighbor volcanic events, if volcanic events are defined as vents or vent pairs. If volcanic events are defined as vents or vent alignments, $15 \text{ km} < h < 18 \text{ km}$ better

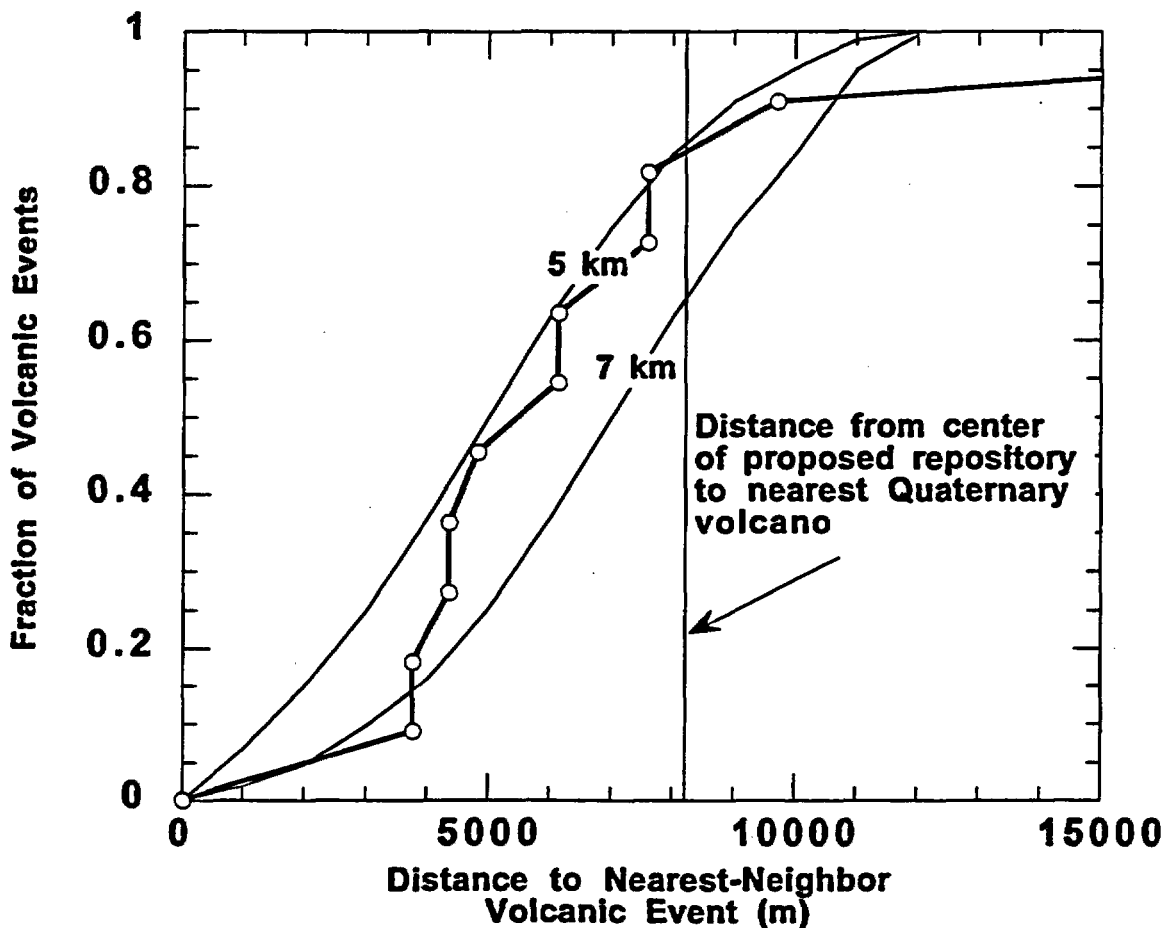


Figure 12. Comparison of observed fraction of volcanic events within a given distance of their nearest-neighbor volcanic event with Gaussian kernel models calculated using $h = 5$ km and $h = 7$ km. Observed curves include vents and vent alignments (open circles) as single volcanic events, calculated from the center of the vent alignment. Buckboard Mesa is an outlier in the distribution as it is approximately 25 km from its nearest neighbor.

approximates the distribution of distances to nearest-neighbor volcanic events, given the distribution of YMR volcanoes. Comparison of the Epanechnikov and Gaussian kernel models suggests the Gaussian kernel models better fit the observed volcano distribution than Epanechnikov distributions, particularly at nearest-neighbor distances greater than 6 km. The difficulty fitting the observed distributions with the Epanechnikov kernel function results from truncation of this distribution at distances greater than h .

Testing models against observed distributions also leads to a natural definition of conservatism. For example, the distance between the proposed repository and its nearest-neighbor Quaternary volcano is 8.2 km. A Gaussian kernel function with $h \geq 7$ km clearly is conservative

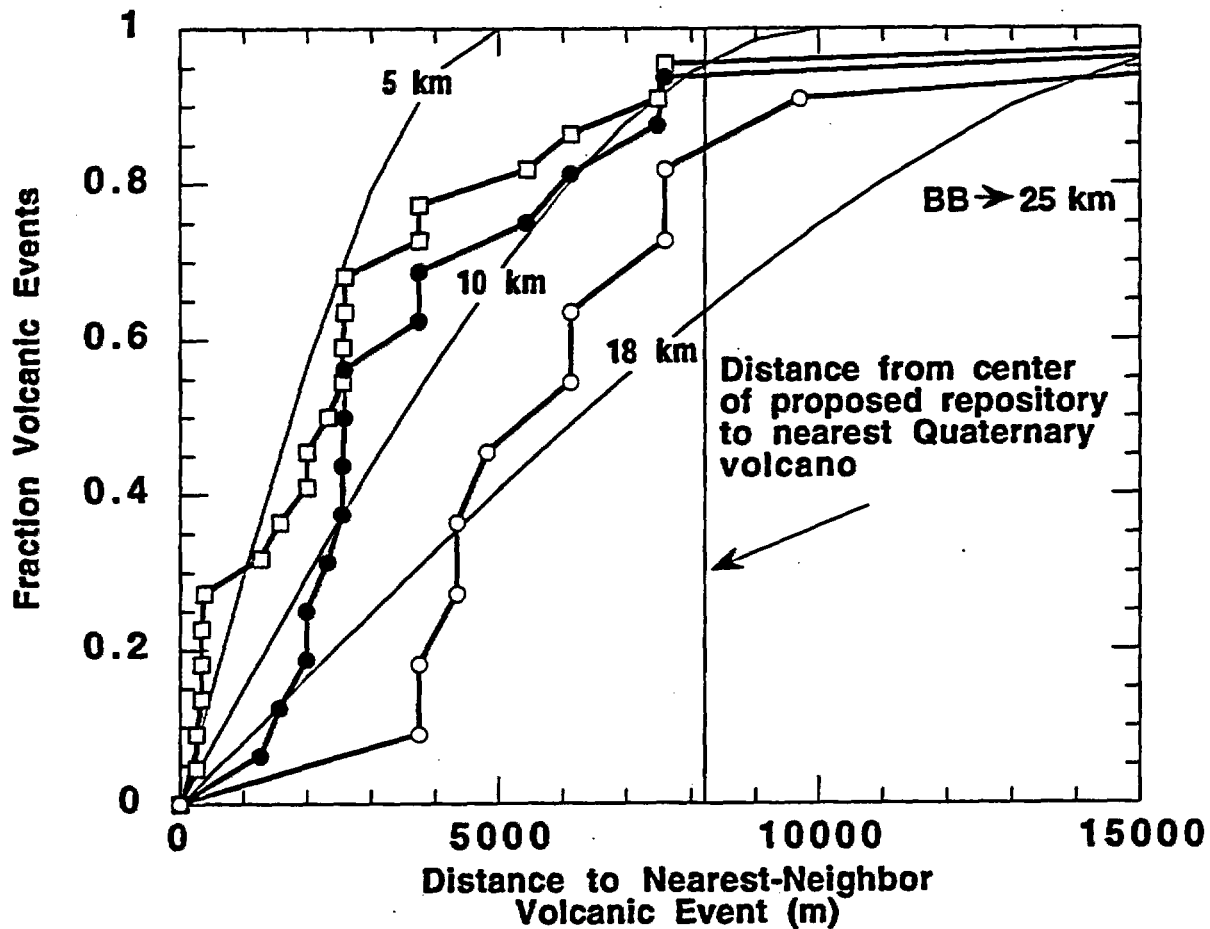


Figure 13. Comparison of observed fraction of volcanoes within a given distance of their nearest-neighbor volcano with Epanechnikov kernel models calculated using $h = 5$ km, 10 km, and 18 km. Observed curves include all vents (open squares), all vents or vent pairs more closely spaced than 1 km (solid circles), and vents and vent alignments (open circles). Buckboard Mesa (BB) is an outlier in the distribution as it is approximately 25 km from its nearest neighbor. The center of the repository site is located 8.2 km from Northern Cone, the nearest Quaternary volcano.

because a greater fraction of volcanic events occur at nearest-neighbor distances less than 8.2 km than predicted by the model, whereas a Gaussian kernel function with $h = 3$ km is not conservative (Figure 11). Similarly, probability models based on Epanechnikov kernel functions and $h \geq 10$ km are conservative where volcanic events are defined as vents and vent pairs, and $h \geq 18$ km where volcanic events are defined as vents and vent alignments.

4.1.4.3.3 Area Affected by Igneous Events

The area affected by igneous events varies with the definition of igneous event (Section 4.1.2). Where igneous events are defined in terms of individual, mappable eruptive units, the resulting probability estimate is for direct disruption of the proposed repository and release of waste into the accessible environment. The probability of a volcanic event disrupting the repository depends on the repository area potentially disrupted by flow of magma through the subsurface conduit of the volcano as the eruption develops. Observations at cinder cones in the process of formation (e.g., Luhr and Simkin, 1993; Fedotov, 1983; Doubik, et al., 1995) are that these eruptions initiate by dike injection at comparatively low ascent velocities, on the order of 1 m s^{-1} , which can deform an area of the ground surface several hundred meters in length. Basaltic eruptions, however, quickly localize into vent areas as the eruption progresses and magma flow velocities increase to around 100 m s^{-1} . Hill (1996) reviewed literature on subsurface areas disrupted by basaltic volcanoes analogous to past volcanic eruptions in the YMR. Based on this review and data collected at Tolbachik volcano, Russia, Hill (1996) concluded that typical subsurface conduit diameters are between 1 m and 50 m at likely repository depths of about 300 m. Vent conduits exposed in the San Rafael volcanic field (Delaney and Gartner, 1995), however, often have diameters on the order of 100 m. Therefore, areas disrupted by vent formation, potentially leading to the release of waste into the accessible environment, are on the order of 0.01 km^2 or less. Conservatively, such a volcanic event centered within 50 m of the repository boundary may result in transport of waste to the surface.

Using this approach, the probability of a volcanic eruption through the repository, given an eruption, can be approximated as:

$$P[\text{eruption through repository} | \text{eruption centered at } x,y] = \begin{cases} 1, & \text{if } x,y \in A_e \\ 0, & \text{otherwise} \end{cases} \quad (15)$$

where the effective area, A_e , is the area of the repository and the region about the repository within one conduit radius of the repository boundary (Geomatrix, 1996).

Other definitions of igneous events result in the need for more complex analyses of area affected because these events have length and orientation (Sheridan, 1992; Geomatrix, 1996). In these cases, probability density functions must be estimated for both the length and orientation of igneous events. Geomatrix (1996) gave the probability of an intrusive igneous event centered on a given location intersecting the repository, which can be expressed as:

$$P[L \geq l_r, \phi_1 \leq \Phi \leq \phi_2] = \int_{l_r}^{\infty} \int_{\phi_1}^{\phi_2} f_L(l) \cdot f_\phi(\phi) d\phi dl \quad (16)$$

where Φ is the azimuth of the igneous event with respect to north, with ϕ_1 and ϕ_2 representing the range of azimuths that would result in intersection with the repository, given an igneous event centered on x, y , a distance l_r from the repository boundary. The probability that the igneous event of half-length, L , will exceed l_r at an azimuth between ϕ_1 and ϕ_2 depends on the probability density functions $f_L(l)$ and $f_\phi(\phi)$ for igneous event half-length and azimuth, respectively.

This characterization of area affected by igneous events must be modified further depending on the type of event considered. Defining igneous events as volcanic vents or vent alignments may result in a probability estimate for volcanic disruption of the repository, if the frequency of vent formation along the alignment is included in the calculation. The length of the vent alignment is taken as the distance between the centers of the first and last volcanoes in the alignment. For example, the length of the Amargosa Aeromagnetic Anomaly A alignment of three vents is 4.0 km (Figure 9). The length of the Quaternary Crater Flat alignment of five vents is 11.2 km, based on the distance between southwest Little Cone and Northern Cone (Figure 7). Six vents occur along the 3.6-km Pliocene Crater Flat alignment. Average vent density along these alignments is on the order of 0.5-2.0 vents per km. This vent density suggests that, if an alignment defined by the distance between the first and last vents in the alignment intersects the repository, a vent will likely form within the repository boundary as a result of this intersection.

Uncertainty increases considerably when the functions $f_L(l)$ and $f_\phi(\phi)$ are introduced because these functions must be estimated from limited YMR geologic data. If the igneous event is defined as the development of a vent or vent alignment, mapped vent locations are useful in constraining the functions $f_\phi(\phi)$ and $f_L(l)$. Considering Plio-Quaternary volcanism in the YMR, six igneous events consist of the formation of isolated vents, and four igneous events resulted in the formation of vent alignments (Figure 14). Of these four vent alignments, two are less than 4 km long, the Pliocene Crater Flat vents and the Sleeping Butte vent pair. The Amargosa Aeromagnetic Anomaly A alignment is slightly longer than 4 km. The Quaternary Crater Flat alignment, one of the youngest and most important volcanic events in the YMR, is also the longest alignment, approximately 11 km long. Although these data provide an idea of the range of alignment lengths possible in the YMR, they are not sufficient to estimate a probability distribution for vent alignment lengths, $f_L(l)$.

In order to compensate for the lack of data within the YMR, analog information can be used. Draper, et al. (1994) note that approximately 30 percent of the vents in the San Francisco volcanic field form alignments. The remaining vents are isolated and appear to have formed during independent episodes of volcanic activity. This value appears comparable to the ratio of vent alignments to individual vents in the YMR. Data on vent alignment lengths from other volcanic fields suggests vent alignments may be considerably longer than the Quaternary Crater Flat alignment. For example, Connor, et al. (1992) identified vent alignments >20-km long

in the Springerville volcanic field, Arizona. Vent alignments of comparable or greater length have been identified in the Michoacán-Guanajuato volcanic field, Mexico (Wadge and Cross, 1988; Connor, 1990), and the Panicked volcanic field, Mexico (Lutz and Gutmann, 1995). Smith, et al. (1990) suggested alignments may be up to 20 km long, with a lower probability of 40-km-long alignments, based on mapping in the Lunar Crater, Reveille Range, and San Francisco volcanic fields. None of these authors, however, developed distributions for vent alignment lengths in these areas. Furthermore, it is not clear that the conditions for vent alignment formation and factors controlling vent alignment length are directly comparable between these different regions and the YMR. As a result, estimation of the distribution function for $f_l(l)$ for YMR vents and vent alignment formation is extremely uncertain.

However, given these caveats, the probability density function for event length can be expressed as:

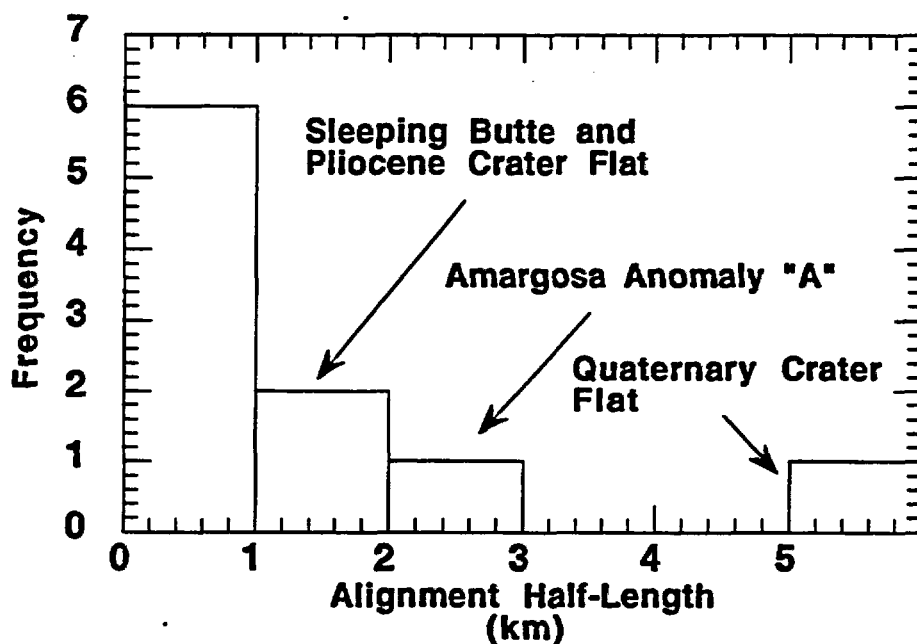


Figure 14. Distribution of Plio-Quaternary vents by vent alignment half-length. Most vents in the Yucca Mountain region occur as isolated vents. The youngest and longest vent alignment in the Yucca Mountain region, the Quaternary Crater Flat alignment, is also closest to the repository site.

$$f_L(l) = \begin{cases} \frac{1}{2}, & l = 0 \\ \frac{U[l_{\min}, l_{\max}]}{2}, & l > 0 \end{cases} \quad (17)$$

By this definition, 50 percent of igneous events have zero length and only disrupt the repository if they fall within the effective area of the repository. The remaining 50 percent of igneous events form alignments that affect areas up to a distance l_{\max} from the point x, y . This percentage assigned to zero-length igneous events is a source of uncertainty in probability estimates and is not well constrained by available data. The probability density function is construed to be a uniform random distribution between l_{\min} and l_{\max} because the distribution of alignment lengths is so poorly known.

Using this definition of $f_L(l)$, probability estimates of intersection of the repository, given an event at x, y , will not be strongly dependent on l_{\min} compared to l_{\max} . The value of l_{\max} can be chosen as 5.6 km, taking the Quaternary Crater Flat alignment as the maximum alignment half-length. Given observations in other volcanic fields, however, l_{\max} may be 10 km or more.

The distribution function for azimuth of alignments or dike zones, $f_\phi(\phi)$, is better constrained by the data on vent alignments, regional stress distribution, and the orientations of high-dilation tendency faults. Three of the alignments in the YMR trend 020° to 030° , perpendicular to the least principle horizontal compressional stress in the region, 028° (e.g., Morris, et al., 1996). Under these circumstances, $f_\phi(\phi)$ may vary over a narrow range. For example,

$$f_\phi(\phi) = U [020^\circ, 035^\circ] \quad (18)$$

Alternatively, $f_\phi(\phi)$ near the repository may respond to the distribution of fault orientations (Figure 15) if ascending magmas tend to exploit faults as low-energy pathways to the surface (Conway, et al., 1997; Jolly and Sanderson, 1997).

Other definitions of igneous events attempt to capture the probability of igneous intrusions intersecting the repository boundary (Sheridan, 1992; Geomatrix, 1996). Igneous intrusions commonly form anastomosing networks at shallow levels in the crust, forming multiple dike segments at a given structural level (e.g., Gartner and Delaney, 1988). Consequently, a term may be added to Eq. (16) to account for the width of igneous events, such as the width of the dike swarm formed during igneous intrusion:

$$P[L \geq l_r, \phi_1 \leq \Phi \leq \phi_2, W \geq w_r] = \int_{l_r}^{\infty} \int_{\phi_1}^{\phi_2} \int_{w_r}^{\infty} f_L(l) \cdot f_\phi(\phi) \cdot f_w(w) \, dw d\phi dl \quad (19)$$

where $f_w(w)$ is a probability density function describing the half-width of the igneous event, which may be a significant fraction of the half-length, and w_r is the shortest distance to the repository boundary perpendicular to the event azimuth, for a given azimuth and event length.

Numerous individual dikes, dike segments, and sills may be located within this zone. Little is known about the distribution $f_w(w)$. In Pliocene Crater Flat, the half-width of the dike swarm appears to be on the order of 200 m. In contrast, Gartner and Delaney (1988) mapped dike zones up to 5 km wide ($W = 2.5$ km) in the San Rafael volcanic field (Figure 8).

Given the spatial density of these igneous features, it is conservative to consider intersection of the area defined by Eq. (19) with the effective repository area as resulting in igneous disruption of the site. This definition of an igneous event, however, does not necessarily result in direct transport of radioactive waste to the surface by erupting magma.

4.1.4.4 Summary

All probability models for volcanic disruption of the proposed repository rely on estimation of parameters to bound the temporal and spatial recurrence rates and magnitudes of igneous events. Ranges of these parameters adopted in the volcanic hazard analysis must be justified using geologic data and models. Estimation of the temporal recurrence rate relies on the frequency of past volcanic events in the YMR. These past recurrence rates indicate volcanism

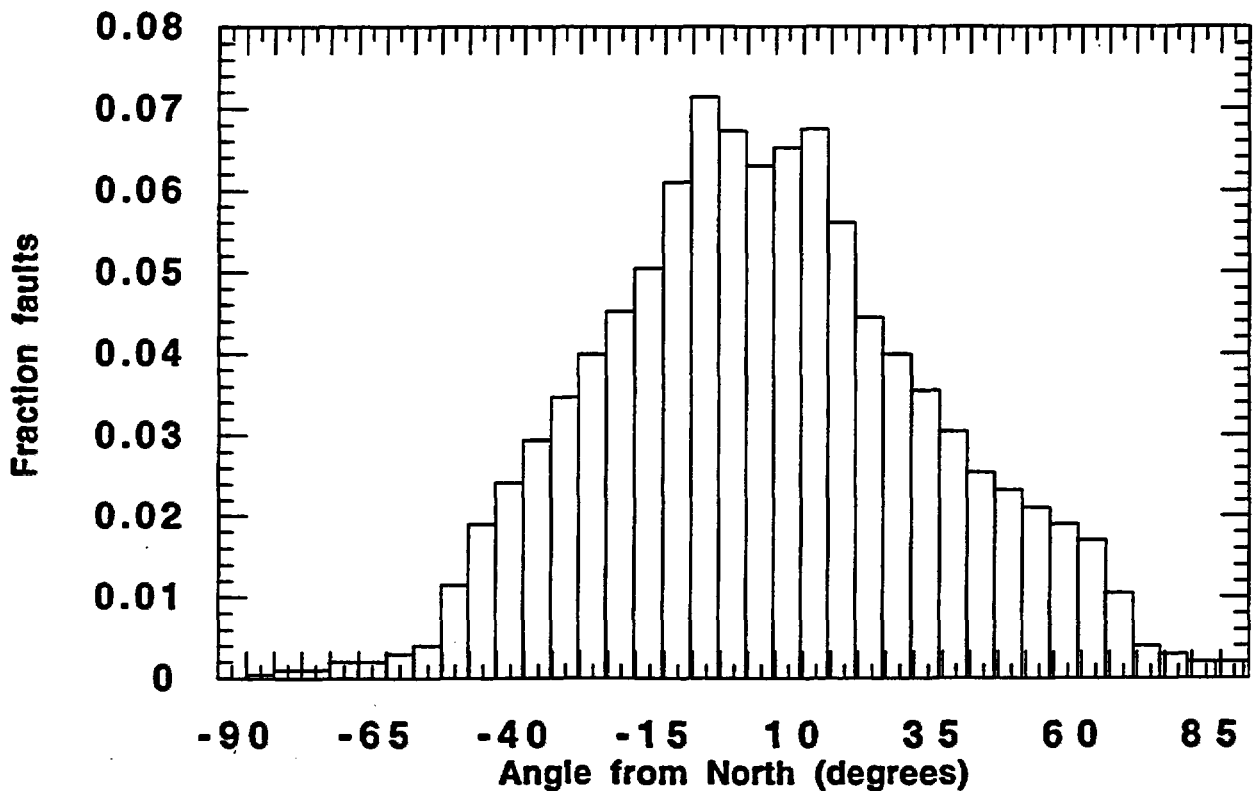


Figure 15. Distribution of the orientation of fault segments with respect to north. This distribution is weighted by fault segment length. Near the repository, $f_e(\phi)$ may vary as a function of this distribution of fault orientations if ascending magmas follow fault planes to the surface.

has persisted throughout the Pliocene and Quaternary at a low recurrence rate compared to many other Basin and Range volcanic fields. Therefore, such low temporal recurrence rates should be used to model probabilities. No evidence exists to indicate that basaltic volcanism has ceased in the YMR. Because the time elapsed since past volcanic eruptions within the YMR is short compared to common repose periods, the YMR should be considered a geologically active basaltic volcanic field, with recurrence rates greater than zero. Conversely, recurrence rates in the YMR are not as large as those in many other WGB volcanic fields, such as the Cima volcanic field where at least 30 volcanic eruptions have occurred since 1.2 Ma. Current evidence suggests that such an intense episode of volcanism is not likely in the YMR during the next 10,000 yr.

The temporal recurrence rate must be specified based on the definitions of igneous events. The current staff estimates for these recurrence rates are 2–12 v/m.y. for igneous events defined as individual mappable units or vents and 1–5 v/m.y. for vents and vent alignments. Temporal recurrence rate for igneous intrusions without volcanic eruptions is not estimated because data is not available to support such estimates. Based on analog data (Conway, et al., 1997), a factor of two or greater is probably reasonable.

Spatial recurrence rate varies across the YMR because of vent clustering and the tendency for volcanism to recur within these clusters. For example, all Quaternary volcanism in the YMR occurs in proximity to Pliocene volcanoes. Estimations of spatial recurrence rate then must rely on patterns in past volcanic activity, which is done using kernel models. Spatial recurrence rates of igneous events at the repository or elsewhere on Yucca Mountain that are assumed to be at or near zero are not supported by existing data. Yet, spatial recurrence rates of zero or a slightly larger than zero regional background value are assumed at the repository in some models presented in Geomatrix, 1996. Staff conclude that the distribution of sparse events does not provide an accurate basis to conclude that spatial recurrence rate within the repository boundary is zero or a low background value. Spatial analyses (e.g., Connor and Hill, 1995) indicate that the repository site is close to the edge of the Crater Flat cluster, within which most YMR Quaternary basaltic volcanism has occurred. A reasonably conservative model would, therefore, indicate that the spatial recurrence rate at the repository is greater than median spatial recurrence rates across the YMR.

Similarly, areas affected by igneous events must be described using parameter estimation, which will vary with the definition of igneous events. If igneous events are defined as individual mappable units and vents, then only those that erupt within the effective area of the repository significantly affect performance. Vent alignment lengths and orientations must be considered if igneous events are defined as vents and vent alignments. Vent alignment length is poorly constrained by available data, but its effect on probability is readily assessed using sensitivity studies. Alignment orientation is well constrained by the correlation between existing vent alignments and crustal stresses. Areas affected by igneous intrusions must be larger than areas affected by individual alignments, but the parameter distributions are poorly constrained.

4.1.5 Probability Criterion 5

4.1.5.1 Acceptance Criterion

Estimates of the probability of future igneous activity in the YMR will be acceptable provided that:

- The models are consistent with tectonic models proposed by NRC and DOE for the YMR.

4.1.5.2 Review Method

NRC staff should determine whether features of proposed probability models, such as boundaries of volcanic source-zones, patterns of vent distribution, and recurrence rate of igneous activity are consistent with tectonic models. It will be acceptable to use more than one tectonic model (consistent with the available data) to obtain an upper bound on probability. At a minimum, NRC staff should determine whether volcanic probability models are consistent with the range of tectonic models discussed in the Structural Deformation and Seismicity (SDS) KTI and used in resolution of other KTIs to assess phenomena such as seismic source characterization and patterns of groundwater flow.

4.1.5.3 Technical Basis

Probability models need to be consistent with tectonic models proposed for the YMR. Tectonic processes affect igneous processes across a large range of scales. Low recurrence-rate basaltic volcanic activity in the Basin and Range may occur where magmas are generated by decompression of fertile mantle during crustal extension (e.g., Bacon, 1982; McKenzie and Bickle, 1988). Magma ascent through the crust is enhanced by crustal structures produced by extension, leading to correlation between basaltic volcanism and structure across a range of scales, from the superposition of individual faults and vents to the occurrence of entire volcanic fields at the margins of extensional basins (Connor, 1990; Parsons and Thompson, 1991; Conway, et al., 1997). Volcanic hazard analysis of the proposed repository must quantify these often complex geological relationships.

The relationship between structure and volcanism has been used to suggest both higher and lower probabilities of volcanic disruption of the repository than are predicted using spatio-temporal patterns in vent distribution alone (Connor and Hill, 1995). Smith, et al. (1990) suggested a narrow northeast-trending structurally controlled source-zone of potential volcanism extends through the repository site, resulting in comparatively high probabilities of volcanic disruption. Alternatively, structure models that exclude the repository from volcanic source-zones result in comparably low probabilities. For example, Crowe and Perry (1989) proposed the north-northwest-trending CFVZ, with an eastern boundary located west of the repository site, effectively isolating the proposed repository. Thus, wide variation in probability estimates is a direct result of the varying ways in which these source zones have been drawn. Part of this dichotomy may be resolved if the relationships between volcanism and structure are considered mechanistically and in light of mapped YMR structural features. In the following, current understanding of these relationships is discussed in terms of:

- Regional tectonic models of Yucca Mountain and surrounding geologic features

- Mechanistic relationships between crustal extension and magma generation
- Local structural controls on magma ascent

4.1.5.3.1 Regional Tectonic Models

Yucca Mountain lies within the Basin and Range Province of the western North American Cordillera; a province characterized by spatially segregated regions of east-west extension between zones of northwest-trending dextral strike-slip or oblique strike-slip faults. Coupled with the overall pattern of crustal extension and transtension are numerous small-volume volcanic fields (Figure 16). Within this tectonic framework, five viable tectonic models that describe the pattern of regional and local deformation around Yucca Mountain emerge from all those that have been proposed in the geologic literature over the past two decades (Stamatakos, et al., 1997b). These five models are:

- Half-graben with deep detachment fault
- Half-graben with moderate depth detachment fault
- Elastic-viscous crust with planar faults with internal block deformation and ductile flow of middle crust
- Pull-apart basin (rhombochasm or sphenochasm)
- Amargosa shear or Amargosa Desert fault system

In a broad sense, these five models can be considered in two general categories of deformation. The first three are dominantly related to extensional deformation, and the latter are dominantly related to strike-slip deformation. Moreover, the five models are not mutually exclusive. Locally extensional-dominated deformation, within Crater Flat for example, can exist within a larger region of transtensional deformation related to a pull-apart basin.

In the deep detachment fault model (e.g., Ferrill, et al., 1996b), the Crater Flat-Yucca Mountain faults are envisioned as soling into the Bare Mountain fault at the base of the seismogenic crust, at approximately 15 km depth (Figure 17a). The faults at Yucca Mountain accommodate strain within the hanging wall of the Bare Mountain fault. This model is dominantly extensional and compatible with a regional strike-slip system in which the Crater Flat-Yucca Mountain domain has largely dip-slip faulting, similar to a pull-apart basin. In addition, the model respects the geologic constraints on the timing of deformation (i.e., variable dips of fault blocks with growth of tuff strata across faults that were active during tuff deposition), as well as rollover in fault blocks. Restored cross-sections, however, are more difficult to balance than with a moderate-depth detachment fault.

The moderate-depth detachment fault model (Young, et al., 1992; Ferrill, et al., 1995; Ofoegbu and Ferrill 1995) is similar to the deep detachment model, but the Crater Flat-Yucca Mountain

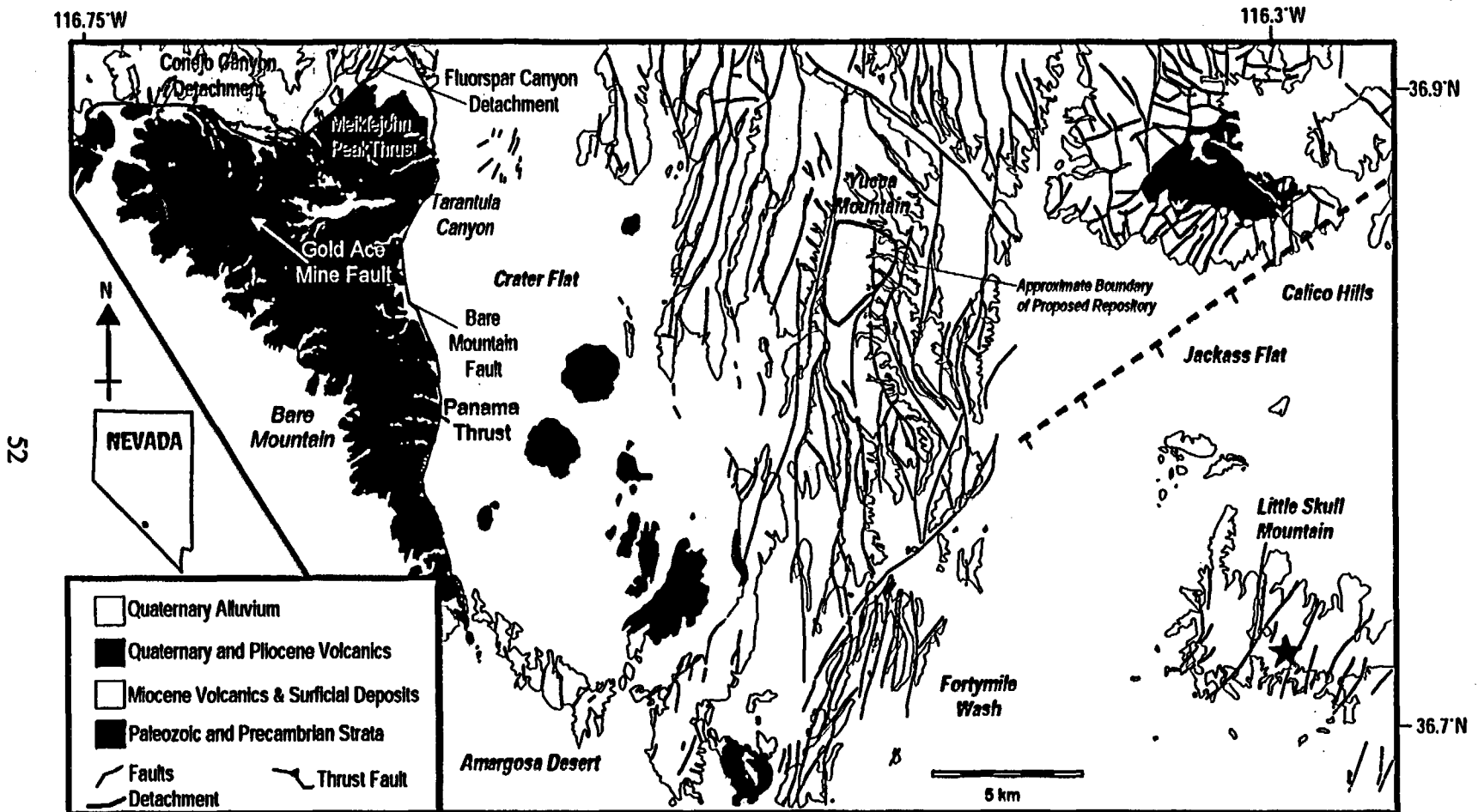


Figure 16. Simplified geologic map of the area around Yucca Mountain showing major geologic units, including Plio-Quaternary volcanoes and faults. From Ferrill, et al., 1996b.

faults sole into a detachment fault at 5–10 km depth (Figure 17b). The detachment then terminates against the deeper, larger Bare Mountain fault. The geometry of this model is the most reasonable for obtaining a balanced, restored cross-section of the upper crustal section.

Both shallow and moderately deep detachment models may influence basaltic magmatic activity in two ways. First, faults that sole into the detachment may serve as conduits for magma ascent in the shallow crust, if these faults provide relatively low-energy pathways to the

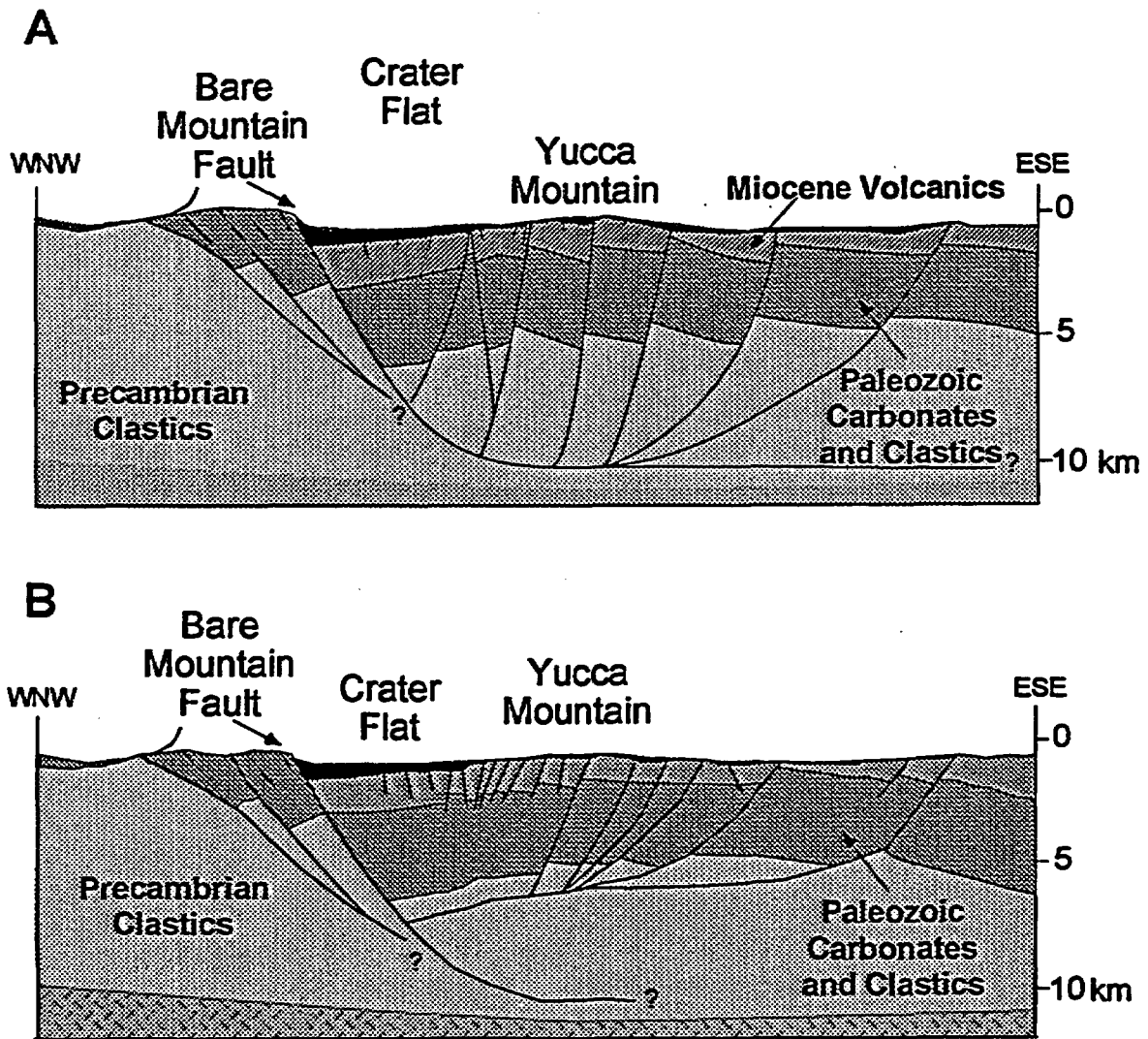


Figure 17. Two balanced cross sections across Bare Mountain, Crater Flat, and Yucca Mountain (from Ferrill, et al., 1996b). The cross sections differ in the depth of the detachment fault. High-angle normal faults at Yucca Mountain intersect this detachment at depths between 5 km (b) and 10 km (a). These high dilation-tendency faults may serve as pathways for ascending magmas.

surface (McDuffie, et al., 1994; Jolly and Sanderson, 1997). Second, dominantly extensional models result in large-scale density contrasts in the shallow crust. Relatively dense PreCambrian and Paleozoic rocks dominate the upper crustal section west of the Bare Mountain fault. East of the Bare Mountain fault, extension results in the formation of a half-graben and the upper crustal section is dominated by less dense tuffs and alluvium. This broad density contrast may influence rates of partial melting, a topic discussed in Section 4.1.5.3.2.

Alternatively, Crater Flat-Yucca Mountain faults have been interpreted as planar to the ductile middle crust (Fridrich, 1997). This is an extension dominant model; fault dips do not become more shallow with depth. This model, which serves as the conceptual basis for the United States Geological Survey boundary element model (Stamatakos, et al., 1997b), assumes the surface geometry of faults and fault blocks cannot be used to constrain deformation at depth. Internal fault-block deformation and ductile flow (and perhaps magma intrusion) at depth are assumed to compensate for variable fault-block dips, which would otherwise produce large triangular-shaped gaps in the subsurface.

The pull-apart basin model envisions Crater Flat as a pull-apart basin that formed in a releasing bend of a north-northwest-trending regional strike-slip system (Fridrich, 1997). The pull-apart basin is a half-graben with a well-defined western edge in the Bare Mountain fault, the diffuse set of Crater Flat-Yucca Mountain faults to the east, and an eastern edge in western Jackass Flats. The regional strike-slip system remains hypothetical, presumably buried beneath Amargosa Desert alluvium southeast of the southern end of the Bare Mountain fault. The pull-apart model explains the vertical axis rotation of the southern reaches of Crater Flat-Yucca Mountain (e.g., Hudson, et al., 1994) as crustal-scale block rotations within overall regional dextral shear. This shear is related to diffuse boundary interactions between the North American and Pacific plates. The model explains the north-northeast arcuate trend of Quaternary volcanic centers of Crater Flat as an alignment along a Reidel shear within the basin.

Fridrich (1997) has proposed two versions of this model. In the rhombochasm version of the pull-apart model, the basin-bounding strike-slip fault trends north-northwest out of Crater Flat and is concealed beneath the Timber Mountain-Oasis Valley calderas. In the sphenochasm version, the northern extent of the bounding strike-slip fault is pinned at the northern end of Crater Flat. Strike-slip deformation increases south and east from the pin point. In response, the basin fans open to the south, and extension on basin bounding normal faults like the Bare Mountain fault increases southward (Scott, 1990; Stamatakos, et al., 1997a).

The Amargosa shear model is similar to the rhombochasm model, with Crater Flat representing a diffuse dextral shear-zone along a major north-northwest-trending crustal shear (e.g., Schweickert and Lahren, 1997). The shear zone extends northward along a hypothetical strike-slip fault extending north-northwest from Crater Flat beneath the Timber Mountain and Oasis Valley calderas. The lack of offset of these calderas is explained as diffuse detachment of the tuffs from underlying crust, in which offset is absorbed by horizontal faults within the tuff layers (Hardyman and Oldow, 1991). The southern extension of the shear links with the Stewart Valley-State Line fault. Total length of the fault and shear zones is greater than 250 km.

The Crater Flat shear zone includes the motion on faults within western Bare Mountain, the

vertical axis rotation within southern Yucca Mountain, and the sites of volcanic activity in Crater Flat. The Quaternary cone alignment is believed to represent a Reidel shear oblique to the main shear axis. Based on a palinspastic reconstruction between southern Bare Mountain and the Striped Hills, this model calls for >30 km of right-lateral offset along the southern extension of this shear since 11.5 Ma (Schweickert and Lahren, 1997). This aspect of the model is suspect because of disparate exhumation ages for Bare Mountain and the Striped Hills, based on fission-track ages (Ferrill, et al., 1997) and paleomagnetic results (Stamatikos, et al., 1997c).

Strike-slip dominated models have been used to infer an entirely different basis for distribution of volcanoes in the YMR other than purely extensional models. For example, Schweickert and Lahren (1997) envision a relatively uniform melt generation region beneath the YMR. In these circumstances, crustal structures such as Reidel shears in pull-apart basins allow magmas to ascend to the surface. Fridrich (1997) also proposed that tensional structures control the ascent of magma through the crust and that volcanism will be limited to areas where these tensional structures exist. Some source-zone probability models (e.g., Crowe and Perry, 1989) propose that Yucca Mountain lies outside of pull-apart basins, and, therefore, the probability of volcanism at Yucca Mountain is extremely low compared with Crater Flat. As noted above, however, the strike-slip fault on the eastern edge of the pull-apart has not been mapped or identified. This lack of direct geologic evidence for a bounding fault on the east side of Crater Flat basin greatly reduces the confidence with which such source zones for basaltic volcanism can be drawn.

Elements of the above tectonic models are not mutually exclusive. For example, predominately strike-slip deformation may have given way to predominantly extensional deformation as regional shear resulted in rotation of the direction of maximum horizontal compressional stress relative to fault planes. In light of these models, it is appropriate to consider mechanistic relationships between crustal extension in the YMR and basaltic magma generation. These relationships rely on a physical link between regional extension of the brittle crust and magma production deeper in the lithosphere.

4.1.5.3.2 Mechanistic Relationships Between Crustal Extension and Magma Generation

Crustal extension controls or strongly influences basaltic magmatism in the WGB (e.g., Leeman and Fitton, 1989; Lachenbruch and Morgan, 1990; Pedersen and Ro, 1992). Magmas that originate in WGB lithospheric mantle, including those of the YMR, were likely produced through decompression melting associated with extension (Farmer, et al., 1989; Hawkesworth, et al., 1995). Decompression melting is favored in zones of mantle lithosphere that have been previously enriched in incompatible elements, which enables melt formation at lower temperatures (e.g., McKenzie and Bickle, 1988). Based on mineralogical phase relationships and geochemical studies, decompression-induced lithospheric melting likely occurs at depths between 40–80 km (Takahashi and Kushiro, 1983; Rogers, et al., 1995). Extension and associated crustal deformation will produce local changes in lithostatic pressure at the base of the crust. Variations in lithostatic pressure produced through this extension may decompress enriched zones in lithospheric mantle sufficiently to partially melt and produce basaltic magma. Thus, lateral changes in lithostatic pressure across the YMR may control areas of future igneous activity.

Crustal extension has resulted in large density differences in the upper 5–6 km of the crust in the YMR due to the displacement of Paleozoic and PreCambrian rocks across the Bare Mountain fault, the formation of the Crater Flat basin, and subsequent deposition of tuff and alluvium in Crater Flat (Figure 18). The average density of a 5.6-km column of rock beneath Crater Flat and Bare Mountain can be calculated from this cross-section using average rock densities for the region (McKague, 1980; Howard, 1985). This difference in average density is 280 kg m^{-3} . Beneath this 5.6-km column, little density difference is expected because any faulting that occurs below 5.6 km does not juxtapose rocks of significantly different densities.

Given lithostatic pressure as

$$P_L = \int_0^z \rho(z)g \, dz \quad (20)$$

where g is gravity (9.8 m/s^2), $\rho(z)$ is rock density at a given depth z , and z is the total depth

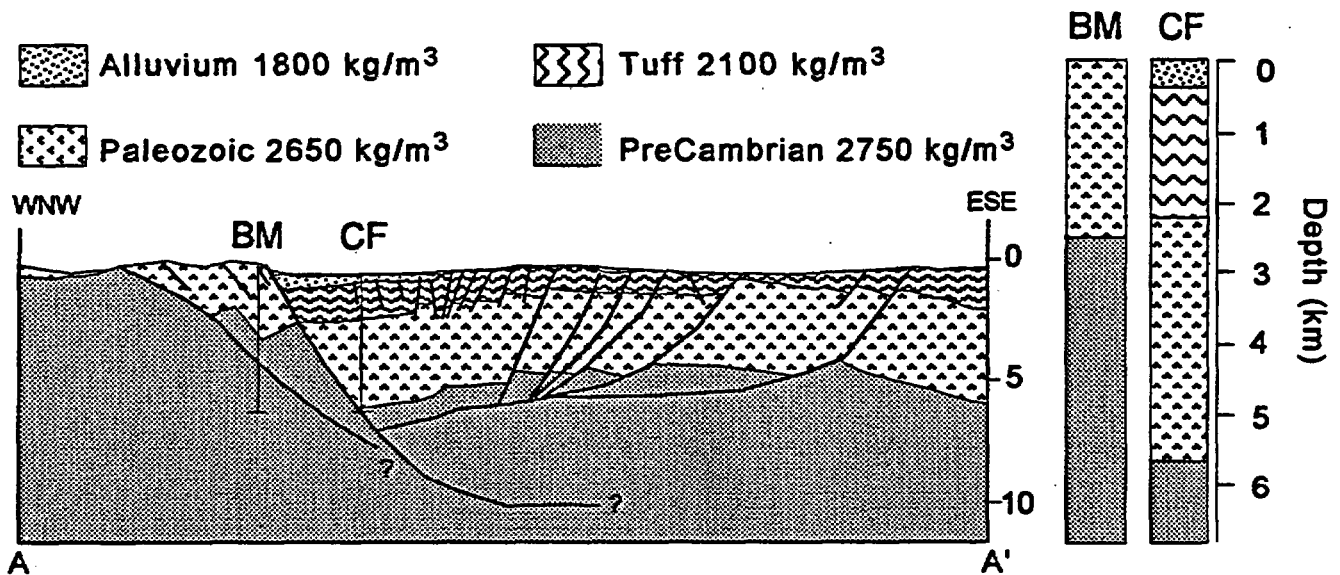


Figure 18. Comparison of density profiles beneath Bare Mountain (BM) and Crater Flat (CF). Profiles are constructed using a balanced cross-section (Ferrill et al., 1996b) and density values from McKague (1980) and Howard (1985). Density differences are assumed to be negligible beneath 5.6 km.

(5.6 km), this density difference in the upper crust produces a lithostatic pressure difference between Bare Mountain and Crater Flat of approximately 15 MPa at a depth equivalent to the base of the Paleozoic section in Crater Flat. This lithostatic pressure estimate excludes topographic effects, because these effects attenuate rapidly with depth (Anderson, 1989).

Lateral changes in density at the surface, such as those produced by topographic variations or the development of a basin, attenuate with depth because of changes in the magnitudes of horizontal stresses relative to vertical stress as a function of depth. In this case lithostatic pressure is best estimated as:

$$P = -\frac{1}{3}(\sigma_{xx} + \sigma_{yy} + \sigma_{zz}) \quad (21)$$

where σ_{xx} , σ_{yy} , and σ_{zz} are the orthogonal normal stresses.

Because of this attenuation, comparatively large-scale density variations are required to create lateral pressure changes in the mantle. Furthermore, lateral density contrast in the crust will cause lateral pressure changes in the mantle only if the Moho discontinuity is not deflected as a result of isostatic compensation (Figure 19). Isostatic compensation is not likely because the scale of features like Bare Mountain and Crater Flat are small compared to the scale of features normally compensated for by isostasy (Anderson, 1989). Existing geophysical data (Brocher, et al., 1996) support a flat Moho discontinuity in the YMR.

Bouguer gravity anomalies indicate that large-scale crustal density variations necessary to produce pressure variation in the mantle at >40 km occur in the YMR (Figure 20). The gravity map is dominated by large negative anomalies produced by Timber Mountain-Oasis Valley calderas and a positive gravity anomaly associated with the Funeral Mountains. A north-trending area of largely negative gravity anomalies extends through Crater Flat and the Amargosa Desert.

These gravity data can be used to create an apparent crustal density map, following the methods of Gupta and Grant (1984), and to infer changes in apparent lithostatic pressure, ΔP_L , at comparatively shallow depths. Construction of the apparent density, or ΔP_L , map from the gravity data requires several assumptions:

- The gravity data must be on a regular grid. In this case, the gravity data were interpolated to a regular grid using a minimum tension bicubic-spline gridding algorithm.
- All density variation occurs due to lateral density variation between grid points. Density is taken to be constant between the surface and a depth, Z , within each grid cell. Density variations in the Earth below Z are not considered to contribute to the gravity anomalies.
- The method assumes a horizontal ground surface. The YMR gravity data have been reduced to a Bouguer anomaly, meaning density variations produced by topography

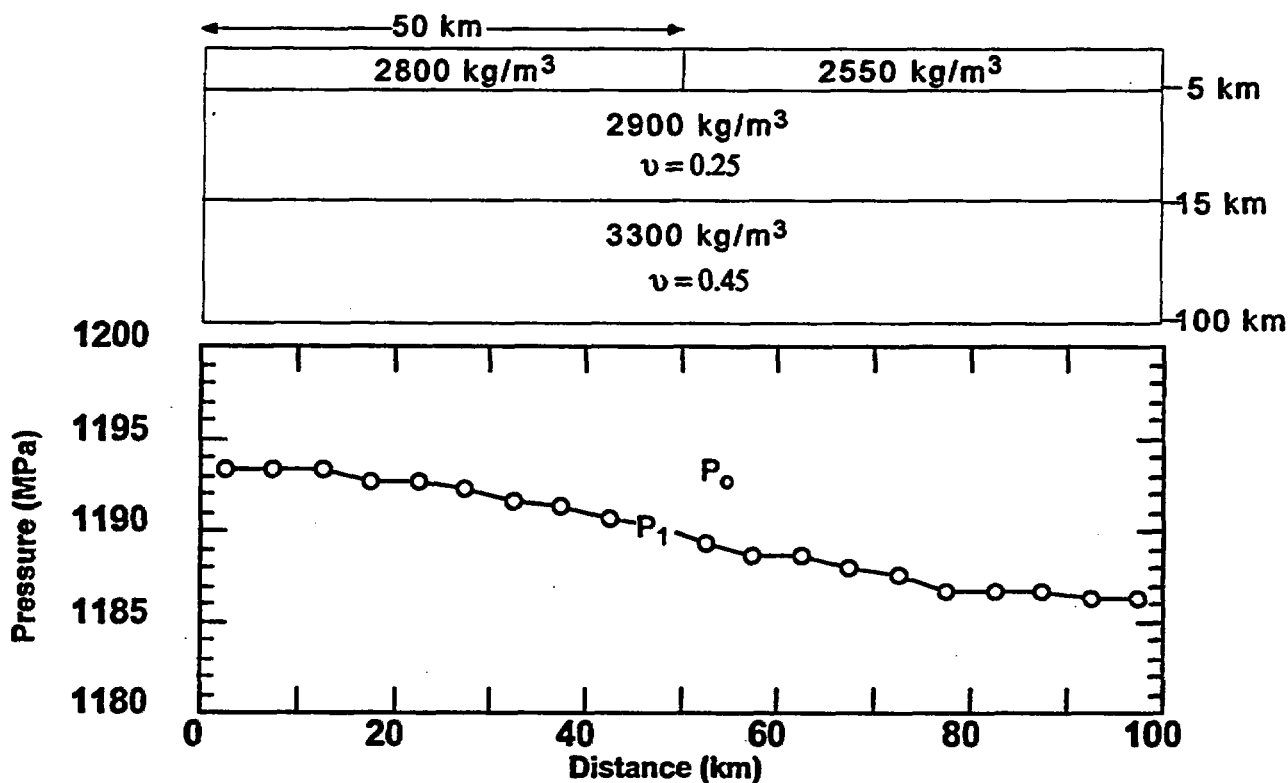
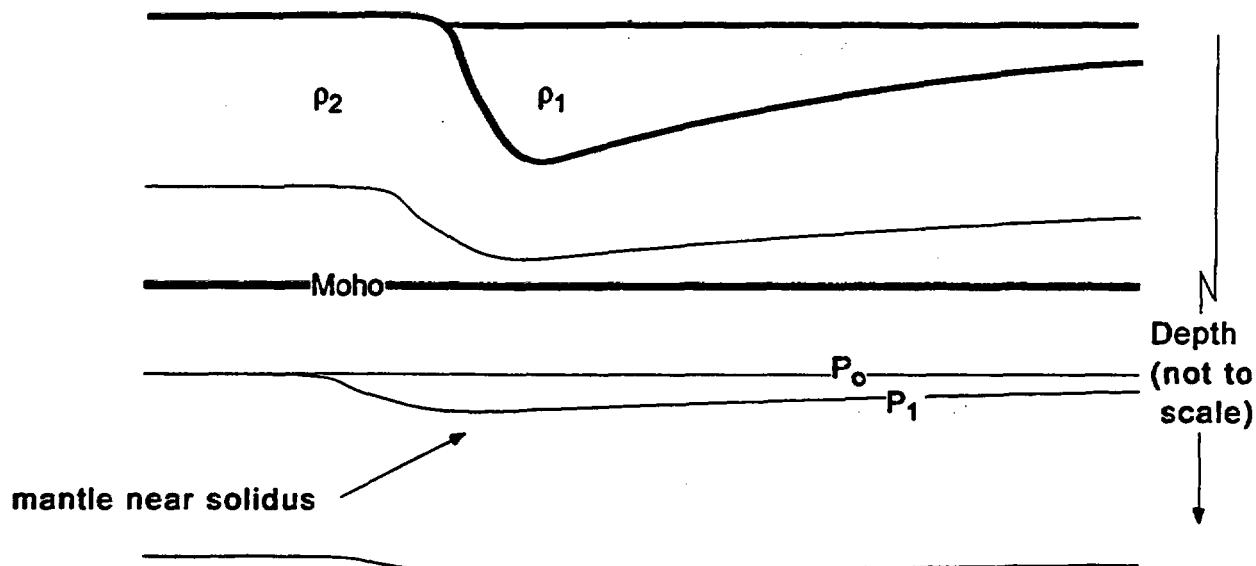


Figure 19. Conceptual model of melt generation in response to crustal extension.
(a) [upper Figure] Extension results in lateral density contrast in the crust that deflects iso-pressure surfaces downward to P_1 from their initial depth P_0 . This local decrease in pressure results in the partial melting of near-solidus mantle. A simple finite element model **(b) [lower Figure]** indicates that pressure changes of 7 MPa are expected at depths of 40 km in response to large density variations in the upper 5 km of the crust, using the bulk densities and values of Poisson's ratio, ν , indicated.

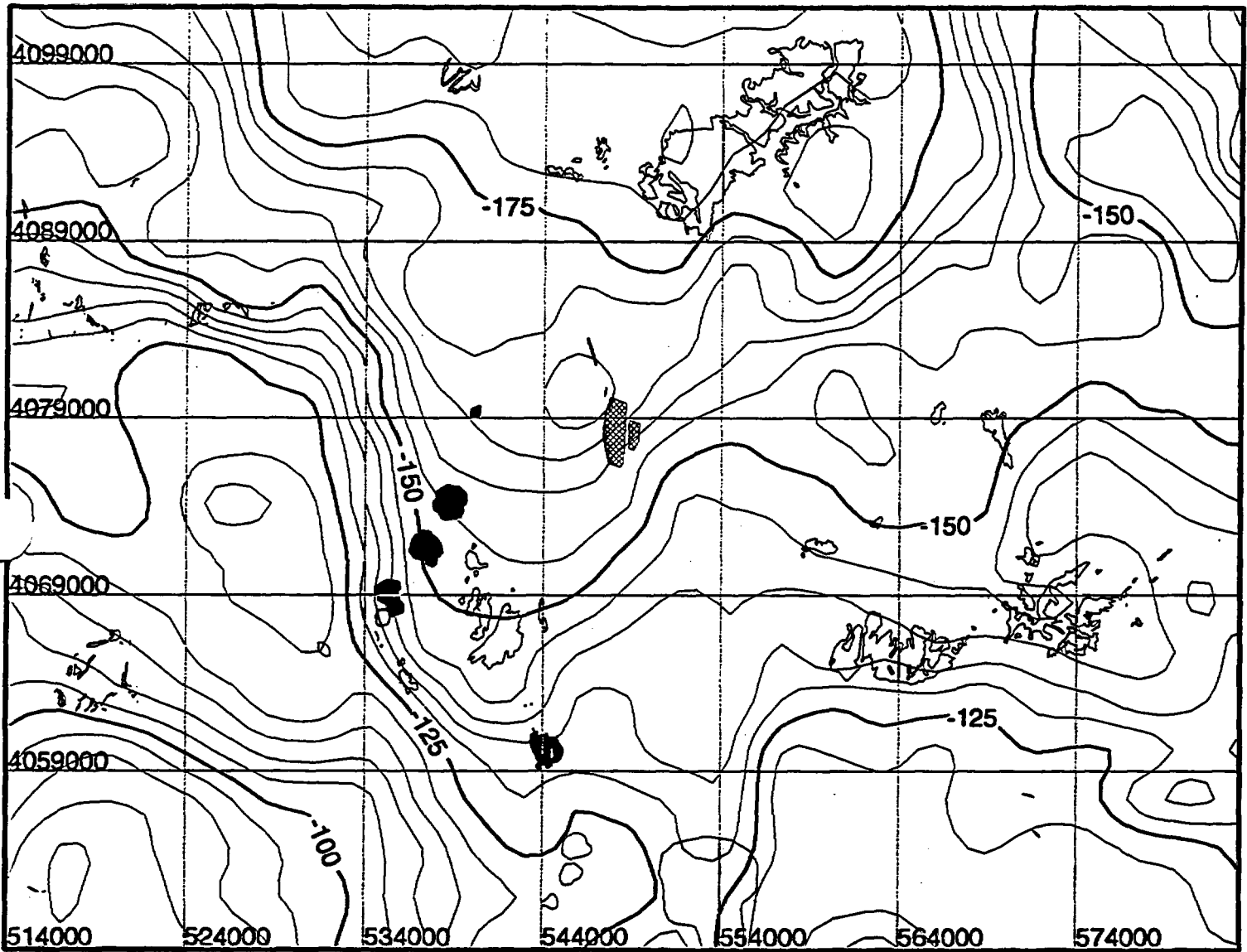


Figure 20. Bouguer gravity anomaly map of the Yucca Mountain region. Data compiled from numerous sources and obtained from the Geophysics Data Repository at Lawrence-Berkeley Laboratory.

and altitude effects have been removed from the gravity map. Using this data set results in lower density variation than expected if topography is factored into the calculation. However, topographic effects have relatively short wavelengths, do not produce significant pressure differences at depths of magma generation, and, therefore, may be neglected.

Using the notation of Gupta and Grant (1984), the gravity anomaly at a point, $\Delta g(x,y)$, at the surface due to density variation at a point, $\Delta\rho(\xi,\eta,\zeta)$ beneath the surface, is:

$$\Delta g(x,y,0) = G \left\{ \frac{\partial}{\partial z} \int_{-\infty}^{\infty} \int_{-\infty}^{\infty} \int_0^z \frac{\Delta\rho(\xi,\eta)d\zeta d\eta d\xi}{\sqrt{(x-\xi)^2 + (y-\eta)^2 + (z-\zeta)^2}} \right\}_{z=0} \quad (22)$$

where G is the universal gravitational constant. Note that in this formulation density does not vary as a function of depth. All density variation is lateral, and the amplitude of the gravity anomaly changes with depth of the anomalous mass only because of the change in distance from the mass anomaly to the gravity meter. Only the vertical component of the gravity anomaly is considered because this is measured by the gravity meter. Differentiating with respect to z gives

$$\Delta g(x,y,0) = G \int_{-\infty}^{\infty} \int_{-\infty}^{\infty} \int_0^z \frac{-\Delta\rho(\xi,\eta)d\zeta d\eta d\xi}{[(x-\xi)^2 + (y-\eta)^2 + \zeta^2]^{3/2}} \quad (23)$$

then integrating across depth

$$g(x,y,0) = G \int_{-\infty}^{\infty} \int_{-\infty}^{\infty} \frac{\Delta\rho(\xi,\eta)d\eta d\xi}{\sqrt{(x-\xi)^2 + (y-\eta)^2}} - G \int_{-\infty}^{\infty} \int_{-\infty}^{\infty} \frac{\Delta\rho(\xi,\eta)d\eta d\xi}{\sqrt{(x-\xi)^2 + (y-\eta)^2 + Z^2}} \quad (24)$$

which expresses the change in gravity in terms of the horizontal distance between the gravity meter and the density anomaly, and the average anomalous density averaged between the surface and depth Z . Because all gravity variations are assumed to result from lateral variations in density, the relationship between gravity anomalies and apparent density anomalies can be expressed using a 2D Fourier transform of the gravity data. The 2D Fourier transform of the gravity field is given by:

$$\Delta g(u,v) = \int_{-\infty}^{\infty} \int_{-\infty}^{\infty} \Delta g(x,y,0) \exp^{i(ux + vy)} dy dx \quad (25)$$

where u and v are wave numbers. Gupta and Grant (1984) developed a simple filter to relate density and gravity in the wave number domain, based on the wavelengths of anomalies:

$$\Delta\rho(u,v) = \frac{1}{2\pi G} \times \frac{\bar{\omega}}{1 - \exp^{-Z\bar{\omega}}} \times \Delta g(u,v) \quad (26)$$

where

$$\tilde{\omega} = \sqrt{u^2 + v^2} \quad (27)$$

The inverse Fourier transform then yields apparent density in the spatial domain:

$$\Delta\rho(x,y) = \frac{1}{2\pi G} \int_{-\infty}^{\infty} \int_{-\infty}^{\infty} \frac{\tilde{\omega}}{1 - \exp^{-Z\tilde{\omega}}} \Delta g(u,v) \, dv du \quad (28)$$

The change in lithostatic pressure across the map region is then

$$\Delta P_z(x,y) = \Delta\rho(x,y)gZ \quad (29)$$

where g is now the average gravitational acceleration, 9.8 m s^{-1} , and Z is the thickness of the crust within which all density changes are assumed to have occurred. Again, no significant density changes, in terms of overall change in lithostatic pressure, are assumed to occur at depths greater than Z .

For $Z = 5000 \text{ m}$, $\Delta\rho(x,y)$ varies from approximately -100 to $+240 \text{ kg m}^{-3}$ across the YMR (Figure 21). The apparent density contrasts across the Bare Mountain fault in southern Crater Flat of $240\text{--}280 \text{ kg m}^{-3}$ are in agreement with density contrasts obtained from the balanced cross-section and measured density values in the region (Figure 18). The most prominent feature of this map is the abrupt change in apparent density from high values west of the Bare Mountain fault to low values east of the Bare Mountain fault. Although this change is most abrupt adjacent to the Crater Flat basin, the apparent density map also reveals that this change persists south of Bare Mountain into the Amargosa Desert, and north of Bare Mountain. The apparent density map also shows that this change in density across the Bare Mountain fault is a long-wavelength feature. Apparent density values remain low east of the Bare Mountain fault for at least 50 km and high west of the Bare Mountain fault to the edge of the gravity map (Figure 21).

Because the magnitude of lateral pressure change will attenuate as a function of depth, only long-wavelength density variations in the crust will produce pressure changes in the mantle at depths of $40\text{--}80 \text{ km}$, the probable depth of magma generation in the YMR. The magnitude of pressure variations resulting from crustal density contrasts calculated across the Bare Mountain fault can be explored using finite element analysis. Based on a simplified geometric representation of the development of the basin, lateral pressure variations on the order of 7 MPa are expected to occur at depths of 40 km (Figure 19), attenuating to 2 MPa at a depth of 80 km , and $\ll 1 \text{ MPa}$ at 100 km . Mantle rocks at depths of $40\text{--}100 \text{ km}$ are under average lithostatic pressures of $1000\text{--}3000 \text{ MPa}$. Thus, a change of $2\text{--}7 \text{ MPa}$ across the density discontinuity represents a small fraction of the total pressure at that depth. This small difference reinforces the idea that extension and deformation of the magnitude observed in the YMR can only result in renewed magmatism if mantle rocks are already near their solidus (Figure 19).

Observations of the distribution of volcanoes in the YMR suggest that these small lithostatic pressure differences are sufficient to generate basaltic melt. Plio-Quaternary volcanoes lie in

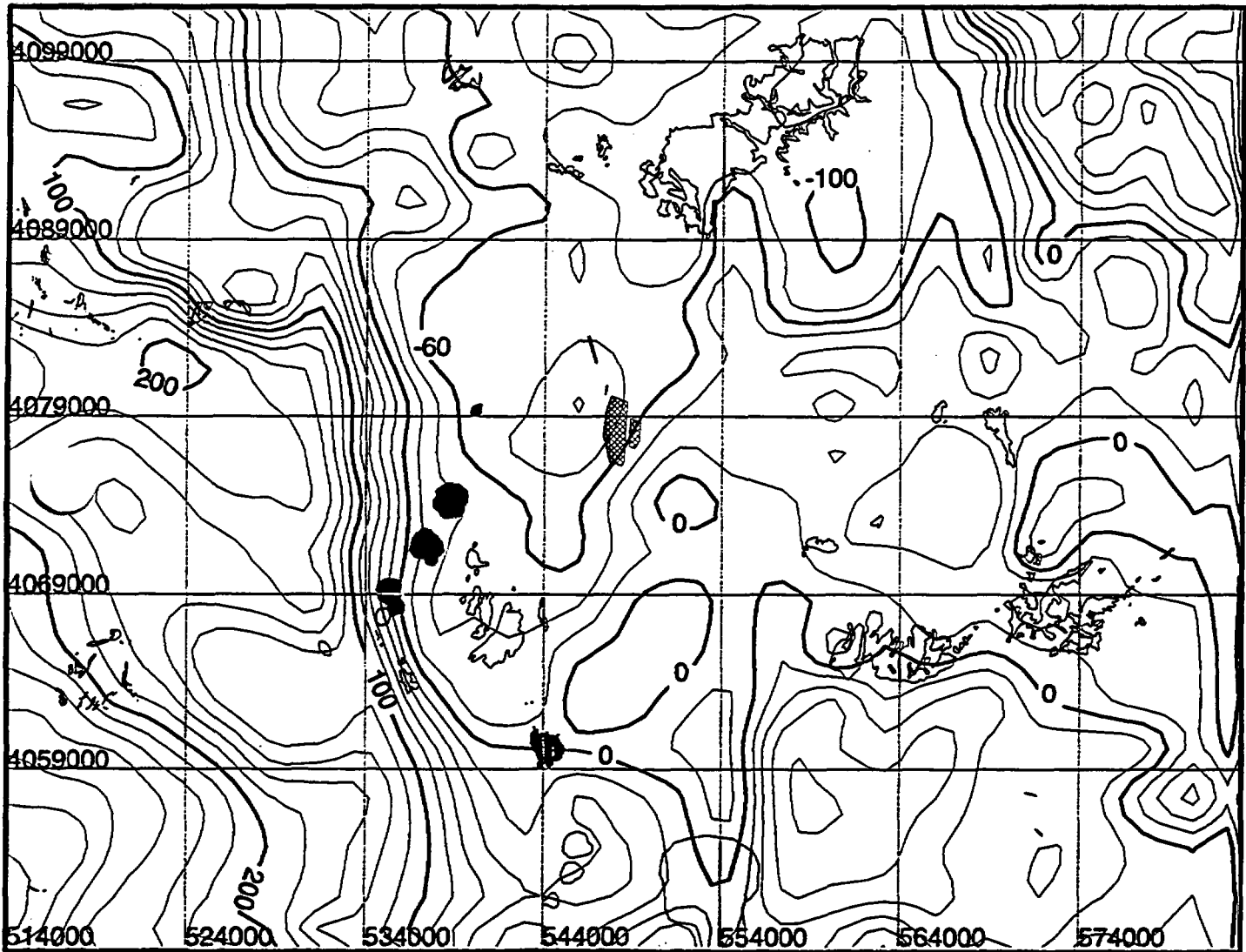


Figure 21. Apparent density variation across the Yucca Mountain region, derived from gravity data. Change from the mean apparent density in the map area is contoured in kg m^{-3} . Volcanoes tend to occur in areas of relatively low average density, east of the Bare Mountain fault.

the lower $\Delta P_L(x,y)$ areas east of the Bare Mountain fault, as expected if decreases in lithostatic pressure result in production of partial melts in the YMR. Nearly all of these volcanoes occur within the gravity low, which, in part, defines the Amargosa Gravity Trough (O'Leary, 1996) (Figure 20). Topographically, Lathrop Wells cinder cone lies outside Crater Flat but, based on gravity data, is within the larger north-trending basin and at the margin of the prominent basement low in southernmost Crater Flat. Aeromagnetic anomalies (Langenheim, et al., 1993) in the Amargosa Desert produced by buried Pliocene(?) basalts also lie within or at the margins of the southern extension of this basin. The easternmost of these buried basalts lies close to the north-trending gravity anomaly demarcating the eastern edge of the Amargosa Desert alluvial basin in this area.

These YMR volcanoes erupted in areas of lower $\Delta P_L(x,y)$ than expected if eruptions occurred randomly throughout the map area. In fact, only one Plio-Quaternary volcano erupted where $\Delta P_L(x,y) > +2$ MPa, and this volcano, Aeromagnetic Anomaly E (Appendix A), erupted in a high gravity-gradient area along the southern projection of the Bare Mountain fault. These observations suggest that long-wavelength density differences in the YMR, dominated by displacement across the Bare Mountain fault and its apparent extension south into the Amargosa Desert, are sufficient to produce the pressure changes in the mantle that cause partial melting and volcanism.

This lithostatic pressure model suggests a correlation between the timing of extension and the timing of volcanism. Magma generated in response to extension, resulting in Quaternary volcanism within vent clusters formed by Miocene and Pliocene basaltic volcanism, occurred because mantle rocks beneath these regions were near their solidus and partially melted when comparatively small amounts of extension took place. A given rate of extension will result in the greatest rate of change in mantle pressure directly beneath the lateral change in crustal density, such as at the Bare Mountain fault. Thus, with continuing extension, mantle in the region of this inflection has the greatest opportunity of producing partial melts as a result of a given amount of crustal extension. Episodes of extension and basaltic volcanism may correlate temporally, because pressure variations in the mantle will likely equilibrate due to ductile flow over time. In other words, pressure changes in the mantle that result from crustal extension will be transitory.

Change in lithostatic pressure also affects magmatism because magmas ascend by buoyant rise. The buoyancy forces acting on the magma are equivalent to the hydrostatic pressure gradient, given by Lister and Kerr (1991) as:

$$P_h = \int_0^z (\rho_{\text{rock}}(z) - \rho_{\text{magma}}) g \, dz \quad (30)$$

where ρ_{rock} and ρ_{magma} are densities of rock and magma, respectively, g is gravitational acceleration, and Z is the depth of magma generation. Rock density varies as a function of depth, most dramatically at the Moho. Because the density of magma is typically less than that of mantle, but greater than most crustal rocks, a level of neutral magma buoyancy exists in the crust. An isolated pod of magma above the level of neutral buoyancy sinks and a pod below the level of neutral buoyancy rises. Magmas fed by conduits respond to the integrated hydrostatic pressure along the conduit but also have flow characteristics that respond to the

local hydrostatic pressure. Thus, dikes propagate laterally above the level of neutral buoyancy (Lister and Kerr, 1991). The level of neutral buoyancy is deeper in the crust beneath basins than beneath mountains. As Quaternary basalts in the YMR demonstrate, basalts do not stagnate in the alluvial basins as they rise through them because hydrostatic pressure is integrated over the depth from origination of the melt. Longer dikes and dike swarms, however, preferably form in these alluvial basins because of the basins' comparatively low lithostatic pressure. Thus, from the perspective of volcanic hazards analysis, understanding changes in lithostatic pressure across the region constrains areas of likely melt generation and areas of likely dike propagation above the level of neutral buoyancy.

4.1.5.3.3 Local Structural Controls on Magma Ascent

Observations in the YMR indicate a strong correlation between structure and volcanism. These observations include vent alignments (Smith, et al., 1990; Connor, et al., 1997) and cinder cones along faults (Section 4.1.4 and Connor, et al., 1997). These observations suggest that structural influences should be considered in probabilistic volcanic hazard analysis of the proposed repository.

Basaltic magmas are transported from the mantle to higher levels in the crust or to the surface by igneous dikes. Propagating dikes, like other hydraulic fractures, typically form perpendicular to the least principal stress and parallel to the principal horizontal stress in extensional terrains (Stevens, 1911; Anderson, 1938).

Under some conditions, pre-existing faults or extension fractures serve as pathways for magma instead of propagating a new dike-fracture. Assuming that a pre-existing fault or extension fracture has no tensile strength, pre-existing fractures dilate (i.e., capture magma) if the fluid pressure exceeds the normal stress resolved on that fracture (Delaney, et al., 1986; Reches and Fink, 1988; Jolly and Sanderson, 1997). The likelihood of dilation and capture is controlled by the magnitude of the three principal stresses (σ_1 , σ_2 , σ_3), fluid pressure, and orientations of pre-existing fractures in the *in situ* stress field.

The ability of any fault or fracture to dilate during magma injection is directly related to the normal stress acting across the fracture. Assuming cohesionless faults, the relative tendency for a fault of a given orientation to dilate in a given stress state (i.e., dilation tendency) can be expressed by comparing the normal stress acting across the fault with the differential stress (e.g., Morris, et al., 1996).

Dilation tendency of the fault is expressed as:

$$T_d = \frac{(\sigma_1 - \sigma_n)}{(\sigma_1 - \sigma_3)} \quad (31)$$

where σ_1 and σ_3 are the maximum and minimum compressional stresses, respectively, and σ_n is the normal stress acting across the fracture. Faults with T_d greater than some threshold value, such as 0.8, are considered to have a high-dilation tendency (Morris, et al., 1996). A Schmidt plot of dilation tendency and fault poles indicates that, in the YMR region, faults oriented 355°–085° with dips >50° have a high dilation-tendency (Figure 22).

In the YMR region, σ_1 is vertical, σ_2 is horizontal and oriented 028° , and σ_3 is horizontal and oriented 298° (Morris, et al., 1996). The relative magnitudes of $\sigma_1:\sigma_2:\sigma_3$ are estimated to be 90:65:25. As a result of this stress pattern, steeply dipping north-northeast-trending faults have a greater dilation tendency than faults of other orientations. Areas with higher concentrations of high dilation-tendency faults, therefore, are more likely to be the areas of volcanic activity. Cinder cone alignments form over prolonged periods of time if high dilation-tendency faults repeatedly serve as conduits for magma ascent (e.g., Conway, et al., 1997).

McDuffie, et al. (1994) provide analytical results that show that the ability of a fault or fault zone to redirect ascending magma depends on the depth at which the dike intersects the fault and the dip of the fault zone. Only high-angle faults with dips greater than $40\text{--}50^\circ$ are capable of dike capture at depths below 1 km. At depths of 10 km, faults dipping at angles less than 70° do not provide low-energy pathways to the surface compared to vertical dike propagation.

Steeply-dipping high-dilation-tendency faults in the YMR include many faults that bound the Yucca Mountain block, such as the Solitario Canyon and Ghost Dance faults. The Solitario Canyon fault adjacent to the repository site hosted dike injection at approximately 10.9 Ma.

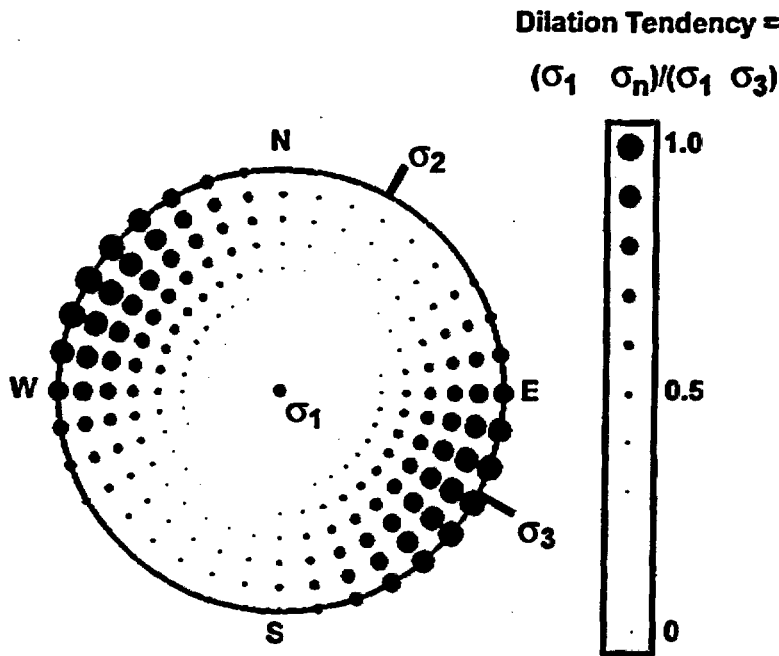


Figure 22. Schmidt plot of fault dilation tendency for Yucca Mountain region stresses. High dilation-tendency faults are oriented $355^\circ\text{--}085^\circ$ with dips greater than 50° (cf. Figure 15).

Moreover, the Solitario Canyon fault extends to the detachment fault at depths of 5–10 km (Figure 16). The distribution of faults with relatively high potentials for acting as magma conduits can be inferred from geologic mapping. In areas of alluvial cover, gravity and magnetic data provide the best indication of the distribution of these faults (e.g., Connor, et al., 1996).

4.1.5.4 Summary

Tectonic setting is important to consider in volcanic hazard analyses at several scales. On regional scales, crustal extension results in changes in pressure in the mantle and gives rise to partial melting. Extension also results in the formation of dip-slip fault systems, which serve as conduits for magma rise. On local scales and at shallow depths, individual dikes may propagate along faults that have high dilation-tendencies and dike lengths may be controlled in part by local lithostatic pressure. Field investigations in the YMR have shown that all of these factors operate in the YMR, partially controlling the distribution and timing of basaltic volcanism.

Sufficient evidence exists to indicate basaltic volcanism in the WGB is linked to crustal deformation. Currently, several tectonic models are in use for the YMR, including detachment fault, simple horst and graben, Amargosa shear, and pull-apart models. Some commonality exists among these models with regard to basaltic volcanism. In particular, all of these models evaluate Crater Flat as an extensional half-graben, bounded on its western margin by the Bare Mountain fault. This structural basin appears to localize volcanism. Detachment fault, pull-apart, and Amargosa shear models all characterize the Bare Mountain fault as a major structure, transecting the brittle crust. The occurrence of the Bare Mountain fault can impact basaltic volcanism at several scales. On a regional scale, the Bare Mountain fault creates a substantial density contrast in the brittle crust. This density contrast causes changes in lithostatic pressure in the mantle that may induce partial melting. The Bare Mountain fault also may serve as a conduit for magma ascent through the brittle crust. The planar fault model is closer to a classical Basin and Range model of horst and graben formation (e.g., Stewart, 1971) than other tectonic models proposed for the YMR. However, this model shares elements with the other tectonic models in that the Bare Mountain fault is a major structure and Crater Flat basin is formed by extension. All of the tectonic models proposed to date include Yucca Mountain in the same structural domain as Crater Flat (O'Leary, 1996; Fridrich, et al., 1997; Schweikert and Lahren, 1997; Young, et al., 1992; Ferrill, et al., 1995; Ofoegbu and Ferrill, 1995; Stamatakos, et al., 1997a).

Results of a number of analyses indicate that incorporation of tectonic models into probability studies increases the probability of volcanic disruption of the proposed repository site compared to models that do not account for the tectonic setting of the site explicitly (Connor, et al., 1996; Hill, et al., 1996). This result primarily reflects the fact that Yucca Mountain is structurally part of the Crater Flat basin, with high dilation-tendency faults bounding and penetrating Yucca Mountain itself. Because of the presence of these structures, the lower limit on probability is represented by the nonhomogeneous Poisson models that do not incorporate structure. Probability models that incorporate tectonic features (e.g., the modified kernel model) are similar to some source-zone models in that the probability surface is elongate in a north-northwest direction, similar to the CFVZ proposed by Crowe and Perry (1989). The same tectonic features that enhance the probability of volcanism in Crater Flat, however, increase the

probability of volcanism at Yucca Mountain, albeit to a lesser degree.

On local scales and at shallow depths, individual basaltic dikes may propagate along faults that have high-dilation tendencies. Dike lengths may be in part controlled by local hydrostatic pressure. Field investigations in the YMR have shown that all of these factors may operate in the YMR, partially controlling the distribution, and possibly the timing, of basaltic volcanism. There is general agreement that volcano distribution is affected by local structural control. Dikes and vent alignments tend to be oriented northeast throughout the region in response to horizontal stresses in the crust. Northeast trends have been accounted for in most analyses (e.g., Geomatrix, 1996; Smith, et al., 1990; Connor, et al., 1997).

4.1.6 Probability Criterion 6

4.1.6.1 Acceptance Criterion

Estimates of the probability of future igneous activity in the YMR will be acceptable provided that:

- The probability values used by DOE in performance assessments reflect the uncertainty in DOE's probabilistic volcanic hazard estimates.

4.1.6.2 Review Method

NRC staff should review these probability values in light of the range of values used in the literature for the YMR and comparable volcanic fields. At a minimum, NRC staff should evaluate probability models by testing their sensitivity to uncertainties about the past distribution of volcanic vents, the recurrence rate of volcanism, and the relationship between igneous activity and tectonism. Probability models must be sufficiently robust to reasonably approximate the current distribution of volcanoes. Probability values need to have estimates of the uncertainties associated with calculated values in order to be acceptable. Uncertainty for reported probability values needs to incorporate both the precision of the probability model (e.g., influence of parameter uncertainty on the range of model results) and accuracy of the probability model (e.g., how well does the model predict the locations of volcanoes). Also, if a conservative value of probability is used in performance assessment then the reasons why this value is considered to be conservative should be clear and transparent.

4.1.6.3 Technical Bases

One of the difficulties inherent in the probabilistic volcanic hazard analysis of the proposed repository is that the small number of volcanoes in the YMR makes it difficult to evaluate models quantitatively. Application of probability models in other volcanic fields (e.g., Condit and Connor, 1996) provides one method of evaluating probability models applied to the YMR. A second, equally important approach to model evaluation is to apply a range of models to estimate the probability of igneous events affecting the proposed repository and evaluate the sensitivity of probability estimates to bound the range of models. In the following, such a sensitivity analysis is performed for a range of models. The models differ primarily in how igneous events are defined and how more realistic, but often less well-constrained, geologic

processes are included in the analysis. These probability models are based on:

- Individual mappable eruptive units and vents
- Vents and vent alignments
- Vents and vent alignments with regional tectonic control
- Igneous intrusions

In the following, annual probabilities of igneous events are calculated and compared using these models and a range of parameters for recurrence rate and area affected by volcanism.

4.1.6.3.1 Individual Mappable Eruptive Units and Vents

Individual mappable eruptive units and vents were used by Connor and Hill (1993, 1995) to estimate the probability of volcanic eruptions at the site. This definition of igneous events involves the fewest assumptions about volcanism, resulting in a straightforward sensitivity analysis.

Assuming that the probability of more than one event in a given year is small, the annual probability of volcanic eruptions within the repository boundary is given by:

$$P[\text{volcanic eruptions within repository boundary}] = 1 - \exp[-\lambda_r \lambda_s A_e] \quad (32)$$

where λ_r is the annual regional recurrence rate of volcanic vent formation, A_e is the effective repository area (Geomatrix, 1996), and λ_s is the spatial recurrence rate of volcanic eruptions at the repository, given a volcanic event in the region. Using a Gaussian kernel:

$$\lambda_s(x,y) = \frac{1}{2\pi h^2 N} \sum_{v=1}^N \exp \left\{ -\frac{1}{2} \left[\left(\frac{x-x_v}{h} \right)^2 + \left(\frac{y-y_v}{h} \right)^2 \right] \right\} \quad (33)$$

where x,y is a Cartesian coordinate within the repository boundary, x_v, y_v is the coordinate of the center of an igneous event, N is the number of such igneous events, h is a smoothing parameter (Section 4.1.4.3). For the following calculations, x,y is 548500, 4078500 and x_v, y_v are in Universal Transverse Mercator coordinates (Appendix A). Based on the analysis in Section 4.1.4.3, a smoothing parameter, $h \geq 5$ km, is appropriate for the Gaussian kernel. An effective repository area of 5.49 km is used in this analysis, based on the current repository design (Figure 7) and a 50-m buffer zone about the repository perimeter. The number of igneous events, N , depends on whether Pliocene and Quaternary or only Quaternary volcanoes are considered in the probability estimate.

Eight igneous events have occurred in the YMR during the Quaternary, if these events are defined as individual mappable eruptive units and vents. Connor and Hill (1995) used this definition for igneous events and varied recurrence rates between 5–10 v/m.y. Here, we model a range of 2–12 v/m.y. A recurrence rate >12 v/m.y. would signal a marked increase in activity

compared to other WGB volcanic fields. Recurrence rates in the Cima volcanic field, California, which is one of the most active basaltic volcanic fields in the WGB, are on the order of 30 v/m.y. (Turrin, et al., 1985). Comparable rates of basaltic volcanism have not occurred during the Plio-Quaternary in the YMR, with the possible exception of in the Funeral Formation. Rates of less than 2 v/m.y. would signal a marked decrease in magmatism in the YMR. No evidence currently available suggests such a decrease is likely. Therefore, the assumption that such a decrease in regional recurrence rate will occur can not be supported for the volcanic hazard analysis.

Estimated probabilities using this model are sensitive to temporal recurrence rate of igneous events in the YMR, λ_r , and choice of h in the calculation of $\lambda_r(x,y)$ (Figure 23). Based on these parameters, the annual probability of volcanic eruptions within the repository boundary is between 0.5×10^{-8} and 3.5×10^{-8} . Probabilities are slightly higher if the distribution of

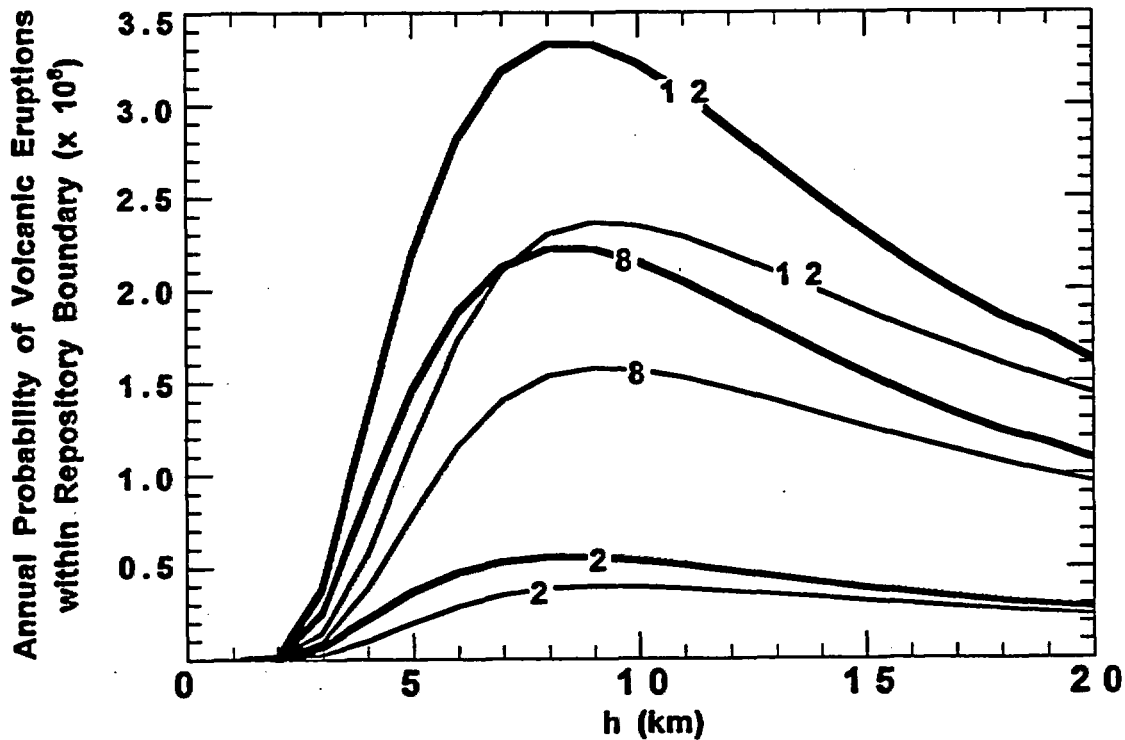


Figure 23. Annual probability of volcanic eruptions within the repository boundary. Igneous events are defined as individual mappable eruptive units and vents. A Gaussian kernel is used with smoothing parameter, h , varying from 0–20 km. Curves are shown for various regional recurrence rates of volcanic vent formation ($\lambda_r = 2 \times 10^{-6}$ v/yr, 8×10^{-6} v/yr, 12×10^{-6} v/yr), based on the distribution of Quaternary volcanoes (heavy lines) and Plio-Quaternary volcanoes (light lines). The effective repository area, A_r , is 5.49 km².

Quaternary volcanoes is considered in estimation of λ_r , rather than the distribution of Plio-Quaternary volcanoes, because Quaternary volcanoes are on average located closer to the repository site. These values are quite close to those calculated by Connor and Hill (1995) using Epanechnikov kernel and nearest-neighbor estimators of spatial and spatio-temporal recurrence rate. Connor and Hill (1995) used $A_e = 8 \text{ km}^2$ and estimated annual probabilities of volcanic disruption of the site between 1×10^{-8} and 5×10^{-8} .

4.1.6.3.2 Vent Alignments

If igneous events are defined as vents and vent alignments, probability of volcanic eruptions within the repository boundary incorporates distance and direction of an igneous event centered at a point, x,y , from the repository boundary. The probability of an igneous event centered at x,y is given by:

$$P_{x,y} [\text{igneous event at } x,y] = 1 - \exp(-\lambda_r \lambda_r \Delta x \Delta y) \quad (34)$$

where λ_r is the regional recurrence rate and λ_r is the spatial recurrence rate at point x,y , calculated using the Gaussian kernel [Eq. (33)]. In practice, λ_r is calculated on a grid of points with map extent X,Y and grid spacing $\Delta x, \Delta y$. This probability is then weighted by the probability that an igneous event centered at x,y , or occurring within $\Delta x, \Delta y$ will result in a volcanic eruption within the repository boundary. For vent alignments in the YMR, the spacing of vents along the alignments is small compared to the size of the repository (Section 4.1.3.2). Vent alignment length is defined as the distance between the centers of the first and last vents on the alignment. Therefore, the probability that an igneous event centered at x,y will result in vent alignment intersection with the repository boundary and subsequent volcanic eruption within the repository boundary is:

$$P_{r,} [\text{volcanic eruptions within repository boundary} | \text{igneous event at } x,y] = \begin{cases} 1, & x, y \in A_e \\ \frac{1}{2} \left[\frac{l_{\max} - l_r}{l_{\max} - l_{\min}} \right], & l_{\min} \leq l_r \leq l_{\max} \\ 0, & l_r > l_{\max} \end{cases} \quad (35)$$

where l_{\min} and l_{\max} are the minimum and maximum alignment half-lengths, respectively, and l_r is the distance from x,y to the nearest repository boundary along the direction of the alignment. For this analysis, vent alignments are assumed to be oriented 028° , perpendicular to the direction of minimum compressional stress in the YMR. Experimentation indicates that choosing a range of values of alignment orientation between 020° and 035° has a negligible effect on probabilities of volcanic eruptions within the repository boundary. Probabilities are sensitive to l_{\max} , which is varied over a range of values in the following analysis, but are not sensitive to the selection of l_{\min} , which for the following calculations is 100 m. As indicated in Eq. (35), 50 percent of all igneous vents are not part of vent alignments in this model. The probability of volcanic eruptions within the repository boundary is then:

P [volcanic eruptions within the repository boundary]

$$= \sum_{i=1}^X \sum_{j=1}^Y P_{xy}(x_i, y_j) \cdot P_b(x_i, y_j) \quad (36)$$

where x_i, y_j are on a rectangular grid of extent X, Y and grid spacing $\Delta x, \Delta y$.

Annual probability of volcanic eruptions within the repository boundary were calculated using $5200 \text{ m} \leq l_{\max} \leq 10,200 \text{ m}$, and $h = 5$ and 7 km (Figure 24). Based on nearest-neighbor vent and vent alignment distances in the YMR, $h \geq 7 \text{ km}$ is reasonably conservative (Figure 11). Using three Quaternary igneous events (Lathrop Wells, Quaternary Crater Flat, Sleeping Butte), results in annual probabilities of volcanic eruptions within the repository boundary between 1×10^{-8} and 3×10^{-8} , assuming a regional recurrence rate of 3 v/m.y. A rate of 5 v/m.y. results in annual probabilities of 6×10^{-8} .

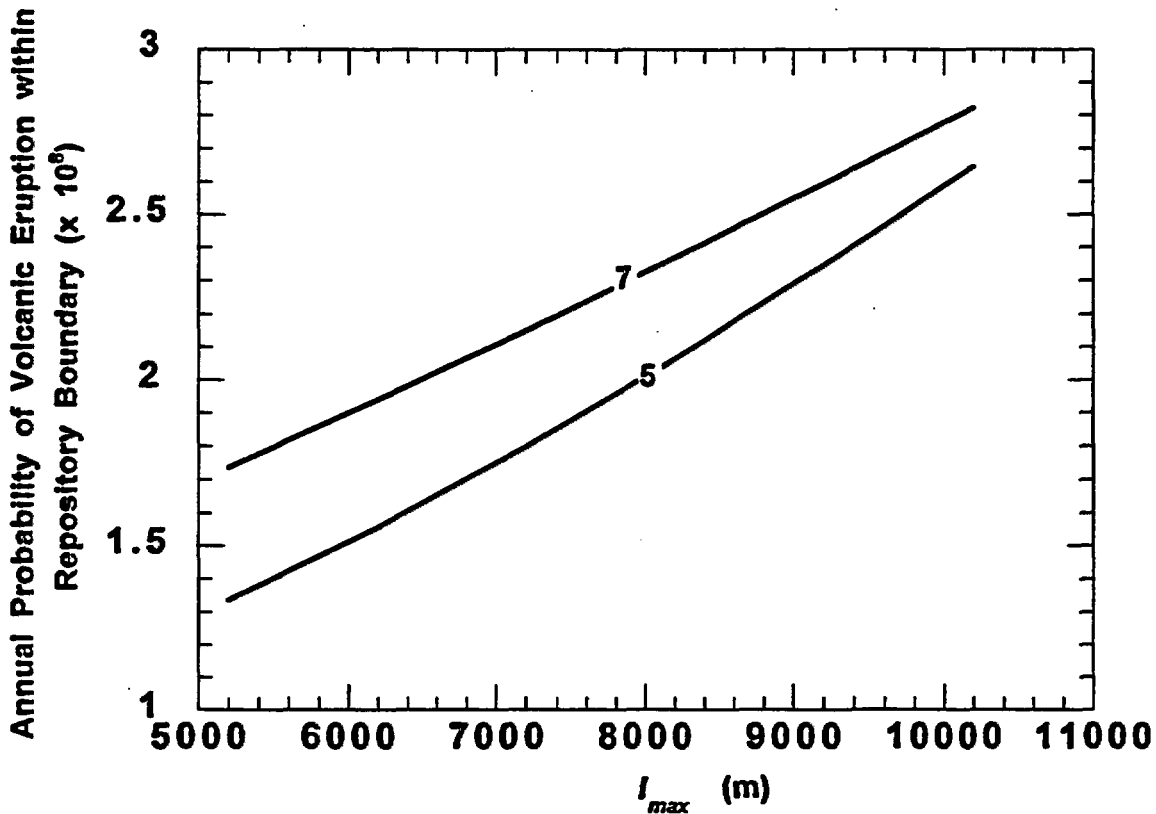


Figure 24. Annual probability of volcanic eruptions within the repository boundary. Igneous events are defined as vents and vent alignments. A Gaussian kernel is used with smoothing parameter, h , of 5 and 7 km (labeled lines) and is based on the distribution of three Quaternary igneous events. Vent alignment half-length, l_{\max} , varied between 5,200 and 10,200 m, roughly changing probability estimates by a factor of two. Probabilities are calculated using $\lambda_i = 3 \times 10^{-6}/\text{yr}$.

4.1.6.3.3 Vent Alignments With Tectonic Control

For a more complete analysis, the above probability estimates should be modified to incorporate additional geologic controls on volcanism. Tectonism in the YMR has led to regional variations in crustal density that may cause variation in rates of partial melting across the YMR (Section 4.1.4.3). These variations are most apparent across the Bare Mountain fault. Plio-Quaternary basaltic volcanism clusters east of this fault, in areas of anomalously low crustal density. In contrast, basaltic volcanism since the mid-Miocene is apparently absent west of the Bare Mountain fault and its southern extension into the Amargosa Desert. Standard Gaussian kernel functions do not take into account these geologic details. As a result, the standard Gaussian kernel [i.e, Eq. (33)] is too simple and overestimates probabilities of volcanic eruptions in some areas, for example on Bare Mountain, and underestimates probabilities elsewhere in the YMR.

The standard Gaussian kernel model developed above was modified by developing a weighting function that accounts for crustal density. The model for basaltic volcanism in extensional environments developed in Section 4.1.5.3 relates lithostatic pressure gradients in the mantle to regional changes in crustal density caused by extension. As illustrated in Figure 19, partial melting occurs where partial melting had occurred previously and close to active graben-bounding faults where slip in the crust causes the greatest pressure change in the mantle.

Pressure change in the mantle is inferred conceptually from simple numerical models of mantle stresses (Figure 19). The weighting function can be estimated from the frequency of volcanic eruptions as a function of crustal density. The distribution of this function, $f_T(x,y)$, was defined based on average crustal densities in the upper 5 km of the crust at the locations of existing volcanoes, derived from application of the density filter to the gravity data set (Figure 25). The Gaussian kernel was then modified to estimate the recurrence rate of volcanism at x,y .

$$K_g(x_p, y_j) = \exp \left\{ -\frac{1}{2} \left[\left(\frac{x_i - x_v}{h} \right)^2 + \left(\frac{y_j - y_v}{h} \right)^2 \right] \right\} \quad (37)$$

$$Q_v = \frac{\sum_{i=1}^X \sum_{j=1}^Y K_g(x_p, y_j)}{\sum_{i=1}^X \sum_{j=1}^Y f_T(x_p, y_j) \cdot K_g(x_p, y_j)} \quad (38)$$

$$\lambda_r(x,y) = \frac{1}{2\pi h^2 N} \sum_{v=1}^N Q_v f_T(x,y) K_g(x,y) \quad (39)$$

Introduction of the ratio Q_v assures that the integral of the modified Gaussian kernel for a single volcano over a large map extent X, Y relative to the smoothing parameter, h , will be unity [Eq. (5)]. The probabilities, however, are redistributed based on crustal density variations in the vicinity of the volcano.

Comparison of the modified and standard kernels was made by contouring $\lambda_i(x,y)$ across the YMR, using the distribution of Quaternary vents and vent alignments and $h = 9,000$ m. As previously, $N = 3$ in this model, defined by Quaternary Crater Flat, Lathrop Wells, and Sleeping Butte as the three Quaternary igneous events. In Figure 26, $\lambda_i(x,y)$ is contoured across the map region using Eq. (33). Given an igneous event in the region, there is a 68-percent chance that the igneous event will occur within this map area. The Sleeping Butte alignment lies north-northwest of the mapped region (see Figure 4). Larger values of $\lambda_i(x,y)$ indicate areas where igneous events are most likely centered. The largest values occur in southern Crater Flat because of the proximity of Lathrop Wells and the Quaternary Crater Flat alignment. In this area, $\lambda_i(x,y)$ varies between 8×10^{-4} volcanic events per square kilometer (v/km^2) and 2×10^{-4} v/km^2 .

Figure 27 is based on the modified kernel [Eqs. (37) to (39)] using the same parameters as used in the standard kernel calculation ($N = 3$, $h = 9,000$ m), but weighting the kernel using crustal densities derived using Eqs. (22) to (29). Use of the modified kernel reduces the area of the $\lambda_i(x,y)$ surface at, for example, the 2×10^{-4} v/km^2 contour, and increases the amplitude of the surface. The $\lambda_i(x,y)$ surface also becomes asymmetric as a result of application of the modified kernel function. Values of $\lambda_i(x,y)$ are greatest in southern Crater Flat, exceeding 1.2×10^{-3} v/km^2 , and decrease abruptly near the Bare Mountain fault. Probability values decrease less abruptly on the eastern boundary of Crater Flat because crustal densities change less rapidly on the eastern edge of the basin. This more gradual change in $\lambda_i(x,y)$ on the eastern edge of the basin is consistent with the proposed model linking crustal extension and basaltic volcanism (Figure 19).

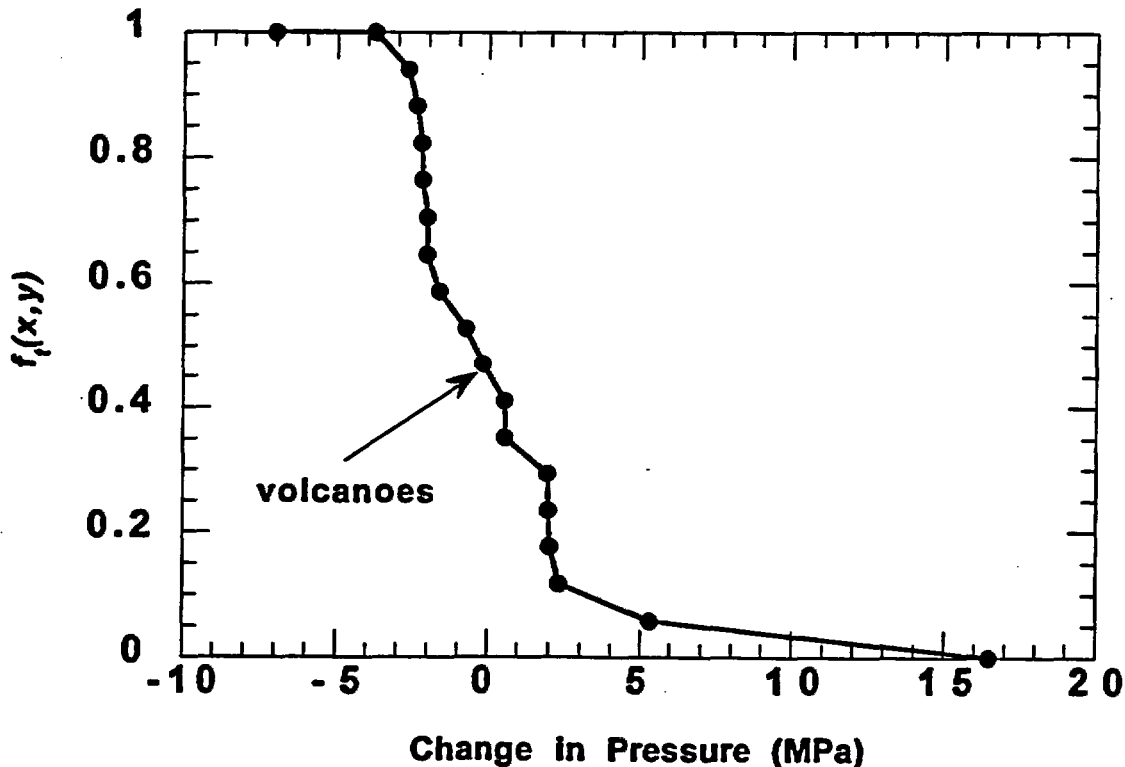


Figure 25. The weighting function, $f_i(x,y)$, is derived from changes in average crustal densities under the locations of Plio-Quaternary Yucca Mountain region Volcanoes.

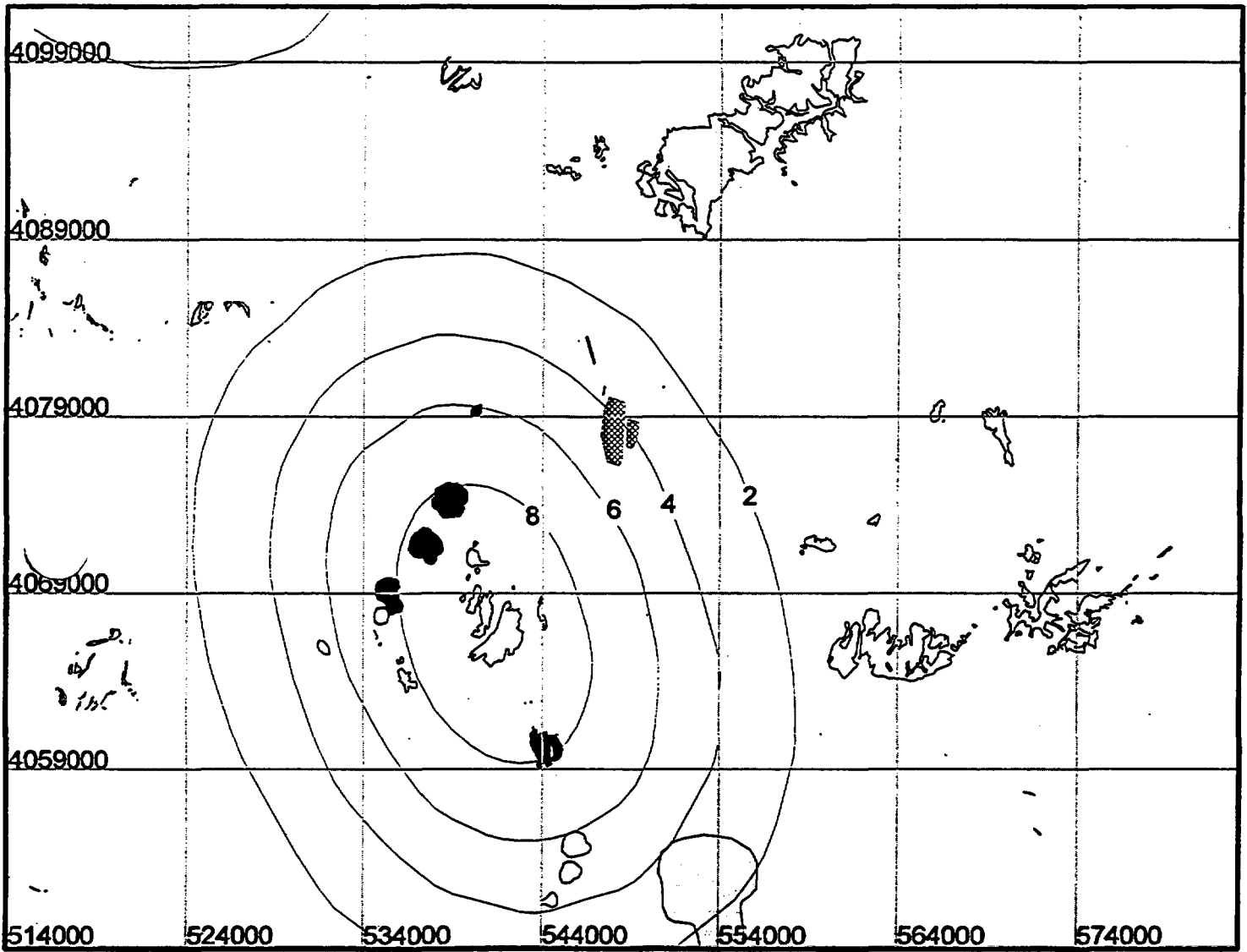


Figure 26. The spatial recurrence rate (v/km^2) is contoured in the area of Yucca Mountain, using the Gaussian kernel function (Eq. 35). In this model, $h = 9,000$ m and $N = 3$, based on the number of igneous events. The contour interval is $2 \times 10^{-4} v/\text{km}^2$. Other symbols are as in Figure 7.

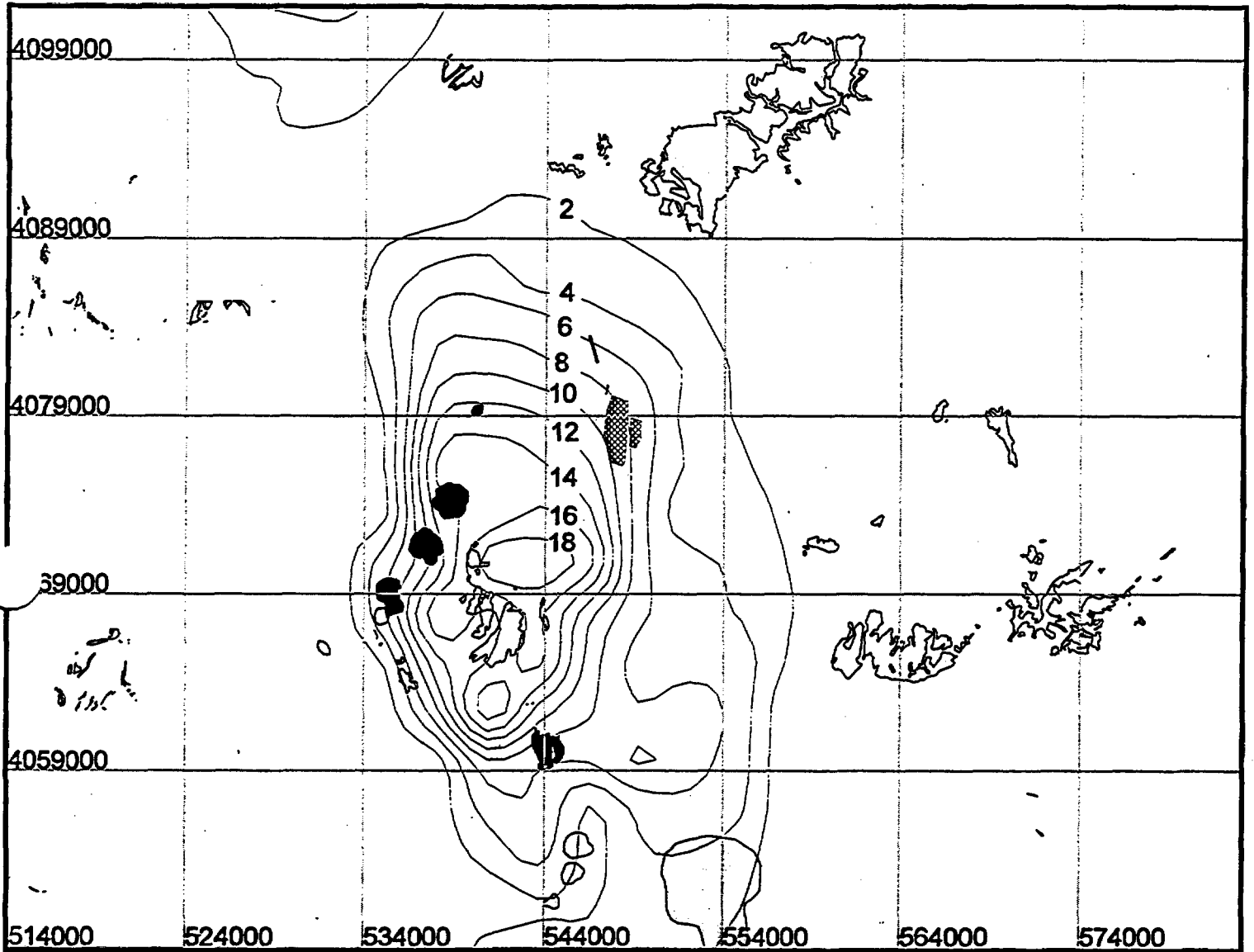


Figure 27. The spatial recurrence rate (v/km^2) is contoured in the area of Yucca Mountain, using the modified Gaussian kernel function (Eq. 37 to 39) to incorporate tectonic control on the probability estimate. In this model, $h = 9,000$ m and $N = 3$, based on the number of igneous events. The contour interval is $2 \times 10^{-4} v/\text{km}^2$. Other symbols are as in Figure 7.

The annual probability of volcanic eruptions within the repository boundary increases when the modified kernel function is used. Annual probability of volcanic eruptions within the repository boundary was calculated using $5,200 \text{ m} \leq l_{max} \leq 10,200 \text{ m}$, and $h = 7 \text{ km}$ (Figure 28). Using the three Quaternary igneous events (Lathrop Wells, Quaternary Crater Flat, Sleeping Butte) results in annual probabilities of volcanic eruptions within the repository boundary between 3×10^{-8} and 5.5×10^{-8} , assuming a regional recurrence rate of 3 v/m.y. Including Pliocene volcanoes in the estimation of $\lambda_r(x,y)$ decreases the annual probability at the repository because many Pliocene volcanoes are located in the Amargosa Desert. Annual probabilities based on the modified kernel distribution and Plio-Quaternary volcanoes vary between 1.5×10^{-8} and 3×10^{-8} , comparable to the annual probabilities estimated using the standard kernel and the distribution of Quaternary vents and vent alignments.

The regional recurrence rate of vent and vent alignment formation is poorly constrained in the YMR. Varying regional recurrence rate of igneous events between 1 and 5 v/m.y. results in

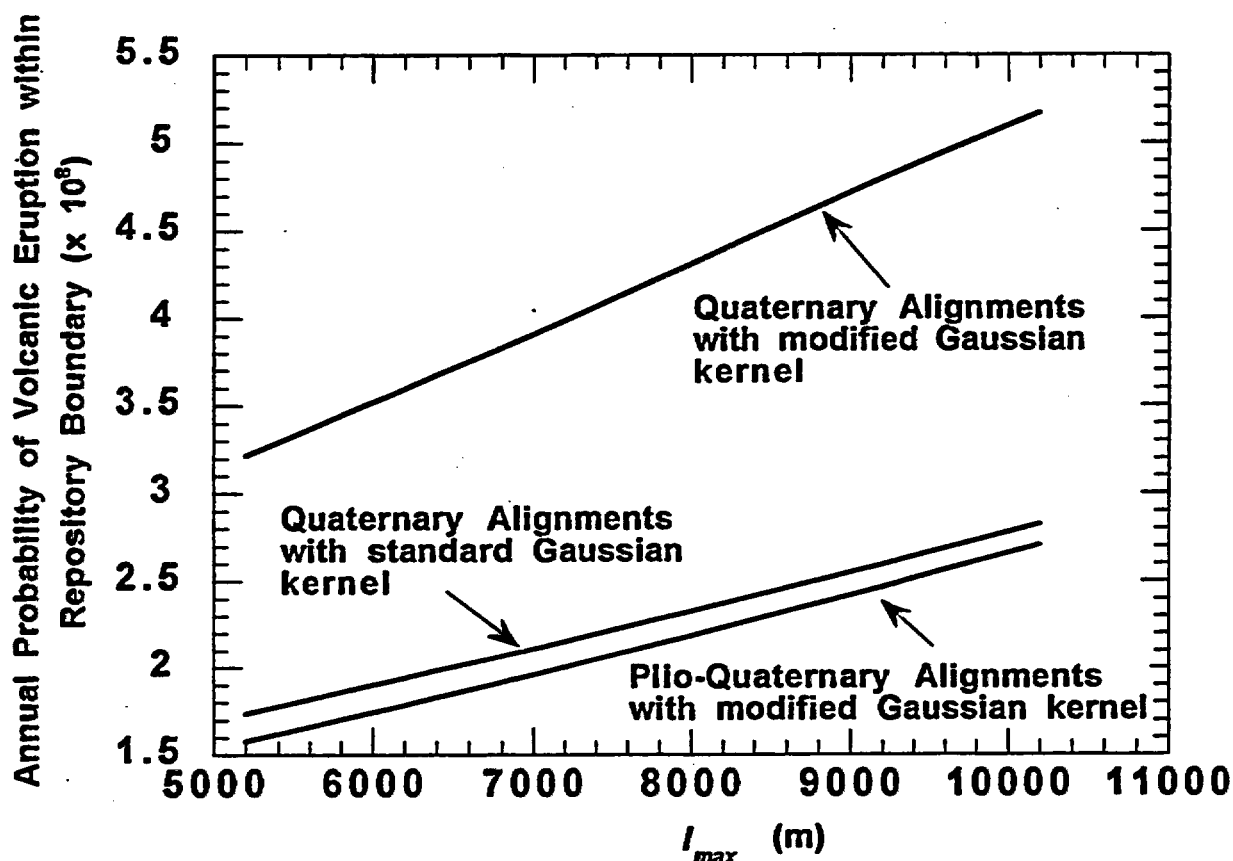


Figure 28. Annual probability of volcanic eruptions within the repository boundary using a modified Gaussian kernel. Igneous events are defined as vents and vent alignments. A modified Gaussian kernel is used with a smoothing parameter, $h = 7 \text{ km}$, based on the distribution of three Quaternary igneous events. Vent alignment half-length, l_{max} , varied between 5,200 and 10,200 m, roughly changing probability estimates by a factor of two. Probabilities are calculated using $\lambda_r = 3 \times 10^{-8} \text{ /yr}$. Curves are shown calculated using Plio-Quaternary events ($N = 12$) and the modified Gaussian kernel, and Quaternary events ($N = 3$) and the standard Gaussian kernel for comparison.

nearly one order of magnitude variation in the annual probability of volcanic eruptions within the repository boundary. Using the modified kernel model, $h = 7$ km, and $5,200 \text{ m} \leq l_{\text{max}} \leq 10,200 \text{ m}$, annual probability of volcanic eruptions within the repository varies between 1×10^{-8} and 9×10^{-8} (Figure 29).

4.1.6.3.4 Igneous Intrusions

The probability of igneous intrusions, such as dike swarms, intersecting the repository is greater than the probability of volcanic eruptions within the repository, because igneous intrusions must have greater areas than vent alignments and most likely occur with greater frequency. All alignments have associated intrusions but not all intrusions produce vent alignments. The recurrence rate of igneous intrusions and their geometry, however, are so poorly constrained by available data that these parameters are not estimated. Based on analogy with the San Rafael volcanic field (Conway, et al., 1997), probabilities of igneous intrusion into the repository boundary may be two to five times the probability of volcanic eruptions within the repository

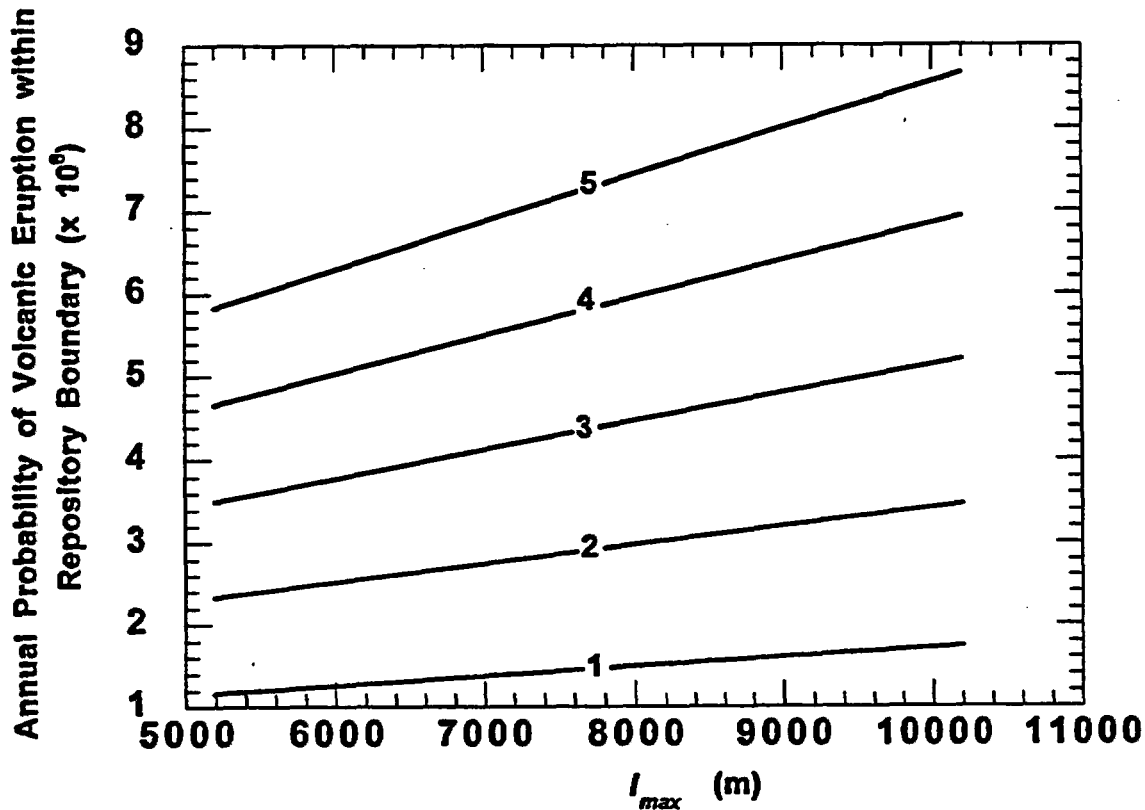


Figure 29. Annual probability of volcanic eruptions within the repository boundary using regional recurrence rates of $\lambda_r = 1 \times 10^{-6}$, 2×10^{-6} , 3×10^{-6} , 4×10^{-6} , and 5×10^{-6} /yr. Igneous events are defined as vents and vent alignments. A modified Gaussian kernel is used with smoothing parameter, $h = 7$ km, based on the distribution of three Quaternary igneous events.

boundary. While such a value is speculative it does provide a basis for development of an interim probability value for igneous intrusion intersecting the repository.

4.1.6.4 Summary

Annual probability of volcanic eruptions within the repository boundary varies between 10^{-8} to 10^{-7} based on a range of models. This range accounts for varying definitions of igneous events and uncertainty in parameter distributions used to estimate probability. Annual probabilities are generally between 1×10^{-8} and 3×10^{-8} for igneous events defined as individual mappable units and vents. This definition of igneous events requires the fewest assumptions about underlying parameter distributions but also neglects some features of vent distribution that are important in the YMR. In particular, the formation of vent alignments is not accounted for in this model. Defining igneous events as vents and vent alignments results in a similar range of probability estimates for the annual probability of volcanic eruptions within the repository boundary, 1×10^{-8} to 6×10^{-8} . Although recurrence rates are lower using this definition of igneous events, the area affected by individual events is greater. The distribution of alignment length and regional recurrence rate of these igneous events introduces the greatest uncertainties into these probability models. Incorporating regional crustal density variation into this model results in a model more closely linked to geologic processes. Based on the crustal density models and similar models presented previously (Hill, et al., 1996; Connor, et al., 1996), the annual probability of volcanic eruptions within the repository boundary is between 1×10^{-8} and 9×10^{-8} . Probabilities of intersection of igneous intrusions with the repository are likely higher, but cannot be confidently estimated from available geologic data. As a value is needed for use in performance assessment, the NRC will assume the rate is a factor of between 2 to 5 higher than for volcanic disruption. Finally, it is noted that this range of probability values, 10^{-8} to 10^{-7} , arises from the application of a variety of models and a range of parameter distributions. Nothing in the above analysis suggests that this range of probabilities has central tendency, that the mean or median of this range of probabilities is significant, or that high or low values in this range are more or less likely. This situation arises because, at least at the current time, it is not feasible to develop an objective basis for assigning likelihood to individual models, due to both lack of data and uncertainty in our understanding of the process. For the purpose of performance assessment the NRC will assume the value of 10^{-7} .

The WGB, which includes Yucca Mountain, is a magmatic province characterized by Quaternary basaltic volcanism (Fitton, et al., 1991). At least 211 basaltic volcanoes <2 Ma occur in the 82,000 km² region defined by Amboy volcano, the Big Pine volcanic field, and the Lunar Crater volcanic field (Figure 3; Luedke and Smith, 1981; Connor and Hill, 1994). Assuming that volcanism is randomly distributed throughout this source-zone (cf. Crowe, et al., 1995; Geomatrix, 1996), volcano recurrence rates are 1.3×10^{-9} yr⁻¹ km⁻². The annual probability of volcanic disruption of any 5-km² area (i.e., repository area) in this source zone is thus 6×10^{-9} . This analysis overlooks the fact that volcanoes cluster within the WGB (Figure 3). The YMR, however, constitutes one of the volcano clusters within the WGB (Connor and Hill, 1995), within which probability should be higher than expected based on a uniform random model. An annual probability of 6×10^{-9} appears a reasonable and general measure of background volcano occurrence for any 5-km² area within the WGB, including the Yucca Mountain repository site. Models that propose an annual probability of volcano formation at the proposed repository site of less than 6×10^{-9} thus do not appear to be reasonable, based on

geologic data.

The likely regional background rate for basaltic intrusions is necessarily higher than that of single volcanoes, due to the larger area affected by a shallow basaltic dike. Using conditions appropriate for the Yucca Mountain repository site, the regional probability of a shallow basaltic intrusion can be assessed by sampling a uniform random distribution of dike half-length between 0.1–4 km and trending 28° from north. The annual probability of igneous disruption of any 5-km² area in the WGB is then 1.7×10^{-8} . This simple calculation does not consider the possibility of unmapped shallow dikes that were emplaced without an associated volcanic eruption, or the presence of misdated Quaternary cinder cones in the WGB. Models that propose an annual probability of igneous dike intersection with the proposed repository site of less than 1.7×10^{-8} do not appear to be reasonably supported.

Uncertainty associated with any probability model consists of two components that measure precision and accuracy. Precision is also referred to as "parameter uncertainty," whereas accuracy often reflects "model uncertainty" (Performance Assessment Working Group, 1997). Of the range of probability models proposed for the YMR, only the spatio-temporal nonhomogeneous models of Connor and Hill (1995) have been evaluated for model accuracy (Condit and Connor, 1996). This initial evaluation demonstrates that these probability models reasonably estimate the locations of basaltic volcanoes in the Springerville volcanic field when basalt petrogenesis remains relatively constant. These models are unsuccessful in estimating the future locations of basaltic volcanoes when the magmatic system undergoes abrupt and large shifts in petrogenesis (Condit and Connor, 1996). The YMR has not undergone similar-magnitude petrogenetic shifts since about 5 Ma (e.g., Crowe, et al., 1986), thus these probability models should be reasonably accurate when applied to the YMR system.

4.1.7 Probability Criterion 7

4.1.7.1 Acceptance Criterion

Estimates of the probability of future igneous activity in the YMR will be acceptable provided that:

- The values used (single values, distributions, or bounds on probabilities) are technically justified and account for uncertainties in probability estimates.

4.1.7.2 Review Method

The NRC considers a range of different approaches for evaluating uncertainty in performance models used in licensing nuclear facilities. The end-members of the uncertainty analysis are represented by a deterministic bound on the upper limits of dose and a probabilistic approach that represents a distribution of model results (Performance Assessment Working Group, 1997). Regardless of the method used, the rationale used in making the analysis and a reasonable and comprehensive understanding of the system being modeled are required for acceptance.

Staff should confirm whether the probability values were directly incorporated or models were appropriately abstracted for use in assessments of repository performance, taking into consideration uncertainties in these estimates.

4.1.7.3 Technical Basis

A deterministic approach evaluates uncertainty by bounding model parameters. Parameter values are generally selected such that overall risk is not underestimated. This approach results in a single, straightforward value that bounds performance but does not provide any quantitative information on the uncertainty associated with this value (Performance Assessment Working Group, 1997). Detailed documentation and justification for parameter values used in this approach are required in order to determine the appropriate level of conservatism needed to represent the range of data.

A probabilistic approach provides a distribution of model results, which in turn provides a quantitative measure of uncertainty. This approach is more objective than a deterministic approach in that a level of conservatism is not implicitly required. The range of parameter values must be reasonable, and appropriate sampling methods must be used in the analysis (Performance Assessment Working Group, 1997). The mean value of a probabilistic analysis is generally used to determine compliance with the performance objective (Performance Assessment Working Group, 1997). For low-level waste licensing, NRC staff also recommended that the 95th percentile of the performance distribution be less than a given value to demonstrate compliance (Performance Assessment Working Group, 1997). As the NRC is using a single value in performance assessment for volcanic probability it is further justification of the use of the value of 10^{-7} .

4.1.7.4 Summary

Based on the range of work currently available, the probability of igneous events at the proposed repository site can be described by single values, mean values of various distributions, entire probability distributions, or bounds on probability distributions. Any of these approaches may be used based on current NRC regulations. Regardless of the value(s) used, the methods used to derive the values must be justified, and the data used to derive the values must be clearly presented.

4.1.8 Probability Criterion 8

4.1.8.1 Acceptance Criterion

Estimates of the probability of future igneous activity in the YMR will be acceptable provided that:

- If used, expert elicitations were conducted and documented using the guidance in the Branch Technical Position on Expert Elicitation (NRC, 1996), or other acceptable approaches.

4.1.8.2 Review Method

If the DOE uses expert elicitation in developing estimates of the probability of future volcanism and igneous intrusion, staff will review the documentation to assure that the expert elicitation (i) followed the procedure described in the Branch Technical Position on expert elicitation (NRC, 1996); (ii) considered the range of models in the relevant literature; (iii) considered the range of data in the relevant literature; and (iv) is consistent with available information, including information developed subsequent to the elicitation.

4.1.8.3. Technical Basis

As summarized in NRC (1996), the NRC expects that subjective judgments of groups of experts will be used by the DOE to assess issues related to overall performance of the proposed high-level radioactive waste repository site at Yucca Mountain. The NRC has traditionally accepted expert judgment as part of a license application to supplement other sources of scientific and technical data. Expert elicitation is commonly used when

- Empirical data are not reasonably obtainable or analyses are not practical to perform
- Uncertainties are large and significant to a demonstration of compliance
- More than one conceptual model can explain, and be consistent with, the available data
- Technical judgments are required to assess whether bounding assumptions or calculations are appropriately conservative

NRC(1996) also summarize a series of technical positions and procedures concerning the use of expert elicitation in demonstrating compliance with geologic repository disposal regulations. These procedures emphasize the need for detailed documentation during the elicitation and for transparency in the aggregation of multiple expert's judgments. An elicitation also should provide a means to evaluate new data that may arise between completion of the elicitation and submittal of licensing documents (NRC, 1996).

The DOE used expert judgement to arrive at a probability value for igneous activity at the repository site (Geomatrix, 1996). Although the report generally followed the NRC Branch Technical Position (BTP) regarding expert elicitation (NRC, 1996), several areas of weakness in the elicitation procedure were noted in the September, 1996 Appendix 7 meeting with DOE:

- Criteria and procedures for incorporating new data into the existing elicitation need to be established and published.
- Central issues need to be deconvoluted as much as possible, so that standard definitions of terms can be used consistently throughout the elicitation.

- Greater balance is needed on the panel to encompass a wider range of viewpoints, along with more thorough documentation of the selection processes and potential conflicts of interest for panel members.
- Intermediate judgments of the experts after the elicitation and any changes of rationales need to be documented.

Following the Appendix 7 meeting, the NRC concluded that the elicitation (Geomatrix, 1996) is generally consistent with the BTP regarding the conduct of an expert elicitation. The NRC will thus give the elicitation the appropriate level of consideration in the review of licensing documents (Bell, 1997).

Staff have performed a technical review of the PVHA elicitation report (Geomatrix, 1996) and, as explained in previous sections of this report, have several technical concerns regarding the PVHA results and their application in the Yucca Mountain program. The most significant concern is that many of the models in the PVHA are critically dependent on the definition of volcanic source-zones. Many of the source-zone models bypass the proposed repository site due to a lack of previous igneous activity at the site (Geomatrix, 1996). Although some geological data appear to suggest such division, critical analyses reveal that these apparent divisions are only manifestations of surficial features and not important to deeper structural control of volcanism (e.g., Stamatakos, et al., 1997b). In addition, larger-scale geologic features that commonly affect the localization of basaltic igneous activity are remarkably similar between the proposed repository site and the locations of past igneous activity. Based on these geologic relationships, staff conclude volcanic source-zones that fail to include the proposed repository site are not reasonably conservative.

According to Geomatrix (1996) mean annual probability of repository disruption is 1.5×10^{-8} yr⁻¹. This is, however, a combined probability for both volcanic and igneous events. Utilizing the source zone models that preclude volcanoes from forming at the repository site, as was done repeatedly in Geomatrix, 1996, requires that the actual probability of volcanic disruption based on this methodology is necessarily lower than 1.5×10^{-8} yr⁻¹. A rough estimate is that the mean PVHA probability for volcanic disruption may be an order of magnitude lower than the combined probability for all classes of igneous events. In order to use probability estimates in performance assessment they must, in some way, be separated into volcanic and intrusive events. DOE is planning additional analysis in this area (TRW, 1997).

4.1.8.4 Summary

There are no generally accepted methodologies for calculating the probabilities of future igneous activity in distributed volcanic fields over periods of 10,000 yr. In addition, more than one conceptual model can be applied to this problem, resulting in a wide range of probability values. DOE is using expert elicitation (Geomatrix, 1996) to evaluate a range of probability models, estimate uncertainties in model results due to reasonable variations in model parameters, and determine a probability distribution for use in performance assessment models.

4.1.9 Probability Criterion 9

4.1.9.1 Acceptance Criterion

Estimates of the probability of future igneous activity in the YMR will be acceptable provided that:

- The collection, documentation, and development of data and models has been performed under acceptable QA procedures, or if data was not collected under an established QA program, it has been qualified under appropriate QA procedures.

4.1.9.2 Review Method

NRC will attend, as observers, DOE-conducted QA audits of program participants who are involved in technical investigations related to igneous activity. NRC will also track the progress made in resolving deficiencies and nonconformities in the program that arise from QA audits and independent review of DOE products.

4.1.9.3 Technical Basis

Both DOE and NRC have approved QA programs for technical investigations conducted by their respective agencies and contractors, and the NRC has stated that the quality of data will be acceptable if the data are developed under an approved QA program (Nuclear Regulatory Commission, 1997). These QA programs detail the procedures necessary to collect, document, and develop data and models in an acceptable manner. Periodic technical audits are conducted by the DOE and the NRC to ensure that appropriate QA procedures are implemented in technical investigations. These audits are usually attended by observers from each agency, who provide an independent assessment of audit effectiveness and conclusions.

Independent technical evaluation is still warranted for many data collected under an approved QA program. One common area of concern is reconciling new data with previously published data, which is a problem that may not be apparent during a routine QA audit. For example, many of the ^3He dates in Crowe, et al. (1995) were internally inconsistent in addition to contradicting previously published values for the same geological units (Hill, 1995). Similar discrepancies were noted in the September 1996 LANL QA audit (e.g., Austin, 1996). Discrepancies between new and previously published data will need to be reconciled in order to provide a solid technical basis for evaluating licensing documents.

Site characterization activities have produced an abundance of data on YMR basaltic volcanoes. In addition to the DOE, the State of Nevada, the U.S. Geological Survey, the CNWRA and the NRC have conducted independent geological investigations in the YMR. Each of these organizations operate under different QA programs. Other researchers associated with universities and national labs also conduct high-quality investigations in the YMR, with varying degrees of formal QA programs. Many of these data are clearly important to licensing issues and must be considered during review of DOE licensing documents. As part of the

license application, DOE will likely qualify many of these externally produced data. Qualification procedures for these externally produced data include production under a QA program equivalent to Nuclear Regulatory Commission (1997), publication through the peer-review process, independent corroboration, or confirmatory testing.

4.1.9.4 Summary

Staff have participated in recent QA audits of DOE and its contractors (e.g., Austin, 1996) and provided numerous reviews of DOE study plans and contractor reports (e.g., Connor, et al., 1993). The NRC staff continue to monitor DOE QA activities related to the IA KTI and disposition of QA deficiencies from the September, 1996, LANL QA audit. Staff have concluded that the LANL QA performance was "marginally effective" and will continue to monitor the DOE/LANL QA program (Austin, 1996). As a result of this audit the DOE audit team concluded that the LANL's QA performance was "marginally effective." The NRC agreed with this finding, and the NRC concerns identified during this audit were deferred to the appropriate DOE deficiency reports (YM-96-D-105 to 108). NRC recently reviewed the remedial actions proposed for these deficiencies and determined that the proposed actions appeared appropriate. Review of the associated Volcanism Synthesis Report is needed to determine if these actions have been effectively carried out and if the concerns have been resolved.

Staff have conducted independent technical investigations in igneous activity to: (i) evaluate DOE data and models likely contained in licensing documents, (ii) develop and test alternative hypotheses to those proposed by the DOE, (iii) evaluate relevant data and models proposed by other agencies such as the State of Nevada, and (iv) reduce uncertainties in models of repository performance. The results of these investigations have been presented in numerous CNWRA reports and peer-reviewed journal articles, many of which are cited in preceding sections of this report. As part of these investigations, staff have compiled all relevant data on the age and location of YMR basaltic igneous features younger than about 11 Ma (Appendix A). These data form the basis for probability models and review of appropriate DOE licensing documents. Staff will continue to evaluate data in the peer-reviewed literature and products from other agencies, in addition to data produced by DOE and its contractors. Although the DOE Volcanism Synthesis Report was not issued in FY97, data presented in Appendix A are used in this IRSR to resolve the igneous activity probability subissue.

4.2 CONSEQUENCES

4.2.1 Acceptance Criterion - Consequences

Acceptance criterion for consequences of igneous activity on repository performance will be developed in FY98.

4.2.2 Review Method - Consequences

Review methods for consequences of igneous activity on repository performance will be developed in FY98.

4.2.3 Technical Basis - Consequences

The technical basis for consequence analysis of volcanic disruption of the repository will be developed in FY98.

4.2.4 Summary - Consequences

To be developed in FY98.

THIS PAGE INTENTIONALLY BLANK

5.0 STATUS OF ISSUE RESOLUTION AT STAFF LEVEL

5.1 STATUS OF RESOLUTION OF PROBABILITY ISSUES

Based on available information, staff conclude that a range in annual probabilities of from 10^{-7} to 10^{-8} bounds the range of credible models on the annual probability of future volcanic activity intersecting the proposed repository site. Although a probability distribution can be constructed to evaluate uncertainty due to parameter variations, this uncertainty is small relative to variations in conceptual models used (i.e., Geomatrix, 1996) or to uncertainties associated with model accuracies. As there is no basis for distinguishing between values in this range, the staff will use an annual probability value of 10^{-7} in performance assessment. The staff does not believe that a meaningful probability for igneous intrusion can be determined with the present data base. Based on field studies at analog sites, the number of intrusive events may be a factor of two or more greater than the number of volcanic events, and the area affected by intrusive events may be orders of magnitude greater than the area effected by volcanic events alone. Based on the analog studies, as interim measure the staff will assume that the probability of an igneous intrusive event is a factor of 2 to 5 higher than that of a volcanic event.

DOE and NRC have not yet reached agreement on the appropriate range of volcanic and intrusive probability estimates to use in performance assessment. As stated above, the staff conclude that a 1×10^{-7} annual probability of volcanic disruption provides a reasonably conservative value for use in performance assessment. During the DOE/NRC Technical Exchange of February 25-26, 1997, DOE agreed that the probability distribution function from their expert elicitation had an upper bound frequency of 10^{-7} ; therefore, there is agreement between NRC and DOE on this value. Further analysis of the probability of volcanic disruption of the site is not warranted until completion of consequence analyses and risk assessment. Also as stated above, as an interim measure the staff will use a factor of 2-5 of the volcanic probability for the probability of igneous intrusion. The staff is not sure what value DOE will be using for intrusive events and awaits the results of the analysis promised in TRW, 1997. As with the volcanic disruption probability the need to determine a defensible value for igneous intrusion is also dependent on evaluating the health effects of this phenomenon; therefore, the staff plans little work on the probability of igneous intrusion until the consequences of igneous intrusion have been evaluated.

5.1.1 Probability Criterion 1

Estimates of the probability of future igneous activity in the YMR will be acceptable provided that:

- The estimates are based on past patterns of igneous activity in the YMR.

Sufficient information exists to define the extent of the YMR igneous system based on past patterns of igneous activity in the YMR. Probability estimates from most models are insensitive to volcanoes older than about 6 Ma or located more than about 30 km from the proposed repository site. Some probability models using nonstationary Poisson or spatially homogeneous Poisson methods, however, are relatively sensitive to spatial and temporal

definitions of the YMR igneous system, and probability estimates derived from these methods will need to be supported with clear definitions of the YMR igneous system.

5.1.2 Probability Criterion 2

Estimates of the probability of future igneous activity in the YMR will be acceptable provided that:

- The definitions of igneous events are used consistently. Intrusive and extrusive events should be distinguished and their probabilities estimated separately.

Sufficient information exists to calculate the probability of volcanic disruption for the proposed repository site, when the event is defined as an individual mappable eruptive unit, or as episodes of vent or vent-alignment formation (e.g., Connor and Hill, 1995; Condit and Connor, 1996). The staff does not consider, however, that there is presently enough information to rigorously define the probability of igneous activity, or the related probability of intrusive activity affecting the repository. Based on preliminary estimates it appears that the effects from intrusions intersecting the repository without volcanic eruption may be significantly less than the effects of volcanic disruption. Further work to rigorously define a probability of igneous intrusion is not warranted until completion of the consequence analysis.

5.1.3 Probability Criterion 3

Estimates of the probability of future igneous activity in the YMR will be acceptable provided that:

- The models are consistent with observed patterns of volcanic vents and related igneous features in the YMR.

Good agreement exists on the basic patterns of basaltic volcanism in the YMR. These patterns include changes in the locus of volcanism with time, recurring volcanic activity within vent clusters, formation of vent alignments, and structural controls on the locations of cinder cones. Each of these patterns in vent distribution has an important impact on volcanic probability models and is considered in current probability models.

5.1.4 Probability Criterion 4

Estimates of the probability of future igneous activity in the YMR will be acceptable provided that:

- Parameters used in probabilistic volcanic hazard assessments, related to recurrence rate of igneous activity in the YMR, spatial variation in frequency of igneous events, and area affected by igneous events, are technically justified and documented by DOE.

Sufficient evidence exists to technically justify parameters related to the recurrence rate of

igneous activity in the YMR, spatial variation in frequency of igneous events, and area affected by igneous events. Staff have conducted independent technical investigations in igneous activity to (i) evaluate DOE data and models, (ii) develop and test alternative hypotheses, and (iii) reduce uncertainties in models of repository performance. The results of these investigations have been presented in numerous CNWRA reports and peer-reviewed journal articles. As part of these investigations, staff have compiled all relevant data on the age and location of YMR basaltic igneous features younger than about 11 Ma (Appendix A). These data form the basis for probability models and review of appropriate DOE licensing documents.

5.1.5 Probability Criterion 5

Estimates of the probability of future igneous activity in the YMR will be acceptable provided that:

- The models are consistent with tectonic models proposed by NRC and DOE for the YMR.

All currently proposed tectonic models indicate that the proposed repository site and the locations of <5-Ma YMR volcanoes are in the same tectonic regime. However, most DOE models propose some type of boundary between Crater Flat and Yucca Mountain. This results in much lower probabilities at the site than for those areas just adjoining in Crater Flat. In most cases the models will not allow, or severely constrain, the probability of a volcanic event forming at Yucca Mountain while allowing dikes from such features to propagate to the site. Although some geologic data appear to suggest such a division, critical analyses reveal that these apparent divisions are only manifestations of surficial features and not important to deeper structural control of volcanism (e.g., Stamatakos, et al., 1997b). Therefore, reasonably conservative probability analyses must be based on source zones that include the proposed repository. The models considered within this IRSR satisfy this requirement.

5.1.6 Probability Criterion 6

Estimates of the probability of future igneous activity in the YMR will be acceptable provided that:

- The probability values used by DOE in performance assessments reflect the uncertainty in DOE's probabilistic volcanic hazard estimates.

Uncertainty associated with any probability model consists of two components that measure precision and accuracy. Precision is also referred to as "parameter uncertainty," whereas accuracy often reflects "model uncertainty" (Performance Assessment Working Group, 1997). Of the range of probability models proposed for the YMR, only the spatio-temporal nonhomogeneous models of Connor and Hill (1995) have been evaluated for model accuracy (Condit and Connor, 1996). This evaluation demonstrates that these probability models reasonably estimate the locations of basaltic volcanoes in the Springerville volcanic field when basalt petrogenesis remains relatively constant. These models are unsuccessful in estimating the future locations of basaltic volcanoes when the magmatic system undergoes abrupt and large shifts in petrogenesis (Condit and Connor, 1996). The YMR has not undergone similar-

magnitude petrogenetic shifts since about 5 Ma (e.g., Crowe, et al., 1986), thus, these probability models should be reasonably accurate when applied to the YMR system.

5.1.7 Probability Criterion 7

Estimates of the probability of future igneous activity in the YMR will be acceptable provided that:

- The values used (single values, distributions, or bounds on probabilities) are technically justified and account for uncertainties in probability estimates.

The DOE has stated that they will use the probability distribution derived from the PHA elicitation (Geomatrix, 1996) to conduct sensitivity studies regarding igneous activity (Brocoum, 1997). In addition, the DOE will use a series of alternative approaches to evaluate model sensitivities to probability values or distributions (Brocoum, 1997). This approach is generally acceptable to the NRC staff (Stablein, 1997).

5.1.8 Probability Criterion 8

Estimates of the probability of future igneous activity in the YMR will be acceptable provided that:

- If used, expert elicitations were conducted and documented using the guidance in the Branch Technical Position on Expert Elicitation (NRC, 1996), or other acceptable approaches.

DOE used expert judgment to arrive at a probability hazard assessment for the proposed repository site (Geomatrix, 1996). While there were areas of weakness, the probability hazard assessment elicitation (Geomatrix, 1996) is generally consistent with the BTP regarding the conduct of an expert elicitation. The NRC will, thus, give the probability hazard assessment elicitation the appropriate level of consideration in review of licensing documents (Bell, 1997).

5.1.9 Probability Criterion 9

Estimates of the probability of future igneous activity in the YMR will be acceptable provided that:

- The collection, documentation, and development of data and models has been performed under acceptable QA procedures, or if data was not collected under an established QA program, it has been qualified under appropriate QA procedures.

The most recent audit which the NRC observed related to the Igneous Activity KTI was in September, 1996, when DOE audited LANL. During this audit the NRC staff observers noted several discrepancies and inconsistencies in the reported data both within the Draft Volcanism

Synthesis Report, and between the draft report and data presented in other reports and journal articles (Austin, 1996). As a result of this audit the DOE audit team concluded that the LANL's QA performance was "marginally effective." The NRC agreed with this finding, and the NRC concerns identified during this audit were deferred to the appropriate DOE deficiency reports (YM-96-D-105 to 108). The NRC recently reviewed the remedial actions proposed for these deficiencies and determined that the proposed actions appeared appropriate. Review of the associated Volcanism Synthesis Report is needed to determine if these actions have been effectively carried out and if the concerns have been resolved.

5.2 STATUS OF CONSEQUENCES ANALYSIS

Acceptance criteria and review procedures for the consequences of the igneous activity subissue will be developed in FY98. As summarized in Hill, et al. (1996) and in numerous sections of the IRSR, considerable work has been conducted relevant to independent assessment of the consequences of volcanic activity on repository performance. This work has progressed to the stage that preliminary dose calculations have been performed for extrusive volcanic scenarios (Section 3). The consequences of direct volcanic disruption of the proposed repository system are included in TPA-3 (Manteufel, et al., 1997); indirect effects of igneous activity on repository performance will be investigated in further detail starting in FY98.

Independent technical investigations also provide a defensible basis for review of DOE consequence studies, which will be presented in the forthcoming Volcanism Synthesis Report. Staff have also used the results of these independent investigations to review aspects of the DOE TSPA program (e.g., Baca and Jarzempa, 1997). Although formal acceptance criteria have not yet been developed, work has progressed to the stage that an IRSR on igneous activity consequences will be written in FY98.

5.3 NRC DISPOSITION OF COMMENTS RELATED TO IGNEOUS ACTIVITY

During review of the DOE Site Characterization Plan, and Study Plans 8.3.1.8.1.1, 8.3.1.8.1.2, and 8.3.1.8.5.1, the NRC developed fifty seven comments and questions related to igneous activity. The change in the overall DOE program has resulted in some of the comments losing validity, and additional information both from DOE and from ongoing work by NRC and CNWRA staff has become available to close many others. As a result thirty four of these comments and questions had been closed prior to the development of this IRSR. NRC disposition of the remaining comments and questions is listed below.

SCA Comment 45: Reliance on volcanic rate calculations that are developed largely independent of consideration of the underlying volcanic-tectonic processes appears likely to underestimate potential impacts on the performance of the repository.

NRC DISPOSITION OF COMMENT: NRC considers this comment resolved. The underlying basis of this comment was a concern as to whether rates of volcanic activity should be considered to be increasing, decreasing, or remaining essentially the same for the period of performance. It must be recognized that, at this time, the underlying processes responsible for volcano formation are very poorly understood.

Recent work by both the State of Nevada (Yogodzinski and Smith, 1995) and the CNWRA (Hill and Connor, 1996) indicates the YMR can be described as lying in a geochemical province that extends south to the Death Valley region and includes the area of the Funeral Formation in the Greenwater Range. The geochemical similarity of various volcanic units indicates that, although not understood, comparable geological processes have acted on all these units. When considering the entire YMR, including the area of the Funeral Formation, the rate of volcanic vent formation has remained relatively constant through the Quaternary and into the Pliocene. The geologic evidence, therefore, suggests that a relatively steady state of volcanic vent formation has occurred for millions of years in the YMR.

The NRC staff, therefore, considers that there is no basis for assuming either an increasing or decreasing rate of volcanic vent formation during the period of repository performance. In review of DOE probability values, and in development of independent probability values, the NRC will use recurrence rates that reflect a relatively steady state of volcanism.

SCA Comment 51: Geophysical survey programs as identified in the SCP may not be sufficient to identify and characterize both the deep crustal and shallow geologic features and their interrelationship.

NRC DISPOSITION OF COMMENT: NRC considers this comment resolved. See Response to Comment 9, Study Plan 8.3.1.8.1.1.

SCA Comment 52: No specific geophysical program appears to be planned to identify volcanic or igneous features and their extent under or close to the site.

NRC DISPOSITION OF COMMENT: NRC considers this comment resolved. See Response to Comment 9, Study Plan 8.3.1.8.1.1.

SCA Question 12: Why has the Lunar Crater area not been included as a possible analog for detailed study of the processes related to basaltic volcanism in the Death Valley-Pancake Range Volcanic Belt?

NRC DISPOSITION OF COMMENT: NRC considers the question resolved. NRC will use its analog studies, primarily at Tolbachik and Cerro Negro, to evaluate volcanic processes and DOE assumptions about volcanic processes.

STUDY PLAN 8.3.1.8.1.1 Comment 1: The use of the term "event" in this study plan appears to be limited to cone formation, and therefore provides an incomplete description of magmatic processes and events, and the requirement to determine consequence of the resultant activity.

NRC DISPOSITION OF COMMENT: NRC considers this comment resolved. As discussed under Probability Criterion 2 the use of the proper definition of event and the ability to carry this definition through the calculations can have a large effect on the resultant probabilities. NRC has carried the calculations through to the probability and will assure that the analyses of DOE also reflect the event definitions.

STUDY PLAN 8.3.1.8.1.1 Comment 2: Use of surface extrusion rates to approximate magma production rates could underestimate the effects of the magmatic process on repository performance.

NRC DISPOSITION OF COMMENT: The NRC considers the comment resolved. Recent work on the size of Little Cones (Stamatakos, et al., 1997a) and the Amargosa magnetic anomalies (Connor, et al., 1997) shows that additional volumes of material have been erupted and were not considered in the various volume predictive calculations presented in the probabilistic hazard assessment report or DOE status reports (e.g., Crowe, et al., 1995).

Examination of Geomatrix, 1996, shows that this approach had a negligible effect on any probability values reported, and the overall effect of this approach, when averaged over the results of the entire panel, appears negligible (Brocoum, 1997).

Although NRC has concerns related to a volume predictive approach, it appears that these concerns do not need to be resolved in evaluating DOE probability models. NRC-preferred probability values do not rely on eruption volumes.

STUDY PLAN 8.3.1.8.1.1, Comment 3: The evaluation of the presence of crustal magma bodies in the vicinity of Yucca Mountain must consider the requirements of 10 CFR Part 60.122(a)(2).

NRC DISPOSITION OF COMMENT: NRC considers this comment resolved. See response to Study Plan 8.3.1.8.1.1, Comment 9.

STUDY PLAN 8.3.1.8.1.1 Comment 4: One of the main activities within this study plan, as stated on page 8, is to estimate the probability of future magmatic disruption of the Yucca Mountain site; however, the probability calculations that this study plan is intended to produce appear too limited to resolve the geologic and regulatory concerns.

NRC DISPOSITION OF COMMENT: The NRC considers this comment resolved. The IRSR provides an acceptable probability for volcanic disruption of the repository and has an interim method for determining the probability of igneous intrusion. If the results of consequence analysis show that a more refined probability for igneous intrusion is necessary, an appropriate concern will be raised.

STUDY PLAN 8.3.1.8.1.1 Comment 5: It is unclear how a volcanic recurrence model can be constructed without knowledge of magmatic events of a size less than that needed to produce a cone.

NRC DISPOSITION OF COMMENT: The NRC considers this comment resolved. See response to Study Plan 8.3.1.8.1.1., Comment 2.

STUDY PLAN 8.3.1.8.1.1 Comment 6: This study plan does not appear to be calculating a "recurrence rate," but rather the average recurrence rate for the sampled population.

NRC DISPOSITION OF COMMENT: NRC considers this comment resolved. The methodology utilized by the DOE in the probabilistic hazard assessment report (Geomatrix, 1996), and by the CNWRA in developing the NRC preferred numbers, alleviates this concern. The IRSR provides an acceptable probability for volcanic disruption of the repository and has an interim method for determining the probability of igneous intrusion.

STUDY PLAN 8.3.1.8.1.1 Comment 7: The study plan does not appear to adequately consider models that assume volcanism is a non-Poissonian process.

NRC DISPOSITION OF COMMENT: NRC considers this comment resolved. The methodology utilized in the probabilistic hazard assessment report (Geomatrix, 1996), and in developing the NRC-preferred probability numbers in this IRSR alleviates this concern as models other than simple homogeneous Poisson processes were considered.

STUDY PLAN 8.3.1.8.1.1 Comment 9: The geophysical program described in the SCP and referred to in this study plan appears too limited to provide the information necessary to develop reasonable probability models.

NRC DISPOSITION OF COMMENT: NRC considers this comment resolved. SCA 51, and 52, Study Plan 8.3.1.8.1.1 Comments 3 and 9, and Study Plan 8.3.1.8.5.1, Comments 1 and 5 and Question 3 all deal in some way with NRC concerns related to DOE program of geophysics as it relates to volcanism.

Due to redirection of the DOE program many planned activities were curtailed. The DOE internal report Synthesis of Borehole and Geophysical Studies at Yucca Mountain, Nevada and Vicinity provides a summary of the DOE program as it stands at present.

Even prior to the DOE program redirection, due to the concerns of NRC with the limitations of the program, NRC authorized the CNWRA to initiate a program of ground magnetic evaluation of several of the known and suspected igneous features in the area of Yucca Mountain to determine if geophysics could cheaply and efficiently resolve many of the basic questions about these features. The ground magnetic work of the CNWRA (Stamatakos, et al., 1997a; Connor, et al., 1997) has demonstrated that there are more buried volcanic bodies in the vicinity of Yucca Mountain than had been suspected during the elicitation of the probabilistic hazard analysis panel (Geomatrix, 1996). These buried features, in general, also lie outside the boundaries of the high-probability zones defined in the Geomatrix report. In addition, the characteristics of these features, such as the size of Little Cones, were not as assumed in Geomatrix, 1996, and there appears to be a strong association of volcanoes with faulting. Based on evaluation of the results of the DOE program and the work of the CNWRA, the following steps have been taken to address these concerns:

1. As additional buried volcanoes have been detected, some in areas outside locations previously known to contain buried volcanoes, it must be assumed that even more buried volcanoes are present, both within and outside the locations known from surface work. As a result the total number of volcanic events utilized in the probability assessments must reflect both the increase in the total number of events and the uncertainty in this number.

2. The subsurface characteristics of known igneous bodies in the vicinity of Yucca Mountain are presently poorly defined. Therefore, conservative assumptions about these features are being used in both probability and consequence analyses.
3. The characteristics and location of smaller igneous intrusive bodies, such as dikes and sills, is poorly known in the YMR. Therefore, undetected dikes and sills must be assumed to exist in the area of Yucca Mountain.
4. Information at present is insufficient to resolve concerns related to potential occurrence of crustal magma bodies in the vicinity of Yucca Mountain. Therefore, it is assumed that a source for magma generation is present in the Yucca Mountain area.
5. There are many open questions regarding the interrelationship of structure and igneous features. The ground magnetics of the CNWRA (Stamatakis, et al., 1997a; Connor, et al., 1997) strongly suggest that there is a strong relationship in the YMR. Therefore, a conservative series of assumptions is being made regarding this kind of interrelationship.
6. The present geologic and geophysical data provides no geologic basis for structural separation of Yucca Mountain and Crater Flat. Rather, the data drives one to the conclusion that Yucca Mountain is part of the Crater Flat basin. Therefore, it is assumed that the Yucca Mountain site lies within the same source region as the basaltic volcanoes of Crater Flat.

It is the staff's opinion that use of the above assumptions can compensate for the limitations of the geophysical program as implemented. These assumptions have been utilized in the development of the probability values contained within the IRSR. Therefore the concerns can be resolved as the IRSR provides an acceptable probability for volcanic disruption of the repository and has an interim method for determining the probability of igneous intrusion.

In evaluation of Yucca Mountain site performance and evaluation of programmatic documents, such as the Viability Assessment, NRC will utilize the value of 10^{-7} for direct volcanic disruption of the repository itself..

STUDY PLAN 8.3.1.8.1.1 Comment 10: The MODEL 1 methodology for calculating the probability for repository disruption presented in Section 3.2.2.2 appears to be incorrect.

NRC DISPOSITION OF COMMENT: NRC considers this comment resolved. The methodology of concern was not used in the development of the probabilistic hazard assessment report or in the development of the NRC-preferred probability numbers by the CNWRA.

STUDY PLAN 8.3.1.8.1.2 Comment 2: The study plan does not address how volatile contents of basaltic eruptions will be described and assessed.

NRC DISPOSITION OF COMMENT: NRC considers this comment open, pending receipt and review of the Volcanism Synthesis report. This comment will be revisited during revisions of the IRSR dealing with volcanic consequences.

STUDY PLAN 8.3.1.8.1.2 Comment 9: The proposed studies for wall-rock fragmentation and subsurface effects do not appear to account for the modification in lithostatic pressures that will occur due to repository construction and operation.

NRC DISPOSITION OF COMMENT: NRC considers this comment open, pending receipt and review of the Volcanism Synthesis report. This comment will be revisited during revisions of the IRSR dealing with volcanic consequences.

STUDY PLAN 8.3.1.8.5.1, R0 Question 3: Have additional analog studies, aside from those presented in this activity, been considered by DOE?

NRC DISPOSITION OF QUESTION: The NRC considers this question resolved. The primary concern remaining on this question was the DOE assumption of waning patterns of volcanism. As is stated in the response to SCA Comment 45, NRC considers the geologic evidence supports a relatively steady state of YMR volcanism from the Pliocene into the Quaternary. Therefore, recurrence rates used in probability calculations will be evaluated utilizing this assumption.

STUDY PLAN 8.3.1.8.5.1 R1 Comment 1: The aeromagnetic data described in Section 2.1.1 may not be sufficient to detect and resolve magnetic anomalies associated with small intrusions that are of regulatory concern.

NRC DISPOSITION OF COMMENT: NRC considers this comment resolved. See response to comment 9, Study Plan 8.3.1.8.1.1.

STUDY PLAN 8.3.1.8.5.1 R1 Comment 4: It is unclear how the volume of eruptive basalt is being calculated.

NRC DISPOSITION OF COMMENT: NRC considers this comment resolved. As was shown in the response to Comment 2, Study Plan 8.3.1.8.1.1, this concern has been somewhat alleviated due to the fact the probability calculations have, in general, not used the volume predictive approach. The concern is applicable, however, when considering the volume of material that must be considered in evaluating consequence of igneous events for performance assessment.

The remaining concern in this comment will be addressed primarily by using independent calculations of volume and values obtained by analogs in determining consequences of igneous events.

STUDY PLAN 8.3.1.8.5.1 R1 Comment 5: It is unclear how the model that assumes northwest-trending structures provide deep-seated control on magma pathways will be tested.

NRC DISPOSITION OF COMMENT: NRC considers this comment resolved. While NRC has remaining concerns as to the geologic basis of the various volcanic zones proposed by DOE, such as the northwest-trending CFVZ, the NRC will rely on independent methods of calculating probability that do not rely on volcanic zone definition, such as the methods of Connor and Hill (1995).

STUDY PLAN 8.3.1.8.5.1 R1 Comment 7: It is unclear how the research discussed in this study plan will resolve alternative petrogenic models.

NRC DISPOSITION OF COMMENT: NRC considers this comment open, pending submittal and review of the Volcanism Synthesis report. This comment will be revisited during revisions of the IRSR dealing with volcanic consequences.

STUDY PLAN 8.3.1.8.5.1 R1 Question 3: How are the intrusive geometries associated with the development of the Crater Flat alignment to be characterized?

NRC DISPOSITION OF COMMENT: NRC considers this comment resolved. See response to Study Plan 8.3.1.8.1.1, Comment 9.

STUDY PLAN 8.3.1.8.5.1 R1 Question 5: If the theory of polycyclic volcanism is correct for the volcanoes in the region of Yucca Mountain, how will it be assured that the age determinations accurately represent the age of the various cones?

NRC DISPOSITION OF COMMENT: NRC considers this comment resolved. The results of recent dating and trenching studies at Lathrop Wells volcano have shown that there has been significant erosion of the cone and that no significant age difference between eruptive units can be demonstrated (see Site Characterization Progress Report #15). As these were two of the main basis points for the theory of polycyclic volcanism, the NRC considered that this theory has been refuted and no longer deserves consideration. This theory also was given little weight during the probabilistic hazard assessment (Geomatrix, 1996).

STUDY PLAN 8.3.1.8.5.1 R1 Question 8: How will volumetric relationships from the different systems in western North America be used to develop specific, time-dependent, volume-predictive models for the Crater Flat system?

NRC DISPOSITION OF COMMENT: NRC considers the comment resolved. The use of volume-predictive methods for developing volcanic probabilities does not appear to be utilized by DOE, therefore, this question is no longer of concern. See also response to Comment 2, Study Plan 8.3.1.8.1.1.

THIS PAGE INTENTIONALLY BLANK

6.0 REFERENCES

- Anderson, E.M. 1938. *The dynamics of sheet intrusion*. Proceedings of the Royal Society of Edinburgh 58: 242–251.
- Anderson, D.L. 1989. *Theory of the Earth*. London: Blackwell Scientific Publications.
- Austin, J.H. 1996. Letter (October 24) to R.A. Milner, U.S. Department of Energy. Washington, DC: U.S. Nuclear Regulatory Commission.
- Ayer, J.E., A.T. Clark, P. Loysen, M.Y. Ballinger, J. Mishima, P.C. Owczarski, W.S. Gregory, and B.D. Nichols. 1988. *Nuclear Fuel Cycle Facility Accident Analysis Handbook*. NUREG-1320. Washington, DC, U.S. Nuclear Regulatory Commission.
- Baca, R.G., and M.S. Jarzempa. 1997. *Detailed Review of Selected Aspects of Total System Performance Assessment — 1995*. IM 5708-761-710. San Antonio, TX: Center for Nuclear Waste Regulatory Analyses.
- Bacon, C.R. 1982. *Time-predictable bimodal volcanism in the Coso Range, California*. Geology 10: 65–69.
- Barnard, R.W., M.L. Wilson, H.A. Dockery, J.H. Gauthier, P.G. Kaplan, R.R. Eaton, F.W. Bingham, and T.H. Robey. 1992. *TSPA 1991: An Initial Total-System Performance Assessment for Yucca Mountain*. Sandia National Laboratories Report SAND91-2795. Albuquerque, NM: Sandia National Laboratories.
- Barr, G.E., E. Dunn, H. Dockery, R. Barnard, G. Valentine, and B. Crowe. 1993. *Scenarios Constructed for Basaltic Igneous Activity at Yucca Mountain and Vicinity*. Sandia National Laboratory Report SAND 91-1653. Albuquerque, NM: Sandia National Laboratory.
- Bell, M.J. 1997. Letter (June 25) to S.J. Brocoum, U.S. Department of Energy. Washington, DC: U.S. Nuclear Regulatory Commission.
- Bemis, K.G., and D.K. Smith. 1993. *Production of small volcanoes in the Superswell region of the South Pacific*. Earth and Planetary Science Letters 118: 251–262.
- Bradshaw, T.K., and E.I. Smith. 1994. *Polygenetic Quaternary volcanism at Crater Flat, Nevada*. Journal of Volcanology and Geothermal Research 63: 165–182.
- Braytseva, O.A., I.V. Melekestev, and V.V. Ponomareva. 1983. *Age divisions of the Holocene volcanic formations of the Tolbachik Valley*. The Great Tolbachik Fissure Eruption. S.A. Fedotov and Y.K. Markhinin, eds. New York, NY: Cambridge University Press: 83–95.
- Brocher, T.M., P.E. Hart, W.C. Hunter, and V.E. Langenheim. 1996. *Hybrid-Source Reflection Profiling Across Yucca Mountain, Nevada: Regional Lines 2 and 3*. U.S. Geological Survey Open-File Report 96-28. Reston, VA: U.S. Geological Survey.

Brocoum, S.J. 1997. Letter (June 4) to J.T. Greeves, U.S. Nuclear Regulatory Commission. Washington, DC: U.S. Department of Energy.

Carr, W.J. 1982. *Volcano-Tectonic History of Crater Flat, Southwestern Nevada, as Suggested by New Evidence from Drill Hole USU-VH-1 and Vicinity*. U.S. Geological Survey Open-File Report 82-457. Reston, VA: U.S. Geological Survey.

Carter Krogh, K.E., and G.A. Valentine. 1995. *Dike and sill emplacement in a shallow extensional setting, Paiute Ridge, NV*. EOS, Transactions of the American Geophysical Union, 76(46): F691.

Champion, D.E. 1991. *Volcanic episodes near Yucca Mountain as determined by paleomagnetic studies at Lathrop Wells, Crater Flat, and Sleeping Butte, Nevada*. Proceedings of the Second Annual International Conference on High-Level Radioactive Waste Management. La Grange Park, IL: American Nuclear Society: 61-67.

Condit, C.D., and C.B. Connor. 1996. *Recurrence rates of volcanism in basaltic volcanic fields: An example from the Springerville volcanic field, Arizona*. Geological Society of America Bulletin 108: 1,225-1,241.

Condit, C.D., L.S. Crumpler, J.C. Aubele, and W.E. Elston. 1989. *Patterns of volcanism along the southern margin of the Colorado Plateau: The Springerville Field*. Journal of Geophysical Research 94(B6): 7,975-7,986.

Connor, C.B. 1990. *Cinder cone clustering in the TransMexican volcanic belt: Structural and petrologic implications*. Journal of Geophysical Research 95: 19,395-19,405.

Connor, C.B. 1993. *Technical and Regulatory Basis for the Study of Recently Active Cinder Cones*. IM-20-5704-141-001. San Antonio, TX: Center for Nuclear Waste Regulatory Analyses.

Connor, C.B., and B.E. Hill. 1993. *Estimating the probability of volcanic disruption of the candidate Yucca Mountain repository using spatially and temporally nonhomogeneous Poisson models*. Proceedings, American Nuclear Society Focus '93 Meeting. La Grange Park, IL: American Nuclear Society: 174-181.

Connor, C.B., and B.E. Hill. 1994. *The CNWRA Volcanism Geographic Information System Database*. CNWRA 94-004. San Antonio, TX: Center for Nuclear Waste Regulatory Analyses.

Connor, C.B., and B.E. Hill. 1995. *Three nonhomogeneous Poisson models for the probability of basaltic volcanism: Application to the Yucca Mountain region, Nevada, U.S.A.* Journal of Geophysical Research 100(B6): 10,107-10,125.

Connor, C.B., C.D. Condit, L.S. Crumpler, and J.C. Aubele. 1992. *Evidence of regional structural controls on vent distribution: Springerville volcanic field, Arizona*. Journal of Geophysical Research 97: 12,349-12,359.

Connor, C.B., B.E. Hill, B.W. Leslie, C. Lin, J.F. Luhr, K.D. Mahrer, G.L. Stirewalt, and

S.R. Young. 1993. *Review of Preliminary Draft: Status of Volcanic Hazard Studies for the Yucca Mountain Site Characterization Project, Dated February 1993*. San Antonio, TX: Center for Nuclear Waste Regulatory Analyses.

Connor, C.B., J. Stamatakos, D. Ferrill, B.E. Hill, S.B.L. Magsino, P. La Femina and R.H. Martin. 1996. Integrating structural models into probabilistic volcanic hazard analyses: An example from Yucca Mountain, NV. EOS, Transactions of the American Geophysical Union. 77(46): F21.

Connor, C.B., S. Lane-Magsino, J.A. Stamatakos, R.H. Martin, P.C. La Femina, B.E. Hill, and S. Lieber. 1997. Magnetic surveys help reassess volcanic hazards at Yucca Mountain, Nevada. EOS, Transactions of the American Geophysical Union 78(7): 73-78.

Conway, M.F., D.A. Ferrill, C.M. Hall, A.P. Morris, J.A. Stamatakos, C.B. Connor, A.N. Halliday, and C. Condit. 1997. *Timing of basaltic volcanism along the Mesa Butte Fault in the San Francisco volcanic field, Arizona, from $^{40}\text{Ar}/^{39}\text{Ar}$ dates: Implications for longevity of cinder cone alignments*. Journal of Geophysical Research 102: 815-824.

Crow, L.H. 1982. *Confidence interval procedures for the Weibull process with applications to reliability growth*. Technometrics 24: 67-71.

Crowe, B.M., and F.V. Perry. 1989. *Volcanic probability calculations for the Yucca Mountain site: Estimation of volcanic rates*. Proceedings Nuclear Waste Isolation in the Unsaturated Zone, Focus '89. La Grange Park, IL: American Nuclear Society: 326-334.

Crowe, B., and F. Perry. 1991. *Preliminary Geologic Map of the Sleeping Butte Volcanic Centers*. Los Alamos National Laboratory Report LA-12101-MS. Los Alamos, NM: Los Alamos National Laboratory.

Crowe, B.M., M.E. Johnson, and R.J. Beckman. 1982. *Calculation of the probability of volcanic disruption of a high-level nuclear waste repository within southern Nevada, USA*. Radioactive Waste Management and the Nuclear Fuel Cycle 3: 167-190.

Crowe, B.M., D.T. Vaniman, and W.J. Carr. 1983. *Status of Volcanic Hazard Studies for the Nevada Nuclear Waste Storage Investigations*. Los Alamos National Laboratory Report LA-9325-MS. Los Alamos, NM: Los Alamos National Laboratory.

Crowe, B.M., K.H. Wohletz, D.T. Vaniman, E. Gladney, and N. Bower. 1986. *Status of Volcanic Hazard Studies for the Nevada Nuclear Waste Storage Investigations*. Los Alamos National Laboratory Report LA-9325-MS, Vol. II. Los Alamos, NM: Los Alamos National Laboratory.

Crowe, B., R. Morley, S. Wells, J. Geissman, E. McDonald, L. McFadden, F. Perry, M. Murrell, J. Poths, and S. Forman. 1992. *The Lathrop Wells volcanic center: Status of field and geochronology studies*. Proceedings of the Third International Conference on High-Level Radioactive Waste Management. La Grange Park, IL: American Nuclear Society: 1,997-2,013.

Crowe, B.M., F.V. Perry, J. Geissman, L. McFadden, S. Wells, M. Murrell, J. Poths, G.A.

Valentine, L. Bowker, and K. Finnegan. 1995. *Status of Volcanic Hazard Studies for the Yucca Mountain Site Characterization Project*. Los Alamos National Laboratory Report LA-12908-MS. Los Alamos, NM: Los Alamos National Laboratory.

Delaney, P.T., and A.E. Gartner. 1995. *Physical Processes of Shallow Mafic Dike Emplacement Near the San Rafael Swell, Utah*. U.S. Geological Survey Open-file Report 95-491. Reston, VA: U.S. Geological Survey.

Delaney, P.T., D.D. Pollard, J.I. Ziony, and E.H. McKee. 1986. *Field relations between dikes and joints: Emplacement processes and paleostress analysis*. Journal of Geophysical Research 91(B5): 4,920-4,938.

Dohrenwend, J.C., L.D. McFadden, B.D. Turrin, and S.G. Wells. 1984. *K-Ar dating of the Cima Volcanic Field, eastern Mojave Desert, California: Late Cenozoic volcanic history and landscape evolution*. Geology 12: 163-167.

Doubik, Y., A.A. Ovsyannikov, C. Connor, R. Martin, and P. Doubik. 1995. Development of the 1975 Tolbachik cinder cone alignment—nature of areal and lateral basaltic volcanism. EOS, Transactions of the American Geophysical Union 76(46): F540.

Draper, G., Z. Chen, M. Conway, C.B. Connor, and C.D. Condit. 1994. Structural control of magma pathways in the upper crust: Insights from the San Francisco volcanic field, Arizona. Geological Society of America Abstracts with Programs 26(7): A-115.

Duffield, W.A., C.R. Bacon, and G.B. Dalrymple. 1980. *Late Cenozoic volcanism, geochronology, and structure of the Coso Range, Inyo County, California*. Journal of Geophysical Research 85(B5): 2,381-2,404.

Eichelberger, J.C., and R. Gooley. 1977. *Evolution of silicic magma chambers and their relationship to basaltic volcanism*. The Earth's Crust, Geophysical Monograph Series, Volume 20. J.G. Heacock, ed. Washington, DC: American Geophysical Union: 57-77.

Einziger, R.E., L.E. Thomas, H.C. Buchanan, and R.B. Scott. 1992. *Oxidation of Spent Fuel in Air at 175 to 195 C*. Journal of Nuclear Material 190: 53

Farmer, G.L., F.V. Perry, S. Semken, B. Crowe, D. Curtis, and D.J. DePaolo. 1989. *Isotopic evidence on the structure and origin of subcontinental lithospheric mantle in southern Nevada*. Journal of Geophysical Research 94: 7,885-7,898.

Faulds, J.E., J.W. Bell, D.L. Feuerbach, and A.R. Ramelli. 1994. *Geologic Map of the Crater Flat Area, Nevada*. Nevada Bureau of Mines and Geology Map 101. Reno, NV: Nevada Bureau of Mines and Geology.

Fedotov, S.A. 1983. *Chronology and features of the southern breakout of the Great Tolbachik fissure eruption, 1975-1976*. The Great Tolbachik Fissure Eruption, Geological and Geophysical Data 1975-1976. S.A. Fedotov and Y. K. Markhinin, eds. Cambridge, MA: Cambridge University Press: 11-26.

- Ferrill, D.A., J.A. Stamatakos, K.H. Spivey, and A.P. Morris. 1995. *Tectonic processes in the central Basin and Range region*. NRC High-Level Radioactive Waste Research at CNWRA, July–December 1995. B. Sagar, ed. CNWRA 95-01S. San Antonio, TX: Center for Nuclear Waste Regulatory Analyses: 6-1 to 6-27.
- Ferrill, D.A., J.A. Stamatakos, S.M. Jones, B. Rahe, H.L. McKague, R.H. Martin, and A.P. Morris. 1996a. *Quaternary slip history of the Bare Mountain fault (Nevada) from the morphology and distribution of alluvial fan deposits*. Geology 24(6): 559–562.
- Ferrill, D.A., G.L. Stirewalt, D.B. Henderson., J.A. Stamatakos, K.H. Spivey, and B.P. Wernicke. 1996b. *Faulting in the Yucca Mountain Region*. CNWRA 95-017. San Antonio, TX: Center for Nuclear Waste Regulatory Analyses.
- Ferrill, D.A., J.A. Stamatakos, A.P. Morris, R.A. Donelick, A.E. Blythe, S.M. Jones, and K. Spivey. 1997. *Geometric, Thermal, and Temporal Constraints on the Tectonic Evolution of Bare Mountain, Nevada*. IM 20-5708-471-731. San Antonio, TX: Center for Nuclear Waste Regulatory Analyses.
- Foland, K.A., and S.C. Bergman. 1992. *Temporal and spatial distribution of basaltic volcanism in the Pancake and Reveille Ranges north of Yucca Mountain*. Proceedings of the Third International Conference on High-Level Radioactive Waste Management. La Grange Park, IL: American Nuclear Society: 2,366–2,371.
- Fridrich, C.J. 1997. *Tectonic evolution of the Crater Flat Basin, Yucca Mountain region, Nevada*. *Cenozoic Basins of the Death Valley Region*. L. Wright and B. Troxel, eds. Geological Society of America Special Paper. Boulder, CO: Geological Society of America. In press.
- Fridrich, C.J., J.W. Whitney, M.R. Hudson, and B.M. Crowe. 1997. *Late Cenozoic extension, vertical-axis rotation, and volcanism in the Crater Flat basin, southwest Nevada*. *Cenozoic Basins of the Death Valley Region*. L. Wright and B. Troxel, eds. Geological Society of America Special Paper. Boulder, CO: Geological Society of America. In press.
- Frizzell, V.A., Jr., and J. Shulters. 1990. *Geologic Map of the Nevada Test Site, Southern Nevada*. Miscellaneous Investigations Map I-2046. Reston, VA: U.S. Geological Survey.
- Gartner, A.E., and P.T. Delaney. 1988. *Geologic Map Showing a Late Cenozoic Basaltic Intrusive Complex, Emery, Sevier, and Wayne Counties, Utah*. Miscellaneous Field Studies Map MF-2052. Reston, VA: U.S. Geological Survey.
- Geomatrix. 1996. *Probabilistic Volcanic Hazards Analysis for Yucca Mountain, Nevada*. Report BA0000000-1717-2200-00082, Rev. 0. San Francisco, CA: Geomatrix Consultants.
- Gudmundsson, A. 1984. *Formation of dykes, feeder-dykes, and the intrusion of dykes from magma chambers*. Bulletin of Volcanology 47: 537–550.
- Gupta, V.K., and F.S. Grant. 1984. *Mineral-exploration aspects of gravity and aeromagnetic surveys in the Sudbury-Cobalt area, Ontario*. The Utility of Regional Gravity and Magnetic

Anomaly Maps. W.J. Hinze, ed. Tulsa, OK: Society of Exploration Geophysicists: 392–412.

Hardyman, R.F., and J.S. Oldow. 1991. *Tertiary tectonic framework and Cenozoic history of the central Walker Lane, Nevada*. Geology and Ore Deposits of the Great Basin, Symposium Proceedings. G.L. Raines, R.E. Lisle, R.W. Schafer, and W.H. Wilkinson, eds. Reno, NV: Geological Society of Nevada.

Hasenaka, T., and I.S.E. Carmichael. 1985. *The cinder cones of Michoacan-Guanajuato, central Mexico: Their age, volume and distribution, and magma discharge rate*. Journal of Volcanology and Geothermal Research 25: 105–124.

Hawkesworth, C., S. Turner, K. Gallagher, A. Hunter, T. Bradshaw, and N. Rogers. 1995. *Calc-alkaline magmatism, lithospheric thinning and extension in the Basin and Range*. Journal of Geophysical Research 100(B7): 10,271–10,286.

Heming, R.F. 1980. *Patterns of Quaternary basaltic volcanism in the northern North Island, New Zealand*. New Zealand Journal of Geology and Geophysics 23: 335–344.

Hill, B.E. 1995. *Current Concerns Regarding DOE/LANL Volcanism Geochemical Data*. AI 5702-441-547. San Antonio, TX: Center for Nuclear Waste Regulatory Analyses.

Hill, B.E. 1996. *Constraints on the Potential Subsurface Area of Disruption Associated with Yucca Mountain Region Basaltic Volcanoes*. IM 5708-461-701. San Antonio, TX: Center for Nuclear Waste Regulatory Analyses.

Hill, B.E. 1997. *CNWRA dose calculations for volcanic disruption of the proposed repository. Presentation to Advisory Committee on Nuclear Waste*. April 22, 1997. Rockville, MD.

Hill, B.E., and C.B. Connor. 1996. *Volcanic Systems of the Basin and Range*. NRC High-Level Radioactive Waste Research at CNWRA, July–December 1995. CNWRA 95-02S. San Antonio, TX: Center for Nuclear Waste Regulatory Analyses: 5-1 to 5-21.

Hill, B.E., C.B. Connor, and J.S. Trapp. 1996. *Igneous activity, NRC High-Level Radioactive Waste Program Annual Progress Report, Fiscal Year 1996*. CNWRA 96-01A. San Antonio, TX: Center for Nuclear Waste Regulatory Analyses: 2-1 to 2-32.

Hill, B.E., B.W. Leslie, and C.B. Connor. 1993. *A Review and Analysis of Dating Techniques for Neogene and Quaternary Volcanic Rocks*. CNWRA 93-018. San Antonio, TX: Center for Nuclear Waste Regulatory Analyses.

Ho, C.H. 1991. *Time trend analysis of basaltic volcanism at the Yucca Mountain site*. Journal of Volcanology and Geothermal Research 46: 61–72.

Ho, C.H. 1992. *Risk assessment for the Yucca Mountain high-level nuclear waste repository site: Estimation of volcanic disruption*. Mathematical Geology 24: 347–364.

Ho, C.H., E.I. Smith, D.L. Feurbach, and T.R. Naumann. 1991. *Eruptive probability calculation*

for the Yucca Mountain site, USA: Statistical estimation of recurrence rates. Bulletin of Volcanology 54: 50–56.

Hogg, R.V., and E.A. Tanis. 1988. *Probability and Statistical Inference*. New York, NY: Macmillan Co.

Howard, N.W. 1985. *Variation in Properties of Nuclear Test Areas and Media at the Nevada Test Site*. UCRL-53721. Livermore, CA: University of California, Lawrence Livermore National Laboratory.

Hudson, M.R., D.A. Sawyer, and R.G. Warren. 1994. *Paleomagnetism and rotation constraints for the Miocene southwestern Nevada volcanic field*. Tectonics 13: 258–277.

Jarzemba, M.S., and P.A. LaPlante. 1996. *Preliminary Calculations of Expected Dose from Extrusive Volcanic Events at Yucca Mountain*. IM 5078-771-610. San Antonio, TX: Center for Nuclear Waste Regulatory Analyses.

Jarzemba, M.S., P.A. LaPlante, and K.J. Poor. 1997. *ASHPLUME Version 1.0 — A Code for Contaminated Ash Dispersal and Deposition, Technical Description and User's Guide*. CNWRA 97-004. San Antonio, TX: Center for Nuclear Waste Regulatory Analyses.

Jolly, R.J.H., and D.L. Sanderson. 1997. *A Mohr circle construction for the opening of a pre-existing fracture*. Journal of Structural Geology 19: 887–892.

Kear, D. 1964. Volcanic alignments north and west of New Zealand's central volcanic region. New Zealand Journal of Geology and Geophysics 7: 24–44.

Kuntz, M.A., D.E. Champion, E.C. Spiker, and R.H. Lefebvre. 1986. *Contrasting magma types and steady-state, volume-predictable basaltic volcanism along the Great Rift, Idaho*. Geological Society of America Bulletin 97: 579–594.

Lachenbruch, A.H., and P. Morgan. 1990. *Continental extension, magmatism and elevation; formal relations and rules of thumb*. Tectonophysics 174: 39–62.

Langenheim, V.E., and D.A. Ponce. 1995. *Depth to Pre-Cenozoic basement in southwest Nevada*. Proceedings of the Sixth Annual International Conference on High-Level Radioactive Waste Management. La Grange Park, IL: American Nuclear Society: 129–131.

Langenheim, V.E., K.S. Kirchoff–Stein, and H.W. Oliver. 1993. *Geophysical investigations of buried volcanic centers near Yucca Mountain, southwestern Nevada*. Proceedings of Fourth Annual International Conference on High-Level Radioactive Waste Management. La Grange Park, IL: American Nuclear Society: 1,840–1,846.

Leeman, W.P. 1970. *The isotopic composition of strontium in Late Cenozoic basalts from the Basin-Range Province, western United States*. Geochimica et Cosmochimica Acta 34: 857–872.

Leeman, W.P., and J.G. Fitton. 1989. *Magmatism associated with lithospheric extension:*

Introduction. Journal of Geophysical Research 94(B6): 7,682–7,684.

Link, R.L., S.E. Logan, H.S. Ng, F.A. Rokenbach, and K.J. Hong. 1982. *Parametric Studies of Radiological Consequences of Basaltic Volcanism*. Sandia National Laboratory Report SAND 81-2375. Albuquerque, NM: Sandia National Laboratory.

Lister, J.R. and R.C. Kerr, 1991. *Fluid-mechanical models of crack propagation and their application to magma transport in dykes*. Journal of Geophysical Research 96: 10,049–10,077.

Luedke, R.G., and R.L. Smith. 1981. *Map Showing Distribution, Composition, and Age of Late Cenozoic Volcanic Centers in California and Nevada*. U.S. Geological Survey Miscellaneous Investigations Series Map I-1091-C. Reston, VA: U.S. Geological Survey.

Luhr, J.F., and T. Simkin. 1993. *Paricutin, the Volcano Born in a Mexican Cornfield*. Phoenix, AZ: Geoscience Press.

Lutz, T.M., 1986. *An analysis of the orientations of large scale crustal structures: a statistical approach based on areal distribution of point-like features*. Journal of Geophysical Research 91: 421–434.

Lutz, T.M., and J.T. Gutmann. 1995. *An improved method of determining the alignment of point-like features and implications for the Panicked volcanic field, Mexico*. Journal of Geophysical Research 100: 17,659–17,670.

Magus'kin, M.A., V.B. Enman, and V.S. Tselishchev. 1983. *Changes in height, volume and shape of the New Tolbachik volcanoes of the Northern Breakout*. The Great Tolbachik Fissure Eruption. Geological and Geophysical Data 1975–1976. S.A. Fedotov, and Ye. K. Markhinin, eds. Cambridge, MA: Cambridge University Press: 307–315.

Manteufel, R.D., R.G. Baca, S. Mohanty, M.S. Jarzemba, S.A. Stothoff, C.B. Connor, G.A. Cragnolino, A. Chowdhury, T.J. McCartin, and T.M. Ahn. 1997. *Total-System Performance Assessment (TPA) Version 3.0 Code: Module Descriptions and User's Guide*. IM 20-5708-762-730. San Antonio, TX: Center for Nuclear Waste Regulatory Analyses.

Margulies, T., L. Lancaster, N. Eisenberg, and L. Abramson. 1992. *Probabilistic analysis of magma scenarios for assessing geologic waste repository performance*. American Society of Mechanical Engineers. Winter Annual Meeting. New York, NY: American Society of Mechanical Engineers.

McBirney, A.R. 1992. *Volcanology. Techniques for Determining Probabilities of Geologic Events and Processes*. International Association for Mathematical Geology, Studies in Mathematical Geology No. 4. R.L. Hunter and C.J. Mann, eds. New York, NY: Oxford University Press: 167–184.

McDuffie, S.M., C.B. Connor, and K.D. Mahrer. 1994. *A simple 2-D stress model of dike-fracture interaction*. EOS, Transactions of the American Geophysical Union 75(16): 345.

McKague, H.L. 1980. *Summary of Measured Medium Properties of Paleozoic Rocks at the DOE Nevada Test Site*. UCRL-52884. Livermore, CA: University of California, Lawrence Livermore National Laboratory.

McKenzie, D., and M.J. Bickle. 1988. *The volume and composition of melt generated by extension of the lithosphere*. Journal of Petrology 29: 625–679.

Morris, A., D.A. Ferrill, and D.B. Henderson. 1996. *Slip-tendency analysis and fault reactivation*. Geology 24(3): 275–278.

Nakamura, K. 1977. *Volcanoes as possible indicators of tectonic stress orientation—principles and proposal*. Journal of Volcanology and Geothermal Research 2: 1–16.

Nuclear Regulatory Commission. 1996. *Branch Technical Position on the Use of Expert Elicitation in the High-Level Radioactive Waste Program*. NUREG-1563. Washington, DC

Nuclear Regulatory Commission. 1997. *Disposal of High-Level Radioactive Wastes in Geologic Repositories*. Code of Federal Regulations, Title 10 — Energy, Chapter 1—U.S. Nuclear Regulatory Commission Part 60.152. Washington, DC: U.S. Government Printing Office.

Ofoegbu, G.L., and D.A. Ferrill. 1995. *Finite Element Modeling of Listric Normal Faulting*. CNWRA 95-008. San Antonio, TX: Center for Nuclear Waste Regulatory Analyses.

O'Leary, D.W. 1996. *Synthesis of tectonic models for the Yucca Mountain area*. Seismotectonic Framework and Characterization of Faulting at Yucca Mountain, Nevada. J.W. Whitney, ed. U.S. Geological Survey Report to the U.S. Department of Energy, Milestone 3GSH100M. Reston, VA: U.S. Geological Survey: 8-1 to 8-153.

Parsons, T., and G.A. Thompson. 1991. *The role of magma overpressure in suppressing earthquakes and topography: Worldwide examples*. Science 253: 1,399–1,402.

Pedersen, T., and H.E. Ro. 1992. *Finite duration extension and decompression melting*. Earth and Planetary Science Letters 113: 15–22.

Performance Assessment Working Group. 1997. *Branch Technical Position on a Performance Assessment Methodology for Low-Level Radioactive Waste Disposal Facilities*. NUREG-1573. Washington, DC: U.S. Nuclear Regulatory Commission.

Ratcliff, C.D., J.W. Geissman, F.V. Perry, B.M. Crowe, and P.K. Zeitler. 1994. *Paleomagnetic record of a geomagnetic field reversal from late Miocene mafic intrusions, southern Nevada*. Science 266: 412–416.

Reches, Z., and J. Fink. 1988. *The mechanism of intrusion of the Inyo Dike, Long Valley Caldera, California*. Journal of Geophysical Research 93(B5): 4,321–4,334.

Rogers, N.W., C.J. Hawkesworth, and D.S. Ormerod. 1995. *Late Cenozoic basaltic magmatism in the Western Great Basin, California and Nevada*. Journal of Geophysical Research 100(B7): 10,287–10,301.

Sagar, B. 1997. *NRC High-Level Radioactive Waste Program Annual Progress Report: Fiscal Year 1996*. NUREG/CR-6513. Washington, DC: U.S. Nuclear Regulatory Commission.

Schweikert, R.A. and M.M. Lahren. 1997. *Strike-slip fault system in the Amargosa Valley and Yucca Mountain, Nevada*. Tectonophysics 272: 25–41.

Scott, R.B. 1990. *Tectonic setting of Yucca Mountain, southwest Nevada*. Basin and Range Extensional Tectonics Near the Latitude of Las Vegas, Nevada. B.P. Wernicke, ed. Geological Society of America Memoir 176: 251–282.

Sheridan, M.F. 1992. *A Monte Carlo technique to estimate the probability of volcanic dikes*. Proceedings of the Third International Conference on High-Level Radioactive Waste Management. La Grange Park, IL: American Nuclear Society: 2,033–2,038.

Silverman, B.W. 1986. *Density Estimation for Statistics and Data Analysis*. New York, NY: Chapman and Hall.

Smith, E.I., D.L. Feuerbach, T.R. Naumann, and J.E. Faulds. 1990. *Annual Report of the Center for Volcanic and Tectonic Studies for the Period 10-1-89 to 9-30-90*. Report 41. Carson City, Nevada: The Nuclear Waste Project Office.

Spence, D.A., and D.L. Turcotte. 1985. *Magma-driven propagation of cracks*. Journal of Geophysical Research 90(B1): 575–580.

Stablein, N.K. 1997. Letter (August 1) to S.J. Brocoum, U.S. Department of Energy. Washington, DC: U.S. Nuclear Regulatory Commission.

Stamatakis, J.A., and D.A. Ferrill. 1996. *Tectonic processes in the central Basin and Range region*. NRC High-Level Radioactive Waste Research at CNWRA, July–December 1995. B. Sagar, ed. CNWRA 95-02S. San Antonio, TX: Center for Nuclear Waste Regulatory Analyses: 6-1 to 6-25.

Stamatakis, J.A., C.B. Connor, and R.H. Martin. 1997a. *Quaternary basin evolution and basaltic volcanism of Crater Flat, Nevada, from detailed ground magnetic surveys of the Little Cones*. Journal of Geology 105: 319–330.

Stamatakis, J.A., D.A. Ferrill, and H.L. McKague. 1997b. *Technical Input on Review and Acceptance Criteria for Issue Resolution Status Report on Tectonic Models*. IM 5708-471-700. San Antonio, TX: Center for Nuclear Waste Regulatory Analyses.

Stamatakis, J.A., D.A. Ferrill, and K.H. Spivey. 1997c. *Paleomagnetic Constraints on the Tectonic Evolution of Bare Mountain, Nevada*. IM 20-5708-471-730. San Antonio, TX: Center

for Nuclear Waste Regulatory Analyses.

Stevens, B. 1911. *The laws of intrusion*. Transactions of the American Institute of Mining Engineers 41: 650–672.

Stewart, J.H. 1971. *Basin and range structure: A system of horsts and grabens produced by deep-seated extension*. Geological Society of America Bulletin 82(4): 1019–1044.

Takada, A. 1994. *The influence of regional stress and magmatic input on styles of monogenetic and polygenetic volcanism*. Journal of Geophysical Research 99: 13,563–13,574.

Takahashi, E., and I. Kushiro. 1983. *Melting of a dry peridotite at high pressures and basalt magma genesis*. American Mineralogist 68: 859–879.

Tanaka, K.L., E.M. Shoemaker, G.E. Ulrich, and E.W. Wolfe. 1986. *Migration of volcanism in the San Francisco volcanic field, Arizona*. Geological Society of America Bulletin 97: 129–141.

Thordarson, T. and S. Self. 1993. *The Laki (Skaftár Fires) and Grímsvotn eruptions in 1783–1785*. Bulletin of Volcanology 55: 233–263.

Tokarev, P.I. 1983. *Calculation of the magma discharge, growth in the height of the cone and dimensions of the feeder channel of Crater 1 in the Great Tolbachik Fissure Eruption, July 1975*. The Great Tolbachik Fissure Eruption. S.A. Fedotov and Y.K. Markhinin, eds. New York, NY: Cambridge University Press: 27–35.

TRW Environmental Safety System Inc. 1997. *Total System Performance Assessment - Viability Assessment (TSPA-VA) Method and Assumptions*. Prepared for U.S. Department of Energy, Office of Civilian Radioactive Waste Management, 1000 Independence Avenue, S.W. Washington, D.C. 20565

Turrin, B.D., D. Champion, and R.J. Fleck. 1991. *$^{40}\text{Ar}/^{39}\text{Ar}$ age of the Lathrop Wells volcanic center, Yucca Mountain, Nevada*. Science 253: 654–657.

Turrin, B.D., D. Champion, and R.J. Fleck. 1992. *Measuring the age of the Lathrop Wells volcanic center at Yucca Mountain: Response*. Science 257: 556–558.

Turrin, B.D., J.C. Dohrenwend, R.E. Drake, and G.H. Curtis. 1985. *K-Ar ages from the Cima volcanic field, eastern Mojave Desert, California*. Isochron/West 44: 9–16.

United States Department of Energy. 1998. *Repository Safety Strategy: U.S. Department of Energy's Strategy to Protect Public Health and Safety After Closure of a Yucca Mountain Repository*. Office of Civilian Radioactive Waste Management, Washington, D.C. 20585

Vaniman, D.T., B.M. Crowe, and E.S. Gladney. 1982. *Petrology and geochemistry of Hawaiite lavas from Crater Flat, Nevada*. Contributions to Mineralogy and Petrology 80: 341–357.

Wadge, G., and A. Cross. 1988. *Quantitative methods for detecting aligned points: An*

application to the vents of the Michoacán-Guanajuato volcanic field, Mexico. Geology 16: 815–818.

Wadge, G., P.A.V. Young, and I.J. McKendrick. 1994. *Mapping lava flow hazards using computer simulation. Journal of Geophysical Research 99: 489–504.*

Walker, G.P.L. 1993. Basaltic-volcano systems. *Magmatic Processes and Plate Tectonics, Geological Society Special Publications 76.* H.M. Prichard, T. Alabaster, N.B.W. Harris, and C.R. Neary, eds. London: Geological Society: 3–38.

Wells, S.G., L.D. McFadden, C.E. Renault, and B.M. Crowe. 1990. *Geomorphic assessment of late Quaternary volcanism in the Yucca Mountain area, southern Nevada: Implications for the proposed high-level radioactive waste repository. Geology 18: 549–553.*

Wells, S.G., B.M. Crowe, and L.D. McFadden. 1992. *Measuring the age of the Lathrop Wells volcanic center at Yucca Mountain: Comment. Science 257: 555–556.*

Whitney, J.W., and R.R. Shroba. 1991. *Comment on Geomorphic assessment of late Quaternary volcanism in the Yucca Mountain area, southern Nevada: Implications for the proposed high-level radioactive waste repository. Geology 18: 661.*

Wilson, M.L., J.H. Gauthier, R.W. Barnard, G.E. Barr, H.A. Dockery, E. Dunn, R.R. Eaton, D.C. Guerin, N. Lu, M.J. Martinez, R. Nilson, C.A. Rautman, T.H. Robey, B. Ross, E.E. Ryder, A.R. Schenker, S.A. Shannon, L.H. Skinner, W.G. Halsey, J.D. Gansemer, L.C. Lewis, A.D. Lamont, I.R. Triay, A. Meijer, and D.E. Morris. 1994. *Total-System Performance Assessment for Yucca Mountain – SNL Second Iteration (TSPA–1993). Sandia National Laboratories Report SAND 93–2675.* Albuquerque, NM: Sandia National Laboratories.

Yogodzinski, G.M., and E.I. Smith. 1995. *Isotopic domains and the area of interest for volcanic hazard assessment in the Yucca Mountain area. EOS, Transactions of the American Geophysical Union 76(46): F669.*

Young, S.R., G.L. Stirewalt, and A.P. Morris. 1992. *Geometric Models of Faulting at Yucca Mountain. CNWSRA 92-008.* San Antonio, TX: Center for Nuclear Waste Regulatory Analyses.

Zoback, M.L. 1989. *State of stress in the northern Basin and Range Province. Journal of Geophysical Research 94: 7,105–7,128.*

APPENDIX A

**COMPILATION OF DATES FOR BASALTIC ROCKS
OF THE YUCCA MOUNTAIN REGION**

Compilation of K-Ar and Ar/Ar dates for post-11 Ma basaltic rocks of the YMR. Units and sample numbers as reported by authors. *Wgt'd mean* corresponds to weighted mean on *n* samples and 1-sigma best estimated errors (Taylor, 1990), multiplied by the square root of the mean square of the weighted deviates (MSWD) if MSWD > 1 (e.g., Fleck et al., 1996). *Average* is average \pm 1 standard deviation of reported dates. *Unkn.* is unknown, *unpub. res.* is unpublished research, and *pers. comm.* is personal communication. Coordinates for vent locations in Universal Transverse Mercator meters, Zone 11, North American Datum 1927. Vent locations determined by cited authors and field observations (B. Hill, unpub. res., 1993-1996).

Lathrop Wells: 543780E, 4060380N. Normal magnetic polarity (Champion, 1991).					
Unit/Sample #	Method	Date (Ma)	$\pm 1 \sigma$ error (Ma)	Notes	Reference
Unkn.	K/Ar	0.06	0.03		Smith et al., 1990
Unkn.	K/Ar	0.23	0.02		Vaniman et al., 1982
Q11a	Ar/Ar	0.14	0.05	Wgt'd mean, n = 8	Turrin et al., 1991
Q11a	Ar/Ar	0.125	0.005		Turrin, 1995
Q12a	Ar/Ar	0.18	0.02	Wgt'd mean, n = 16	Turrin et al., 1991
Q12a/31472	Ar/Ar	0.142	0.019		Turrin et al., 1992
Q13	Ar/Ar	0.22	0.05	Wgt'd mean, n = 4	Turrin et al., 1991
Qs2?/Qsu	Ar/Ar	0.15	0.05	Wgt'd mean, n = 8	Turrin et al., 1991
Q12a/TSV-1	K/Ar	0.29	0.2		Vaniman and Crowe, 1981
Qs3/TSV-129-78	K/Ar	0.30	0.10		Vaniman et al., 1982
Average: 0.18 \pm 0.08 Ma, MSWD = 4.92, Wgt'd mean = 0.13 \pm 0.01 Ma					
Not included in Lathrop Wells data set due to questionable apparent accuracy					
Unkn./71	K/Ar	2.0	0.6	Anomalously old	Marvin et al., 1973
Lava	K/Ar	0.30	0.02	Wgt'd mean, n = 25	Sinnock and Easterling, 1983

Little Black Peak: 522120E, 4110340N. Normal magnetic polarity (Champion, 1991).					
Unit/Sample #	Method	Date (Ma)	$\pm 1\sigma$ error (Ma)	Notes	Reference
NNTS 89-110	K/Ar	0.17	0.16		Fleck et al., 1996
NNTS 89-111	K/Ar	0.19	0.10		Fleck et al., 1996
Unkn. lava	K/Ar	0.21	0.13		Crowe & Perry, 1991
Unkn. lava	K/Ar	0.22	0.10		Crowe & Perry, 1991
Unkn. lava	K/Ar	0.24	0.22		Crowe et al., 1982
Unkn. lava	K/Ar	0.29	0.11		Crowe et al., 1982
Unkn. lava	K/Ar	0.32	0.15		Crowe et al., 1982
TSV-5-77	K/Ar	0.33	0.03		Fleck et al., 1996
TSV-6-77	K/Ar	0.39	0.07		Fleck et al., 1996
Average: 0.26 ± 0.07 Ma, MSWD = 0.69, Wgtd mean = 0.31 ± 0.02 Ma					

Hidden Cone: 523400E, 4112600N. Normal magnetic polarity (Champion, 1991).					
Unit/Sample #	Method	Date (Ma)	$\pm 1\sigma$ error (Ma)	Notes	Reference
Unkn. lava	K/Ar	0.32	0.20		Crowe & Perry, 1991
RDSBa14	K/Ar	0.34	0.07		Fleck et al., 1996
NNTS 89-109	K/Ar	0.37	0.07		Fleck et al., 1996
Unkn. lava	Ar/Ar	0.38	0.02		Turrin, 1995
TSV-64-78	K/Ar	0.40	0.09		Fleck et al., 1996
913-8B2	K/Ar	0.43	0.11		Fleck et al., 1996
Average: 0.37 ± 0.04 Ma, MSWD = 0.14, Wgtd mean = 0.38 ± 0.02 Ma					

Northern Cone: 540350E, 4079360N. Reversed magnetic polarity (Champion, 1991).					
Unit/Sample #	Method	Date (Ma)	$\pm 1\sigma$ error (Ma)	Notes	Reference
Unkn. lava	K/Ar	1.04	0.03	"unpublished USGS date"	Crowe et al., 1995
Unkn. lava	K/Ar	1.05	0.07	Feldspar separate	Smith et al., 1990
NNTS 7-86	K/Ar	1.06	0.05		Fleck et al., 1996
TSV-128-78	K/Ar	1.07	0.04		Vaniman et al., 1982
TSV-128-78	K/Ar	1.09	0.03		Fleck et al., 1996
Unkn. lava	K/Ar	1.09	0.07	Feldspar separate	Faulds et al., 1994
TSV-128	K/Ar	1.14	0.3		Vaniman and Crowe, 1981
Unkn. lava	K/Ar	1.66	0.5	"unpublished USGS date"	Crowe et al., 1995
Average: 1.15 ± 0.21 Ma, MSWD = 0.44, Wgtd mean = 1.07 ± 0.02 Ma Age must be <0.98 Ma or >1.05 Ma to correspond with C1r.1n subchron boundaries in Cande and Kent (1992).					

Black Cone: 538840E, 4074120N. Reversed magnetic polarity (Champion, 1991).					
Unit/Sample #	Method	Date (Ma)	$\pm 1\sigma$ error (Ma)	Notes	Reference
Northern flow	K/Ar	0.71	0.06	Feldspar separate	Smith et al., 1990
NNTS 9-86	K/Ar	0.79	0.09		Fleck et al., 1996
Lava S of cone	K/Ar	0.8	0.06	"unpublished USGS date"	Crowe et al., 1995
NNTS 8-86	K/Ar	0.82	0.07		Fleck et al., 1996
Summit lava lake	K/Ar	0.83	0.09	"unpublished USGS date"	Crowe et al., 1995
NNTS-106-89	K/Ar	0.91	0.07		Fleck et al., 1996
S lava/BC6FVP	Ar/Ar	0.94	0.05		Crowe et al., 1995
Duplicate of BC3FVP	Ar/Ar	0.96	0.15		Crowe et al., 1995
NNTS 105-89	K/Ar	1.03	0.06		Fleck et al., 1996
N lava/BC12FVP	Ar/Ar	1.05	0.08		Crowe et al., 1995
Summit lava lake/BC1FVP	Ar/Ar	1.05	0.14		Crowe et al., 1995
TSV-2A-77	K/Ar	1.06	0.05		Fleck et al., 1996
TSV-2-77	K/Ar	1.07	0.05		Fleck et al., 1996
TSV-2A	K/Ar	1.07	0.4		Vaniman and Crowe, 1981
Lava lake S	K/Ar	1.09	0.12	Feldspar separate	Smith et al., 1990
TSV-2	K/Ar	1.09	0.3		Vaniman and Crowe, 1981
Average: 0.95 ± 0.12 Ma, MSWD: 3.12, Wgtd mean = 0.94 ± 0.03 Ma Age must be <0.98 Ma or >1.05 Ma to correspond with C1r. In subchron boundaries in Cande and Kent (1992).					

Red Cone: 537580E, 4071880N. Reversed magnetic polarity (Champion, 1991).					
Unit/Sample #	Method	Date (Ma)	$\pm 1\sigma$ error (Ma)	Notes	Reference
NNTS 10-86	K/Ar	0.84	0.12		Fleck et al., 1996
Flow E of cone	K/Ar	0.84	0.15	"unpublished USGS date"	Crowe et al., 1995
Sandia 6	K/Ar	0.93	0.1		Fleck et al., 1996
Top of main cone	K/Ar	0.95	0.08	Feldspar separate	Smith et al., 1990
Sandia 7	K/Ar	0.97	0.04		Fleck et al., 1996
Sandia 5	K/Ar	0.97	0.06		Fleck et al., 1996
Scoria-mound dike	K/Ar	0.98	0.1	Feldspar separate	Smith et al., 1990
Main cone	K/Ar	1.01	0.06	Feldspar separate	Smith et al., 1990
Flow E of cone	K/Ar	1.07	0.34	"unpublished USGS date"	Crowe et al., 1995
NNTS 11-86	K/Ar	1.09	0.2		Fleck et al., 1996
Sandia 213	K/Ar	1.09	0.16		Fleck et al., 1996
Sandia 214	K/Ar	1.11	0.09		Fleck et al., 1996
TSV-378-81	K/Ar	1.5	0.1		Vaniman et al., 1982
Average: 1.03 ± 0.17 Ma, MSWD = 2.64, Wgtd mean = 1.01 ± 0.04 Ma Age must be <0.98 Ma or >1.05 Ma to correspond with Clr.1n subchron boundaries in Cande and Kent (1992).					
Not included in Red Cone data set due to questionable apparent accuracy					
Lab B	K/Ar	1.12	0.27	Average n = 6	Sinnock and Easterling, 1983
Lab C	K/Ar	1.55	0.15	Average n = 6	Sinnock and Easterling, 1983
Lab A	K/Ar	1.55	0.31	Average n = 6	Sinnock and Easterling, 1983

Little Cones: 535200E, 4069360N; bocca at 535480E, 4069560N. Reversed magnetic polarity (Champion, 1991).

Unit/Sample #	Method	Date (Ma)	$\pm 1\sigma$ error (Ma)	Notes	Reference
SE lava	K/Ar	0.76	0.2		Crowe et al., 1995
NE cone summit	K/Ar	0.77	0.04	Feldspar separate	Smith et al., 1990
Unkn.	Ar/Ar	0.904	0.011	sanidine xenocryst	Heizler et al., 1994
SE lava/CF15FVP	Ar/Ar	1.02	0.1		Crowe et al., 1995
Unkn./TSV-3-77	K/Ar	1.04	0.05		Fleck et al., 1996
SW lava/TSV-3	K/Ar	1.11	0.3		Vaniman and Crowe, 1981
<p>Average: 0.93 ± 0.15 Ma, MSW = 4.18 Ma, Wgt Mean = 0.90 ± 0.02 Ma Age must be <0.98 Ma or >1.05 Ma to correspond with C1r. In subchron boundaries in Cande and Kent (1992).</p>					

Buckboard Mesa: 555180E, 4109200N; second vent possible at about 555500E, 4108500N (Lutton, 1969). Normal magnetic polarity (Minor et al., 1993).

Unit/Sample #	Method	Date (Ma)	± 1σ error (Ma)	Notes	Reference
TSV-413-82	K/Ar	2.7	0.2		Marvin et al., 1989
WDH-12	K/Ar	2.77	0.08		Fleck et al., 1996
Unkn.	K/Ar	2.79	0.1		Crowe et al., 1982
Unkn.	K/Ar	2.82	0.04		Crowe et al., 1982
WDH-11	K/Ar	2.82	0.04		Fleck et al., 1996
NNTS-15	Ar/Ar	2.91	0.01		Turrin, 1995
Unkn.	K/Ar	2.93	0.03		Crowe et al., 1995
NNTS 16-86	K/Ar	2.95	0.06		Fleck et al., 1996
Unkn.	K/Ar	3.07	0.29		Crowe et al., 1995
NNTS 15-86	K/Ar	3.21	0.12		Fleck et al., 1996
<p>Average: 2.90 ± 0.15 Ma, MSWD = 2.50 Ma, Wgtd Mean = 2.90 ± 0.01 Ma Age must be 2.60–3.05 Ma to correspond with C2An.1n subchron boundaries in Cande and Kent (1992).</p>					

Crater Flat: 540330E, 4070050N; 540420E, 4068780N; 540360E, 4068440N; 540680E, 4068820N; 540700E, 4068260N; possible vent area at 540300E, 4071600N. All reversed magnetic polarity (Champion, 1991).

Unit/Sample #	Method	Date (Ma)	$\pm 1\sigma$ error (Ma)	Notes	Reference
Sandia 32	K/Ar	3.59	0.06		Fleck et al., 1996
Sandia 17	K/Ar	3.64	0.03		Fleck et al., 1996
VH-1-126	K/Ar	3.64	0.10		Fleck et al., 1996
CF79-26-1	K/Ar	3.64	0.13		Vaniman and Crowe, 1981
S vent/CF10FVP	Ar/Ar	3.65	0.06		Crowe et al., 1995
Central vent/CF12FVP	Ar/Ar	3.69	0.05		Crowe et al., 1995
Sandia 212	K/Ar	3.69	0.06		Fleck et al., 1996
Sandia 217	K/Ar	3.70	0.11		Fleck et al., 1996
Sandia 211	K/Ar	3.71	0.11		Fleck et al., 1996
Sandia 20	K/Ar	3.73	0.02		Fleck et al., 1996
Sandia 215	K/Ar	3.73	0.04		Fleck et al., 1996
Sandia 31	K/Ar	3.73	0.17		Fleck et al., 1996
N lava/CF14FVP	Ar/Ar	3.75	0.04		Crowe et al., 1995
Unkn.	K/Ar	3.75	0.12		Crowe et al., 1995
NNTS-14-86	K/Ar	3.75	0.07		Fleck et al., 1996
Sandia 19	K/Ar	3.77	0.05		Fleck et al., 1996
Sandia 29	K/Ar	3.78	0.06		Fleck et al., 1996
Sandia 30	K/Ar	3.79	0.03		Fleck et al., 1996
Sandia 18	K/Ar	3.81	0.08		Fleck et al., 1996
CF79-72-24-8	K/Ar	3.84	0.15		Marvin et al., 1989
CF79-24-8	K/Ar	3.85	0.13		Fleck et al., 1996
NNTS-14	Ar/Ar	3.86	0.02		Turrin, 1995
Unkn.	K/Ar	3.91	0.2		Crowe et al., 1995
NNTS-13-86	K/Ar	4.01	0.13		Fleck et al., 1996

Average: 3.75 ± 0.10 Ma, MSWD = 2.94, Wgtd mean = 3.76 ± 0.02 Ma

Age must be 3.55–4.03 Ma to correspond with C2An.3n–C3n. In subchron boundaries in Cande and Kent (1992).

Crater Flat: 540330E, 4070050N; 540420E, 4068780N; 540360E, 4068440N; 540680E, 4068820N; 540700E, 4068260N; possible vent area at 540300E, 4071600N. All reversed magnetic polarity (Champion, 1991).

Unit/Sample #	Method	Date (Ma)	$\pm 1\sigma$ error (Ma)	Notes	Reference
Not included in Crater Flat data set due to questionable apparent accuracy					
Lava 4, Lab B	K/Ar	3.69	0.09	Average n = 6	Sinnock and Easterling, 1983
Lava 3, Lab B	K/Ar	3.73	0.06	Average n = 6	Sinnock and Easterling, 1983
Lava 3, Lab C	K/Ar	3.89	0.17	Average n = 6	Sinnock and Easterling, 1983
Lava 4, Lab C	K/Ar	4.00	0.13	Average n = 6	Sinnock and Easterling, 1983
Lava 4, Lab A	K/Ar	4.22	0.08	Average n = 6	Sinnock and Easterling, 1983
Lava 3, Lab A	K/Ar	4.27	0.46	Average n = 6	Sinnock and Easterling, 1983

**Amargosa Desert Aeromagnetic Anomaly "B": Estimated vent location 553700E, 4052900N.
Reversed magnetic polarity (Langenheim et al., 1993).**

Unit/Sample #	Method	Date (Ma)	$\pm 1\sigma$ error (Ma)	Notes	Reference
Well FF-25-1	Ar/Ar	3.85	0.05		Crowe et al., 1995
Well FF-25-1	Ar/Ar	4.11	0.07		B. Turrin, unpub. res., 1995
Well FF-25-1	Ar/Ar	4.19	0.05		B. Turrin, unpub. res., 1995
Well FF-25-1	Ar/Ar	4.19	0.06		B. Turrin, unpub. res., 1995
Well FF-25-1	Ar/Ar	4.19	0.07		B. Turrin, unpub. res., 1995
Well FF-25-1	Ar/Ar	4.15	0.07		B. Turrin, unpub. res., 1995
Well FF-25-1	Ar/Ar	4.16	0.06		B. Turrin, unpub. res., 1995
Well FF-25-1	Ar/Ar	4.16	0.05		B. Turrin, unpub. res., 1995
<p>Average: 4.13 ± 0.11 Ma, MSWD = 4.95, Wgtd Mean = 4.11 ± 0.05 Ma. Age must be 3.55–4.03 Ma or 4.12–4.27 Ma to correspond with C2An.3n–C3n.1n subchron boundaries in Cande and Kent (1992).</p>					

Amargosa Desert Aeromagnetic Anomalies "A": Estimated vent locations for A1: 546100E, 4055100N; A2: 546100E, 4053100N; A3: 544500E, 4051400N (Connor et al., 1997). All reversed magnetic polarity. Age of 4.1 ± 0.1 Ma estimated by analogy with Anomaly B.

Amargosa Desert Aeromagnetic Anomaly "C": Estimated vent location 547000E, 4042900N. Reversed magnetic polarity (Langenheim et al., 1993). Age of 4.1 ± 0.1 Ma estimated by analogy with Anomaly B.

Amargosa Desert Aeromagnetic Anomaly "D": Estimated vent location 549400E, 4040000N. Normal magnetic polarity (Langenheim et al., 1993). Age of 4.1 ± 0.1 Ma estimated by analogy with Anomaly B and correspondence with 4.03–4.13 Ma C3n.1n normal subchron in Cande and Kent (1992).

Amargosa Desert Aeromagnetic Anomaly "E": Estimated vent location 538300E, 4047200N. Normal magnetic polarity (Langenheim et al., 1993). Age of 4.1 ± 0.1 Ma estimated by analogy with Anomaly B and correspondence with 4.03–4.13 Ma C3n.1n normal subchron in Cande and Kent (1992).

Magnetic Anomaly, SW Crater Flat: Estimated vent location 535000E, 4067800N, normal magnetic polarity (Kane and Bracken, 1983; Connor et al., 1997). Age of 6 ± 1 Ma estimated by applying 0–1 Ma sedimentation rate of 0.03 mm yr^{-1} at Little Cones (Stamatikos et al., 1997) to modeled 150–200 m depth of burial to causative body (Connor et al., 1997).

Thirsty Mountain: Main vent location 529520E, 4112150N. Small boccas at 529480E, 4112040N and 529540E, 4111680N. Reversed magnetic polarity (Fleck et al., 1996).

Unit/Sample #	Method	Date (Ma)	$\pm 1\sigma$ error (Ma)	Notes	Reference
913-6A	K/Ar	4.60	0.04		Fleck et al., 1996
913-6B	K/Ar	4.66	0.03		Fleck et al., 1996
913-6C	K/Ar	4.61	0.10		Fleck et al., 1996
NE-10-1-91-1	Ar/Ar	4.68	0.03		Crowe et al., 1995
NE-10-1-91-2	Ar/Ar	4.88	0.04		Crowe et al., 1995

Average: 4.69 ± 0.11 Ma, MSWD = 7.34, Wgtd Mean = 4.69 ± 0.05 Ma.

Age must be 4.61–4.69 Ma to correspond with C3n.3n normal subchron boundaries in Cande and Kent (1992).

Nye Canyon: Main vent locations are North unit: 604680E, 4094260N; Middle unit: 602170E, 4088960N; South unit 600950E, 4085920N and 600550E, 4085450N; Ring dike main vent: 599160E, 4085820N; Scarp Canyon vent: 597930E, 4082470N (Hinrichs and McKay, 1965; Tschanz and Pampeyan 1970; Crowe et al., 1986). Normal magnetic polarity (D. Champion, unpub. res., 1994).

Unit/Sample #	Method	Date (Ma)	$\pm 1\sigma$ error (Ma)	Notes	Reference
North/TSV-293-80	K/Ar	6.3	0.2		Crowe et al., 1983a
Middle/TSV-63D	K/Ar	6.8	0.2		Crowe et al., 1983a
South/TSV-96	K/Ar	7.2	0.2		Crowe et al., 1983a
South/L-7420	Ar/Ar	7.27	0.03		B. Turrin, unpub. res., 1995
Ring dike/L-7405	Ar/Ar	7.34	0.03		B. Turrin, unpub. res., 1995
Middle/L-7400	Ar/Ar	7.36	0.05		B. Turrin, unpub. res., 1995
<p>Average: 7.05 ± 0.07 Ma, MSWD = 7.14, Wgtd Mean = 7.30 ± 0.05 Ma. Age must be 7.25–7.38 Ma to correspond with C4n.1n subchron boundaries in Cande and Kent (1992).</p>					

Frenchman Flat: Basaltic lava in drill holes Ue5I (286–293 m), 595260E, 4080980N; and Ue5K (289–299 m), 593520E, 4081480N (Carr et al., 1975). Drill hole locations used as vent proxies. Carr et al. (1975) show 2 discrete lavas based on interpretations of magnetic and gravity data. Magnetic polarity unknown.

Unit/Sample #	Method	Date (Ma)	± 1σ error (Ma)	Notes	Reference
UE5-I/940'	Ar/Ar	8.57	0.21		Turrin, 1995
UE5-I/950'	Ar/Ar	8.4	0.16		Turrin, 1995
UE5-I/960'	Ar/Ar	8.67	0.08		Turrin, 1995
UE5-K/960'	Ar/Ar	8.37	0.21		Turrin, 1995
UE5-K/970'	Ar/Ar	8.43	0.19		Turrin, 1995
UE5-K/980'	Ar/Ar	8.59	0.29		Turrin, 1995

Average: 8.51 ± 0.12 Ma, MSWD = 0.83, Wgt'd Mean = 8.57 ± 0.06 Ma.

Yucca Flat: Basaltic lava in drill holes UE1h (226–308 m), 582980E, 4095280N; UE1j (415–429 m), 582440E, 4096580N; and UE6d (about 1000 m depth; Carr, 1984), 583740E, 4093400N (Fernald et al., 1975). Drill hole locations used as vent proxies. Magnetic polarity unknown.

Unit/Sample #	Method	Date (Ma)	± 1σ error (Ma)	Notes	Reference
UE1h/784'	K/Ar	8.1	0.3		Carr, 1984

Rocket Wash: Main vent location estimated at 536100E, 4109100N (Lipman et al., 1966; O'Conner et al., 1966; Crowe et al., 1995). Unknown magnetic polarity.

Unit/Sample #	Method	Date (Ma)	± 1σ error (Ma)	Notes	Reference
Lava	K/Ar	8	0.2		Crowe et al., 1983a

Paiute Ridge: Main vent locations estimated at 592400E, 4106800N; 592800E, 4105900N (Beyers and Barnes, 1967; Crowe et al., 1983b); 593400E, 4105500N. Cogenetic vents in northern Scarp Canyon at 594800E, 4107900N and 595800E, 4106300N. Other small, dike-fed vents are possible in the complex. Transient normal-to-reversed magnetic polarity (Ratcliff et al., 1994).

Unit/Sample #	Method	Date (Ma)	$\pm 1\sigma$ error (Ma)	Notes	Reference
Scarp Canyon dike	K/Ar	8.7	0.3		Crowe et al., 1983b
TSV-309-80	K/Ar	8.5	0.3		Crowe et al., 1983b
Sanidine xenocrysts	Ar/Ar	8.65	0.1		Ratcliff et al., 1994
Sanidine xenocrysts	Ar/Ar	8.66	0.18		Ratcliff et al., 1994
Sanidine phenocryst	Ar/Ar	8.59	0.07		Ratcliff et al., 1994
Average: 8.62 ± 0.08 Ma, MSWD = 0.13, Wgted Mean = 8.61 ± 0.05 Ma.					

Pahute Mesa: Main vent locations estimated at 548900E, 4133300N; 554100E, 4134500N; and 562400E, 4132700N (Ekren et al., 1966; Noble et al., 1967; Crowe et al., 1995). Unknown magnetic polarity.

Unit/Sample #	Method	Date (Ma)	$\pm 1\sigma$ error (Ma)	Notes	Reference
NE Basalt Ridge / TSV-55	K/Ar	8.8	0.1		Crowe et al., 1983a
Basalt Ridge / TSV-17	K/Ar	10.4	0.4		Crowe et al., 1983a
Basalt Ridge dike/TSV-16	K/Ar	9.1	0.7		Crowe et al., 1983a
Average: 9.4 ± 0.9 Ma, MSWD = 7.57, Wgted Mean = 8.9 ± 0.1 Ma.					
TSV-17 overlays 9.40 ± 0.03 Ma Rocket Wash Tuff of the Thirsty Canyon Group (Ekren et al., 1966; Sawyer et al., 1994). Correlative lavas 20 km W of Basalt Ridge overlay 9.15 ± 0.02 Ma Gold Flat Tuff of the Thirsty Canyon Group (Rogers et al., 1968; Sawyer et al., 1994).					

Basalt of Sleeping Butte: Vent locations at 525700E, 4112100N; 524300E, 4113600N; others likely. Unknown magnetic polarity.

Unit/Sample #	Method	Date (Ma)	$\pm 1\sigma$ error (Ma)	Notes	Reference
913-8C	Ar/Ar	9.70	0.13		Fleck et al., 1996
913-6I	Ar/Ar	9.70	0.21		Fleck et al., 1996
913-8D	Ar/Ar	9.29	0.06		R. Fleck, unpub. res., 1995
RDSBc23	Ar/Ar	9.81	0.07		R. Fleck, unpub. res., 1995
RDSBb1	Ar/Ar	9.84	0.07		Fleck et al., 1996
NNTS 89-107	Ar/Ar	9.85	0.19		Fleck et al., 1996

**Average: 9.7 ± 0.2 Ma, MSWD = 9.89, Wgtd Mean = 9.6 ± 0.1 Ma.
Overlain by 9.40 ± 0.04 Ma Rocket Wash Tuff (Fleck et al., 1996; Sawyer et al., 1994).**

Solitario Canyon: Vent location estimated at 546800E, 4082400N, after Scott and Bonk (1984). Unknown magnetic polarity.

Unit/Sample #	Method	Date (Ma)	$\pm 1\sigma$ error (Ma)	Notes	Reference
TSV-168-79	K/Ar	10.0	0.4		Crowe et al., 1983a
dike	K/Ar	11.7	0.3	Groundmass feldspar separate	Smith et al., 1997

Large disparity in ages precludes averaging. Dike intrudes 12.70 ± 0.03 Ma Tiva Canyon Tuff (Sawyer et al., 1994). Compositionally distinct from other Miocene Crater Flat basalt (i.e., Crowe et al., 1986).

Miocene Basalt of SW Crater Flat: Vent locations estimated at 536400E, 4064000N; and 534700E, 4066500N after Swadley and Carr (1987) and Connor et al. (1997). Reversed magnetic polarity.

Unit/Sample #	Method	Date (Ma)	$\pm 1\sigma$ error (Ma)	Notes	Reference
Main vent area	K/Ar	10.5	0.1		Crowe et al., 1983a
W Lava/DFCF-1	Ar/Ar	11.19	0.13		This report
W Lava/DFCF-2	Ar/Ar	11.29	0.12		This report

Average: 11.0 ± 0.4 Ma, MSWD = 15.73, Wgtd mean = 10.9 ± 0.3 Ma.
Overlies 11.45 ± 0.03 Ma Ammonia Tanks Tuff of the Timber Mountain Group (Sawyer et al., 1994). Compositionally similar to basalt in VH-2 drill core (i.e., Crowe et al., 1986).

Basalt of VH-2: Vent location(s) unknown, estimated at VH-2 location 537900E, 4072950N. May extend S and W of VH-2 (Crowe et al., 1995). Reversed magnetic polarity (Carr and Parrish, 1985).

Unit/Sample #	Method	Date (Ma)	$\pm 1\sigma$ error (Ma)	Notes	Reference
VH-2-1200	K/Ar	11.3	0.4		Carr and Parrish, 1985

Overlies 11.45 ± 0.03 Ma Ammonia Tanks Tuff of the Timber Mountain Group (Sawyer et al., 1994). Compositionally similar to Miocene basalt in SW Crater Flat (i.e., Crowe et al., 1986). Possibly correlative dike in VH-1 drill core intruding Topopah Spring Tuff at 353 m (Carr, 1982).

Basalt of Skull Mountain: Unknown vent locations and magnetic polarity.					
Unit/Sample #	Method	Date (Ma)	± 1σ error (Ma)	Notes	Reference
Unkn.	K/Ar	10.2	0.5		Crowe et al., 1983a
Overlies 11.45 ± 0.03 Ma Ammonia Tanks Tuff of the Timber Mountain Group (Sargent and Stewart, 1971). May correlate with basalt in eastern Amargosa Desert (i.e., Swadley, 1983).					

Basalt of Kiwi Mesa: Vent locations at 568940E, 4078740N and 568820E, 4079000N; others possible. Unknown magnetic polarity.					
Unit/Sample #	Method	Date (Ma)	± 1σ error (Ma)	Notes	Reference
TSV-382-81	K/Ar	11.2	0.5	Kiwi Mesa basalt at Little Skull Mountain	Marvin et al., 1989
TSV-382-81	K/Ar	11.4	0.5	Kiwi Mesa basalt at Little Skull Mountain	Marvin et al., 1989
Unkn.	K/Ar	9.7	0.3		Crowe et al., 1983a
TSV-370-81	K/Ar	9.9	0.4		Marvin et al., 1989
TSV-370-81	K/Ar	10.0	0.4		Marvin et al., 1989
Average: 10.4 ± 0.9 Ma, MSWD = 3.34, Wgtd Mean = 10.2 ± 0.3 Ma. Overlies 11.45 ± 0.03 Ma Ammonia Tanks Tuff of the Timber Mountain Group (Ekren and Sargent, 1965).					

Basalt of Little Skull Mountain: Unknown vent locations and magnetic polarity. Multiple flow units, compositionally diverse (Crowe et al., 1986).

Unit/Sample #	Method	Date (Ma)	$\pm 1\sigma$ error (Ma)	Notes	Reference
Upper lava	K/Ar	8.4	0.4		Crowe et al., 1995
Overlies 11.45 ± 0.03 Ma Ammonia Tanks Tuff of the Timber Mountain Group (Sargent and Stewart, 1971). Date thought too young (Crowe et al., 1995) based on correlation with basalt of Jackass Flat.					

Basalt of Jackass Flat: Unknown vent locations and magnetic polarity.

Unit/Sample #	Method	Date (Ma)	$\pm 1\sigma$ error (Ma)	Notes	Reference
TSV-372-81	K/Ar	11.0	0.5	"Poor date"	Marvin et al., 1989
TSV-372-81	K/Ar	9.6	0.4	"Preferred date"	Marvin et al., 1989
Overlies 12.80 ± 0.03 Ma Topopah Spring Tuff of the Timber Mountain Group (McKay and Williams, 1964). Marvin et al. (1989) identify 11.0 Ma date as "poor" and the 9.6 Ma date as the "preferred date" based on analytical uncertainties.					

Basalt of Northeastern Amargosa Desert: Near-vent location at 563300E, 4046500N (i.e., Swadley, 1983); other locations likely. Compositionally distinct from Basalt of Southeastern Amargosa Desert; contains quartz phenocrysts (?) and may correlate with Basalt of Little Skull Mountain. Likely correlates with shallow, highly reflective unit in western part of AV-1 seismic reflection line (Brocher et al., 1993). Unusual shallow inclination to paleomagnetic direction may correlate with Basalt of Southeastern Amargosa (D. Champion, pers. comm., 1995).

Basalt of Southeastern Amargosa Desert: Exposed only in drill cores and cuttings at drill holes MSH-C (565300E, 4039700N; 149-157 m) and water wells around 569200E, 4043600N (Johnston, 1968). Likely correlates with shallow, highly reflective unit in eastern part of AV-1 seismic reflection line (Brocher et al., 1993).

Unit/Sample #	Method	Date (Ma)	± 1σ error (Ma)	Notes	Reference
MSH-C-501	K/Ar	9.6	0.1		R. Fleck, unpub. res. 1996

Shallow inclination to MSH-C paleomagnetic direction (30°) similar to direction of Northeastern Amargosa Desert basalt outcrops (D. Champion, pers. comm. 1995). Fine-grained holocrystalline olivine-pyroxene basalt compositionally distinct from Northeastern Amargosa Desert basalt (Hill and Luhr, unpub. res. 1997).

Basalt of the Specter Range: Small outcrops of subvolcanic basalt in the Specter Range at 571500E, 4057600N and 571900E, 4055350N (Sargent and Stewart, 1971). Compositionally primitive and distinct from other basalts within 20 km (Hill and Luhr, unpub. res.). Intrudes carbonate rocks of the Cambrian Bonanza King Formation (Sargent and Stewart, 1971).

Basalt of Dome Mountain: Unknown vent locations, normal magnetic polarity (Minor et al., 1993).					
Unit/Sample #	Method	Date (Ma)	± 1σ error (Ma)	Notes	Reference
Unkn.	K/Ar	10.8	0.5		Kistler, 1968
Upper/RR30a16R	Ar/Ar	10.4	0.4		R. Fleck, unpub res., 1995
Main/RR30a4	Ar/Ar	10.7	0.2		R. Fleck, unpub res., 1995
Lower/RR30a14	Ar/Ar	10.7	0.07		R. Fleck, unpub res., 1995
Basal/RR30a15	Ar/Ar	10.5	0.05		R. Fleck, unpub res., 1995
<p>Average: 10.6 ± 0.2 Ma, MSWD = 1.98, Wgtd mean = 10.58 ± 0.06 Ma. Overlies 11.2–11.4 Ma Beatty Wash Formation and is overlain by 10.3 Ma Rhyolite of Shoshone Mountain (Christiansen and Lipman, 1965; Minor et al., 1993). Date concordant with 9.78–10.83 normal polarity chron C5n.2n (Candie and Kent, 1992).</p>					

Basalt of the Amargosa Range: Diffuse outcrops of highly eroded basaltic rock between 505000E, 4077000N and 521000E, 4062000N, on the eastern flank of the Amargosa Range, Nevada.					
Unit/Sample #	Method	Date	± 1σ error	Notes	Reference (Ma) (Ma)
Basalt BF-383	K/Ar	9.0	0.3		Marvin et al., 1989
Basalt BF-380	K/Ar	10.3	0.4		Marvin et al., 1989
Basalt BF-379	K/Ar	7.5	0.3		Marvin et al., 1989
<p>Basalts BF-383 and -380 overlay 11.45 ± 0.03 Ma Ammonia Tanks Tuff of the Timber Mountain Group (Marvin et al., 1989; Sawyer et al., 1994).</p>					

Beatty Basalt: Vents preserved at 525300E, 4085600N; 527400E, 4085200N; and 514800E, 4090800N (Maldonado and Hausback, 1990); other vents likely. Unknown magnetic polarity. Diffuse outcrops of highly eroded basaltic rock between 502000E, 4081000N and 529000E, 4092000N.

Unit/Sample #	Method	Date	$\pm 1\sigma$ error	Notes	Reference (Ma) (Ma)
Lava Tb2	K/Ar	10.3	0.4		Maldonado and Hausback (1990)
Basalt BF-380A	K/Ar	8.1	0.4		Marvin et al., 1989
Tb1/102887-3	K/Ar	10.7	0.2		Monsen et al., 1992

Lava TB2 overlain by 10.0 ± 0.4 Ma locally erupted latite lavas (unit TI), Maldonado and Hausback (1990). Basalt BF-380A overlies 9.36 ± 0.02 Ma Pahute Mesa Tuff of the Thirsty Canyon Group (Marvin et al., 1989; Sawyer et al., 1994).

Basalt of the Grapevine Mountains: Eroded vents at 476400E, 4101800N, 476800E, 4102700N, and 477900E, 4106600N; more vents likely to west. Poor age constraints, likely late Pliocene or Pleistocene (Albers and Stewart, 1972). Similar isotopic character as YMR basalts (Yogodzinski and Smith, 1995; Hill and Connor, 1996).

Basalt of the Funeral Formation: Over 25 vents exposed between about 515000E, 4010000N and 542000E, 4030000N (McAllister, 1970, 1971, 1973; Conway et al., 1997). Normal and reversed magnetic polarities. Similar isotopic character as YMR basalts (Yogodzinski and Smith, 1995; Hill and Connor, 1996).

Unit/Sample #	Method	Date	$\pm 1\sigma$ error	Notes	Reference (Ma) (Ma)
TSV-383-81	K/Ar	4.0	0.1		Marvin et al., 1989
N Ryan area	K/Ar	4.03	0.12		McAllister, 1973
E Black Mtns.	K/Ar	4.90	Unkn.		Asmerom et al., 1994
Funeral Fm., upper?	K/Ar	3.20	Unkn.		Asmerom et al., 1994

Basalt of Southern Death Valley: Cinder Hill vent at 523900E, 3977100N. Multiple vents possible for Shoreline Butte, summit 526200E, 3973700N. Unknown magnetic polarities. Similar isotopic character as YMR basalts (Yogodzinski and Smith, 1995; Hill and Connor, 1996).

Unit/Sample #	Method	Date	$\pm 1\sigma$ error	Notes	Reference (Ma) (Ma)
Shoreline Butte	K/Ar	1.5	Unkn.		Wright and Troxel, 1984
Cinder Hill	K/Ar	0.69	Unkn.		Wright and Troxel, 1984

APPENDIX REFERENCES

Albers, J.P., and J.H. Stewart. 1972. *Geology and Mineral Deposits of Esmeralda County, Nevada*. Nevada Bureau of Mines and Geology Bulletin 78. Reno, NV: University of Nevada.

Asmerom, Y., S.B. Jacobsen, and B.P. Wernicke. 1994. *Variations in magma source regions during large-scale continental extension, Death Valley region, western United States*. Earth and Planetary Science Letters 125: 235–254.

Beyers, F.M., and H. Barnes. 1967. *Geologic Map of the Paiute Ridge Quadrangle, Nye County, Nevada*. U.S. Geological Survey Geological Quadrangle Map GQ-577. Reston, VA: U.S. Geological Survey.

Brocher, T.M., M.D. Carr, K.F. Fox, and P.E. Hart. 1993. *Seismic reflection profiling across Tertiary extensional structures in the eastern Amargosa Desert, southern Nevada, Basin and Range province*. Geological Society of America Bulletin 105: 30–46.

Cande, S.C., and D.V. Kent. 1992. *A new geomagnetic polarity time scale for the late Cretaceous and Cenozoic*. Journal of Geophysical Research 97(B10): 13,917–13,951.

Carr, W.J. 1982. *Volcano-Tectonic History of Crater Flat, Southwestern Nevada, as Suggested by New Evidence from Drill Hole USU-VH-1 and Vicinity*. U.S. Geological Survey Open-File Report 82-457. Reston, VA: U.S. Geological Survey.

Carr, W.J. 1984. *Regional and Structural Setting of Yucca Mountain, Southwestern Nevada, and Late Cenozoic Rates of Tectonic Activity in Part of the Southwestern Great Basin, Nevada and California*. U.S. Geological Survey Open-File Report 84-854. Reston, VA: U.S. Geological Survey.

Carr, W.J., and L.D. Parrish. 1985. *Geology of Drill Hole USW VH-2, and Structure of Crater Flat, Southwestern Nevada*. U.S. Geological Survey Open-File Report 85-475. Reston, VA: U.S. Geological Survey.

Carr, W.J., G.D. Bath, D.L. Healey, and R.M. Hazelwood. 1975. *Geology of Northern Frenchman Flat, Nevada Test Site*. U.S. Geological Survey Open-File Report 474-216. Reston, VA: U.S. Geological Survey.

Champion, D.E. 1991. *Volcanic episodes near Yucca Mountain as determined by paleomagnetic studies at Lathrop Wells, Crater Flat, and Sleeping Butte, Nevada*. Proceedings of the Second Annual International Conference on High-Level Radioactive Waste Management. La Grange Park, IL: American Nuclear Society: 61–67.

Christiansen, R.L., and P. Lipman. 1965. *Geologic Map of the Topopah Spring NW Quadrangle, Nye County, Nevada*. U.S. Geological Survey Geological Quadrangle Map GQ-444. Reston, VA: U.S. Geological Survey.

Connor, C.B., S. Lane-Magsino, J.A. Stamatakos, R.H. Martin, P.C. La Femina, B.E. Hill, and S. Lieber. 1997. *Magnetic surveys help reassess volcanic hazards at Yucca Mountain, Nevada*. EOS, Transactions of the American Geophysical Union 78(7): 73-78.

Conway, F.M., C. Connor, B. Hill, and D. Ferrill. 1997. *Landsat TM, SPOT and SLAR interpretation of volcanic and structural features of the Greenwater and Saline Ranges, Inyo County, California, USA*. Volcanic Activity and the Environment, IAVCEI Abstracts. Unidad Editorial: Guadalajara, Mexico. 68.

Crowe, B., and F. Perry. 1991. *Preliminary geologic map of the Sleeping Butte Volcanic Centers*. Los Alamos National Laboratory Report LA-12101-MS. Los Alamos, NM: Los Alamos National Laboratory.

Crowe, B.M., M.E. Johnson, and R.J. Beckman. 1982. *Calculation of the probability of volcanic disruption of a high-level nuclear waste repository within southern Nevada, USA*. Radioactive Waste Management and the Nuclear Fuel Cycle 3: 167-190.

Crowe, B.M., D.T. Vaniman, and W.J. Carr. 1983a. *Status of Volcanic Hazard Studies for the Nevada Nuclear Waste Storage Investigations*. Los Alamos National Laboratory Report LA-9325-MS. Los Alamos, NM: Los Alamos National Laboratory.

Crowe, B., S. Self, D. Vaniman, R. Amos, and F. Perry. 1983b. *Aspects of potential magmatic disruption of a high-level radioactive waste repository in southern Nevada*. Journal of Geology 91: 259-276.

Crowe, B.M., K.H. Wohletz, D.T. Vaniman, E. Gladney, and N. Bower. 1986. *Status of Volcanic Hazard Studies for the Nevada Nuclear Waste Storage Investigations*. Los Alamos National Laboratory Report LA-9325-MS, Vol. II. Los Alamos, NM: Los Alamos National Laboratory.

Crowe, B.M., F.V. Perry, J. Geissman, L. McFadden, S. Wells, M. Murrell, J. Poths, G.A. Valentine, L. Bowker, and K. Finnegan. 1995. *Status of Volcanic Hazard Studies for the Yucca Mountain Site Characterization Project*. Los Alamos National Laboratory Report LA-12908-MS. Los Alamos, NM: Los Alamos National Laboratory.

Ekren, E.B., and K.A. Sargent. 1965. *Geologic Map of the Skull Mountain Quadrangle, Nye County, Nevada*. U.S. Geological Survey Geological Quadrangle Map GQ-387. Reston, VA: U.S. Geological Survey.

Ekren, E.B., R.E. Anderson, P.P. Orkild, and E.N. Hinrichs. 1966. *Geologic Map of the Silent Butte Quadrangle, Nye County, Nevada*. U.S. Geological Survey Geological Quadrangle Map GQ-493. Reston, VA: U.S. Geological Survey.

Faulds, J.E., J.W. Bell, D.L. Feuerbach, and A.R. Ramelli. 1994. *Geologic Map of the Crater Flat Area, Nevada*. Nevada Bureau of Mines and Geology Map 101. Reno, NV: Nevada Bureau of Mines and Geology.

Fernald, A.T., F.M. Beyers, Jr., and J.P. Ohi. 1975. *Lithologic Logs and Stratigraphic Units of Drill Holes and Mined Shafts in Areas 1 and 6, Nevada Test Site*. U.S. Geological Survey Report 474-206. Reston, VA: U.S. Geological Survey.

Fleck, R.J., B.D. Turrin, D.A. Sawyer, R.G. Warren, D.E. Champion, M.R. Hudson, and S.A. Minor. 1996. *Age and character of basaltic rocks of the Yucca Mountain region, southern Nevada*. Journal of Geophysical Research 100(B4): 8,205–8,227.

Heizler, M.T., W.C. McIntosh, F.V. Perry, and B.M. Crowe. 1994. *$^{40}\text{Ar}/^{39}\text{Ar}$ Results of Incompletely Degassed Sanidine: Age of Lathrop Wells Volcanism*. U.S. Geological Survey Circular 1107. Reston, VA: U.S. Geological Survey: 113.

Hill, B.E., and C.B. Connor. 1996. *Volcanic Systems of the Basin and Range. NRC High-Level Radioactive Waste Research at CNWRA, July–December 1995*. CNWRA 95-02S. San Antonio, TX: Center for Nuclear Waste Regulatory Analyses: 5-1 to 5-21.

Hinrichs, E.N., and E.J. McKay. 1965. *Geologic Map of the Plutonium Valley Quadrangle, Nye and Lincoln Counties, Nevada*. U.S. Geological Survey Geological Quadrangle Map GQ-384. Reston, VA: U.S. Geological Survey.

Johnston, R.H. 1968. *U.S. Geological Survey Tracer Study, Amargosa Desert, Nye County, Nevada, Part 1: Exploratory Drilling, Tracer Well Construction and Testing, and Preliminary Findings*. U.S. Geological Survey Open-File Report 68-152. Reston, VA: U.S. Geological Survey.

Kane, M.F., and R.E. Bracken. 1983. *Aeromagnetic Map of Yucca Mountain and Surrounding Regions, Southwest Nevada*. U.S. Geological Survey Open-File Report 83-616. Reston, VA: U.S. Geological Survey.

Kistler, R.W. 1968. *Potassium-argon ages of volcanic rocks in Nye and Esmeralda Counties, Nevada*. Geological Society of America Memoir 110. Boulder, CO: Geological Society of America: 251–262.

Langenheim, V.E., K.S. Kirchoff-Stein, and H.W. Oliver. 1993. *Geophysical investigations of buried volcanic centers near Yucca Mountain, southwestern Nevada*. Proceedings of Fourth Annual International Conference on High-Level Radioactive Waste Management. La Grange Park, IL: American Nuclear Society: 1,840–1,846.

Lipman, P.W., W.D. Quinlivan, W.J. Carr, and R.E. Anderson. 1966. *Geologic Map of the Thirsty Canyon SE Quadrangle, Nye County, Nevada*. U.S. Geological Survey Geological Quadrangle Map GQ-489. Reston, VA: U.S. Geological Survey.

Lutton, R.J. 1969. *Internal structure of the Buckboard Mesa basalt*. Bulletin of Volcanology 33: 579–593.

Maldonado, F., and B.P. Hausback. 1990. *Geologic Map of the Northeast Quarter of the Bullfrog 15-Minute Quadrangle, Nye County, Nevada*. U.S. Geological Survey Miscellaneous Investigations Map I-2049. Reston, VA: U.S. Geological Survey.

Marvin, R.F., H.H. Mehnert, and E.H. McKee. 1973. A summary of radiometric ages of Tertiary volcanic rocks in Nevada and eastern California. Part III: southeastern Nevada. Isochron/West 6: 1-30.

Marvin, R.F., H.H. Mehnert, and C.W. Naeser. 1989. *U.S. Geological Survey radiometric ages: Compilation C, part three: California and Nevada*. Isochron/West 52: 3-11.

McAllister, J.F. 1970. *Geology of the Funeral Creek Borate Area, Death Valley, Inyo County, California*. California Division of Mines and Geology Map Sheet 14. Sacramento, CA: California Division of Mines and Geology.

McAllister, J.F. 1971. *Preliminary Geologic Map of the Funeral Mountains in the Ryan Quadrangle, Death Valley Region, Inyo County, California*. U.S. Geological Survey Map 71-187. Reston, VA: U.S. Geological Survey.

McAllister, J.F. 1973. *Geologic Map and Sections of the Amargosa Valley Borate Area - Southeast Continuation of the Furnace Creek Area - Inyo County, California*. U.S. Geological Survey Miscellaneous Geological Investigations Map I-782. Reston, VA: U.S. Geological Survey.

McKay, E.J., and W.P. Williams. 1964. *Geologic Map of the Jackass Flats Quadrangle, Nye County, Nevada*. U.S. Geological Survey Geological Quadrangle Map GQ-368. Reston, VA: U.S. Geological Survey.

Minor, S.A., D.A. Sawyer, R.R. Wahl, V.A. Frizzell, Jr., S.P. Schilling, R.G. Warren, P.P. Orkild, J.A. Coe, M.R. Hudson, R.J. Fleck, M.A. Lanphere, W.C. Swadley, and J.C. Cole. 1993. *Preliminary Geologic Map of the Pahute Mesa 30'x60' Quadrangle, Nevada*. U.S. Geological Survey Open-File Report 93-299. Reston, VA: U.S. Geological Survey.

Monsen, S.A., M.D. Carr, M.C. Reheis, and P.P. Orkild. 1992. *Geologic Map of Bare Mountain, Nye County, Nevada*. U.S. Geological Survey Map I-2201. Reston, VA: U.S. Geological Survey.

Noble, D.C., R.D. Krushensky, E.J. McKay, and J.R. Ege. 1967. *Geologic Map of the Dead Horse Flat Quadrangle, Nye County, Nevada*. U.S. Geological Survey Geological Quadrangle Map GQ-614. Reston, VA: U.S. Geological Survey.

O'Conner, J.T., R.E. Anderson, and P.W. Lipman. 1966. *Geologic Map of the Thirsty Canyon Quadrangle, Nye County, Nevada*. U.S. Geological Survey Geological Quadrangle Map GQ-524. Reston, VA: U.S. Geological Survey.

Ratcliff, C.D., J.W. Geissman, F.V. Perry, B.M. Crowe, and P.K. Zeitler. 1994. *Paleomagnetic record of a geomagnetic field reversal from late Miocene mafic intrusions, southern Nevada*. Science 266: 412-416.

Rogers, C.L., E.B. Ekren, D.C. Noble, and J.E. Weir. 1968. *Geologic Map of the Northern Half of the Black Mountain Quadrangle, Nye County, Nevada*. U.S. Geological Survey Miscellaneous Geologic Investigations Map I-545. Reston, VA: U.S. Geological Survey.

Sargent, K.A., and J.H. Stewart. 1971. *Geologic Map of the Specter Range NW Quadrangle, Nye County, Nevada*. U.S. Geological Survey Geological Quadrangle Map GQ-884. Reston, VA: U.S. Geological Survey.

Sawyer, D.R., R.J. Fleck, M.A. Lanphere, R.G. Warren, D.E. Broxton, and M.R. Hudson. 1994. *Episodic caldera volcanism in the Miocene southwestern Nevada volcanic field: Revised stratigraphic framework, $^{40}\text{Ar}/^{39}\text{Ar}$ geochronology, and implications for magmatism and extension*. Geological Society of America Bulletin 106: 1,304–1,318.

Scott, R.B., and J. Bonk. 1984. *Preliminary Geologic Map of Yucca Mountain, Nye County, Nevada, with Geologic Sections*. U.S. Geological Survey Open-File Report 84-494. Reston, VA: U.S. Geological Survey.

Sinnock, S., and R.G. Easterling. 1983. *Empirically Determined Uncertainty in Potassium-Argon Ages for Plio-Pleistocene Basalts from Crater Flat, Nye County, Nevada*. Sandia National Laboratory Report SAND 82-2441. Albuquerque, NM: Sandia National Laboratory.

Smith, E.I., D.L. Feuerbach, T.R. Naumann, and J.E. Faulds. 1990. *Annual Report of the Center for Volcanic and Tectonic Studies for the Period 10-1-89 to 9-30-90*. Report 41. Carson City, Nevada: The Nuclear Waste Project Office.

Smith, E.I., S. Morikawa, and A. Sanchez. 1997. *Summary of the Activities of the Center for Volcanic and Tectonic Studies, University of Nevada, Las Vegas, for the Period 1986–1996*. Carson City, Nevada: The Nuclear Waste Project Office.

Stamatakis, J.A., C.B. Connor, and R.H. Martin. 1997. *Quaternary basin evolution and basaltic volcanism of Crater Flat, Nevada, from detailed ground magnetic surveys of the Little Cones*. Journal of Geology 105: 319–330.

Swadley, W.C. 1983. *Map Showing Surficial Geology of the Lathrop Wells Quadrangle, Nye County, Nevada*. U.S. Geological Survey Miscellaneous Investigations Series Map I-1361. Reston, VA: U.S. Geological Survey.

Swadley, W.C., and W.J. Carr. 1987. *Geologic Map of the Quaternary and Tertiary Deposits of the Big Dune Quadrangle, Nye County, Nevada, and Inyo County, California*. U.S. Geological Survey Miscellaneous Investigations Series Map I-1767. Reston, VA: U.S. Geological Survey.

Taylor, J.K. 1990. *Statistical Techniques for Data Analysis*. Boca Raton, FL: CRC Press.

Tschanz, C.M., and E.H. Pampeyan. 1970. *Geology and Mineral Deposits of Lincoln County, Nevada*. Nevada Bureau of Mines and Geology Bulletin 73. Reno, NV: Nevada Bureau of Mines and Geology.

Turrin, B. 1995. *Geochronology data for the Yucca Mountain Region. Presentation to the DOE Probabilistic Volcanic Hazard Assessment Elicitation Panel, February 22, 1995 Meeting in Phoenix, Arizona.* San Francisco, CA: Geomatrix Consultants.

Turrin, B.D., D. Champion, and R.J. Fleck. 1991. *$^{40}\text{Ar}/^{39}\text{Ar}$ age of the Lathrop Wells volcanic center, Yucca Mountain, Nevada.* Science 253: 654–657.

Turrin, B.D., D. Champion, and R.J. Fleck. 1992. *Measuring the age of the Lathrop Wells volcanic center at Yucca Mountain: Response.* Science 257: 556–558.

Vaniman, D., and B. Crowe. 1981. *Geology and Petrology of the Basalts of Crater Flat: Applications to Volcanic Risk Assessment for the Nevada Nuclear Waste Storage Investigations.* Los Alamos National Laboratory Report LA-8845-MS. Los Alamos, NM: Los Alamos National Laboratory.

Vaniman, D.T., B.M. Crowe, and E.S. Gladney. 1982. *Petrology and geochemistry of Hawaiiite lavas from Crater Flat, Nevada.* Contributions to Mineralogy and Petrology 80: 341–357.

Wright, L.A., and B.W. Troxel. 1984. *Geology of the North 1/2 Confidence Hills 15 Minute Quadrangle, Inyo County, California.* California Division of Mines and Geology Map Sheet 34. Sacramento, CA: California Division of Mines and Geology.

Yogodzinski, G.M., and E.I. Smith. 1995. *Isotopic domains and the area of interest for volcanic hazard assessment in the Yucca Mountain area.* EOS, Transactions of the American Geophysical Union 76(46): F669.